frontiers | Research Topics

100 years of quantum science and technology

Edited by
Karl Hess, Fedor Jelezko and
Bryan Dalton

Published in
Frontiers in Quantum Science and Technology

INTERNATIONAL YEAR OF
Quantum Science
and Technology

ISSN 1664-8714
ISBN 978-2-8325-7498-0
DOI 10.3389/978-2-8325-7498-0

Generative AI statement
Any alternative text (Alt text) provided alongside figures in the articles in this ebook has been generated by Frontiers with the support of artificial intelligence and reasonable efforts have been made to ensure accuracy, including review by the authors wherever possible. If you identify any issues, please contact us.

About Frontiers

Frontiers is more than just an open access publisher of scholarly articles: it is a pioneering approach to the world of academia, radically improving the way scholarly research is managed. The grand vision of Frontiers is a world where all people have an equal opportunity to seek, share and generate knowledge. Frontiers provides immediate and permanent online open access to all its publications, but this alone is not enough to realize our grand goals.

Frontiers journal series

The Frontiers journal series is a multi-tier and interdisciplinary set of open-access, online journals, promising a paradigm shift from the current review, selection and dissemination processes in academic publishing. All Frontiers journals are driven by researchers for researchers; therefore, they constitute a service to the scholarly community. At the same time, the *Frontiers journal series* operates on a revolutionary invention, the tiered publishing system, initially addressing specific communities of scholars, and gradually climbing up to broader public understanding, thus serving the interests of the lay society, too.

Dedication to quality

Each Frontiers article is a landmark of the highest quality, thanks to genuinely collaborative interactions between authors and review editors, who include some of the world's best academicians. Research must be certified by peers before entering a stream of knowledge that may eventually reach the public - and shape society; therefore, Frontiers only applies the most rigorous and unbiased reviews. Frontiers revolutionizes research publishing by freely delivering the most outstanding research, evaluated with no bias from both the academic and social point of view. By applying the most advanced information technologies, Frontiers is catapulting scholarly publishing into a new generation.

What are Frontiers Research Topics?

Frontiers Research Topics are very popular trademarks of the *Frontiers journals series*: they are collections of at least ten articles, all centered on a particular subject. With their unique mix of varied contributions from Original Research to Review Articles, Frontiers Research Topics unify the most influential researchers, the latest key findings and historical advances in a hot research area.

Find out more on how to host your own Frontiers Research Topic or contribute to one as an author by contacting the Frontiers editorial office: frontiersin.org/about/contact

100 years of quantum science and technology

Topic editors

Karl Hess — University of Illinois at Urbana-Champaign, United States

Fedor Jelezko — University of Ulm, Germany

Bryan Dalton — Swinburne University of Technology, Australia

Citation

Hess, K., Jelezko, F., Dalton, B., eds. (2026). *100 years of quantum science and technology*. Lausanne: Frontiers Media SA. doi: 10.3389/978-2-8325-7498-0

Table of contents

frontiers | Frontiers in Quantum Science and Technology

TYPE Editorial
PUBLISHED 28 January 2026
DOI 10.3389/frqst.2026.1755907

OPEN ACCESS

EDITED BY
Luca Lepori,
QSTAR, Italy

REVIEWED BY
Eric Bittner,
University of Houston, United States

*CORRESPONDENCE
Karl Hess,
karlfhess@gmail.com

RECEIVED 27 November 2025
ACCEPTED 20 January 2026
PUBLISHED 28 January 2026

CITATION
Hess K (2026) Editorial: Quantum information theory.
Front. Quantum Sci. Technol. 5:1755907.
doi: 10.3389/frqst.2026.1755907

Editorial: Quantum information theory

Karl Hess*

Center for Advanced Study, University of Illinois, Urbana, IL, United States

KEYWORDS

bell inequalities, contextual probabilities, EPR experiments, hidden variables / ontological variables, quantum entanglement, quantum information theory, quantum measurement problem, quantum nonlocality

Editorial on the Research Topic
Editorial: Quantum science and technology

Quantum information theory has evolved into a rapidly expanding and significant field of research. The papers presented in this section address a specific subset of this discipline—namely, the nature of quantum entanglement and the fundamental question of whether quantum information must inherently rely on probabilities that are intrinsic features of nature, rather than mere reflections of our ignorance regarding the details of underlying physical events. These issues trace back to the Einstein–Bohr debates, which were given formal logical and mathematical structure following the seminal contributions of Einstein, Podolsky, and Rosen (EPR), and later through John Stuart Bell's formulation of his celebrated inequality.

Subsequent experimental work, inspired by the ideas of EPR and Bell, led to major advances, particularly in polarization-based measurements capable of resolving single photon-pair detections. The paper by Carl Kocher in this section provides a detailed and lucid account of the first photon-based experiment demonstrating entanglement. Following this experimental milestone, it became reasonable to assert that EPR-type experiments offered compelling evidence for the entanglement—i.e., the significant correlation—of photon-pair measurements, consistent with the existence of certain intrinsic properties of the photon pairs responsible for the observed correlations, as originally suggested by EPR.

However, theoretical and experimental investigations by John Clauser and others soon revealed discrepancies between measurement results and Bell-type inequalities for specific sets of polarizer-angle pairs. After extensive theoretical analysis, Bell concluded that these discrepancies could only be explained by invoking nonlocal, instantaneous influences—faster than the speed of light—which contradicted the spirit of Einstein's relativity and which Einstein famously described as "spooky." Recognizing the extraordinary implications of his claim, Bell emphasized the necessity of definitive experimental proof that photon-pair measurements could not influence one another through any signal propagating at or below the speed of light. Alain Aspect and his collaborators provided a groundbreaking solution by developing experiments that rapidly switched polarizer angles in between measurement, ensuring that the actual pair-measurements could not influence each other within the light-speed limit.

These fast-switching experiments were later refined by research groups led by Alain Aspect, John Clauser, and Anton Zeilinger—whose team even conducted photon-pair

measurements between distant Canary Islands. Their collective achievements were recognized with the 2022 Nobel Prize in Physics. In their Nobel lectures, they emphasized Bell's postulated quantum nonlocalities. Many researchers have since endorsed this interpretation, arguing that such instantaneous influences u nderpin t he c omputational a dvantages o f quantum systems. However, no direct empirical proof of this claim exists, and Bell's theoretical framework remains the principal foundation for associating quantum superposition with nonlocality. Consequently, Bell's inequalities have become a central defense against more conventional, Einsteinian interpretations of quantum phenomena.

Despite extensive experimental progress, substantial doubts remain concerning the theoretical soundness of Bell's framework—doubts that extend well beyond the familiar experimental loopholes. These reservations center on the mathematical consistency of Bell-type derivations, as numerous previously neglected mathematical and physical factors have been identified t hat c an y ield v iolations o f B ell-type i nequalities. The introduction of rapid polarizer switching partially mitigated these concerns by not only ensuring that photon pairs emitted at the source could not depend on the polarizer settings, but also by suggesting that the observing experimenters (conventionally named Alice and Bob) are spatially separated, mutually unaware of each other's settings, and free to choose their polarizer orientations independently. Under these conditions, explanations of the observed correlations seem to necessarily invoke instantaneous, nonlocal influences.

The analyses presented in this section challenge that conclusion, showing, for example, that such reasoning implicitly disregards the stratagems of Einstein's theory of relativity. Yes, Alice and Bob are causally disconnected during the pair-measurement process and cannot possibly perform any mutual or relative assessment of outcomes in real time. However, a relative assessment may be carried out by theoreticians who retrospectively can check the consistency of their model—after all measurement data have been collected.

Gerard 't Hooft identified fundamental problems in Bell's framework early on and consistently expressed skepticism toward prevailing interpretations involving quantum superposition. Despite his distinguished reputation and profound contributions to theoretical physics, his deterministic perspective was largely disregarded and, at times, unfairly associated with "conspiratorial" thinking. This section includes one of 't Hooft's important papers, which demonstrates that the standard quantum-mechanical harmonic oscillator possesses an exact duality with a fully classical system, thereby revealing the potential existence of hidden ontological variables—a possibility often denied in textbooks emphasizing Bell's conclusions. 't Hooft's ideas and findings indicate the need for a more extensive investigation into underlying classical variables that are more basic than the quantum variables usually employed.

Several other contributions in this section further demonstrate that Bell's work possesses only limited validity and cannot be exclusively grounded in considerations of locality or determinism. Karl Hess and Jürgen Jakumeit show that crucial mathematical details within set-theoretic probability frameworks were neglected by Bell and his followers, despite their importance for the validity of Bell-type proofs. From a mathematical standpoint, the cardinality of the number M of Einstein's "elements of reality" (the properties of entangled photons) relative to the number N of measurements determines whether Bell-type proofs hold; they do so only when $M \ll N$. This insight also clarifies the success of Mermin's well-known elementary proofs, which typically assume $M = 8$. There is, however, no physical justification for restricting the number of photon-pair properties to eight. Hess and Jakumeit further point out that for finite M, Bell-type inequalities can only be derived by neglecting the physically necessary symmetry associated with the invariance of average measurement outcomes under certain polarizer rotations.

Marian Kupczynski promotes a statistical interpretation of quantum mechanics and critically reexamines Bell's theorem and its implications. Drawing upon Bertrand's paradox, he emphasizes the contextual nature of probabilities and their intrinsic dependence on the specific experimental conditions and measurement protocols. Kupczynski argues that if one introduces additional setting-dependent local variables—representing the physical characteristics of measuring instruments and procedures—into Bell's probabilistic framework, then quantum correlations can be accounted for without invoking nonlocalities.

Kupczynski's explanation also relies on the invariance of certain global physical laws with respect to rotations of the coordinate system employed to describe the EPR experiments, thereby guaranteeing consistency with the observed quantum statistics. His conclusions are extensively supported by numerous references in his review, which collectively reinforce the contextual and statistical foundations of his interpretation.

Taken together, these analyses suggest that while the 2022 Nobel Prize recognized remarkable experimental achievements, its interpretative emphasis on instantaneous influences and quantum superposition may have led the field astray. The use of Bell-type inequalities by Aspect, Clauser, and Zeilinger remains conceptually problematic. The photon-pair entanglement-experiments described by Carl Kocher can, in fact, be interpreted consistently with Einstein's notion of physical reality. Kocher's contribution in this section elucidates the essential details of the first EPR experiment with entangled photons and provides clear explanations of the factors underlying entanglement.

The contribution by Ana Maria Cetto and Luis de la Peña offers an additional compelling rationale to reconsider quantum-mechanical interpretations by taking the underlying physics of quantum phenomena into account. They establish a link between particle spin and quantum statistics, which results from the particles' response to the shared background radiation field. This approach has significant implications for understanding entanglement.

Finally, Theodorus Maria Nieuwenhuizen's paper presents a rigorous Hamiltonian treatment of the Curie–Weiss measurement model for spin-1 systems, distinguishing the stages of dephasing, decoherence, and registration. The associated H-theorem for the "dynamical free energy" illustrates relaxation toward a stable pointer state. This ensemble-based treatment, in which the density matrix becomes diagonal, provides valuable insight into the quantum measurement problem, without solving it.

Author contributions

KH: Writing – original draft, Writing – review and editing.

Funding

The author(s) declared that financial support was not received for this work and/or its publication.

Conflict of interest

The author(s) declared that this work was conducted in the absence of any commercial or financial relationships that could be construed as a potential conflict of interest.

The author KH declared that they were an editorial board member of Frontiers at the time of submission. This had no impact on the peer review process and the final decision.

Generative AI statement

The author(s) declared that generative AI was not used in the creation of this manuscript.

Any alternative text (alt text) provided alongside figures in this article has been generated by Frontiers with the support of artificial intelligence and reasonable efforts have been made to ensure accuracy, including review by the authors wherever possible. If you identify any issues, please contact us.

Publisher's note

frontiers | Frontiers in Quantum Science and Technology

TYPE Perspective
PUBLISHED 22 August 2024
DOI 10.3389/frqst.2024.1451239

OPEN ACCESS

EDITED BY
Karl Hess,
University of Illinois at Urbana-Champaign, United States

REVIEWED BY
Bengt Norden,
Chalmers University of Technology, Sweden
Juergen Jakumeit,
Access e.V., Germany

*CORRESPONDENCE
Carl A. Kocher,
kocher@mailaps.org

RECEIVED 18 June 2024
ACCEPTED 01 July 2024
PUBLISHED 22 August 2024

CITATION
Kocher CA (2024), Quantum entanglement of optical photons: the first experiment, 1964–67. *Front. Quantum Sci. Technol.* 3:1451239. doi: 10.3389/frqst.2024.1451239

Quantum entanglement of optical photons: the first experiment, 1964–67

Carl A. Kocher*

Quantum Foundry, University of California, Santa Barbara, Santa Barbara, CA, United States

The first experimental observation of entangled visible light was achieved by optically exciting free atoms of calcium and detecting pairs of photons emitted in a two-stage cascade. The polarizations of the entangled photons were observed to be correlated, in agreement with quantum theory. This review describes the rationale, methodology, challenges, and results, including experimental details not previously published.

KEYWORDS

entanglement, EPR paradox, atomic cascade, photon counting, reduction postulate, polarization correlation, Bell inequalities

1 Introduction

In the mid-1960s, as a young experimental physicist at the University of California, Berkeley, I was fascinated by quantum theory and impressed by its success in describing small systems such as atoms and molecules. Of particular interest was the 1935 article by Einstein, Podolsky, and Rosen (Einstein et al., 1935), which notes that if particles have a common origin, measurements of their properties (such as spin states) may be correlated. The correlation remains, even if the particles move apart and are spatially separated. In this hypothetical situation, quantum effects would be apparent on a macroscopic scale.

Although the term "entanglement" was coined by Schrödinger in the 1930s, it was not in common use in the 1960s. In simple terms, entanglement is a property of a system containing two or more particles, in which the quantum state of a particle depends on, and is linked to, the states of others. Electrons, for example, are entangled in every atom, every molecule, every material. So it would be fair to say that entanglement is everywhere. And experiments on entangled systems can reveal aspects of Nature that may seem surprising and quite remarkable.

I was interested in finding the simplest possible system for studying the effects of entanglement, and began feasibility studies for a low-energy experiment that could be set up in a small laboratory with a limited budget. Inspired by the Einstein-Podolsky-Rosen gedanken experiment, it would deal with the spin states of just two entangled particles.

If the particles were electrically charged, like low-energy electrons, there would be no clean way to extract them without exposure to stray fields that would affect the spins. Therefore it seemed natural to consider visible light, in which the photons have no charge and are non-interacting. When atoms emit light, there is no need to extract the photons: Nature performs the extraction process for us.

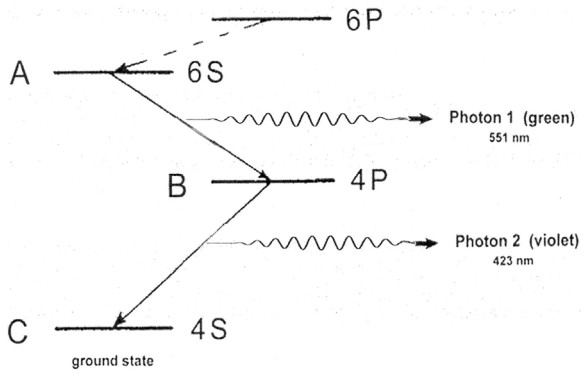

FIGURE 1
Photons emitted in a two-stage cascade.

2 Experimental concept

If a free atom is excited, it can make a transition to a lower-energy state, via the spontaneous emission of electromagnetic radiation in the form of a photon. Although the photon may be detected as a point-particle, it propagates as an extended wave packet, spreading as it moves out from the atom, carrying angular momentum (spin) as well as energy.

Figure 1 shows several singlet-state energy levels for an isolated calcium atom. If the atom is initially in state A, it can give up energy in two stages, A → B and B → C, with the emission of Photon 1 (green light, 551 nm) and Photon 2 (violet light, 423 nm). The corresponding spectral lines are seen in the emission spectrum of calcium.

An ensemble of excited calcium atoms is shown at the center of Figure 2, with the green and violet photons detected by photomultiplier detectors (PM) along a common axis.

Narrow-band interference filters pass the desired wavelengths while blocking other light. Pulses from the detectors are recorded as atoms proceed through the two-stage cascade A → B → C. For identification of photon pairs from the same atom, the detector pulses can be fed into a coincidence circuit that "clicks" only when photons arrive at the two detectors at nearly the same time.

Since light propagates as a wave, even in the quantum realm, the experiment can incorporate familiar optical components such as lenses, interference filters, linear polarizers, and glass vacuum windows, through which the photons can pass prior to detection.

The spin state of a photon corresponds to its polarization state, as noted in Section 3.2, where the two-photon final state is discussed. In the visible region of the spectrum, polarizations can be studied with ordinary linear polarizers, commonly known as Polaroid sheets. In the experiment, a rotatable linear polarizer is mounted in front of each detector, so that the coincidence counting rate can be recorded as a function of the angular orientations of the polarizers.

This experiment would be the first attempt to count and analyze single optical photons and pairs of photons emitted in an atomic cascade. (Kocher, 1967a; Kocher and Commins, 1967).

Why did I choose calcium? 1) Efficient linear polarizers are available for polarization measurements at the green and violet calcium wavelengths. 2) Single-photon detection by photomultiplier detectors is possible, although somewhat inefficient, for light at these wavelengths. 3) Entanglement calculations are simple and unambiguous for calcium, as the initial and final states, A and C, are spherically symmetric. Spherical symmetry requires that all internal angular momenta for the atom (orbital, electron spin, and nuclear spin) must be zero. States A and C are S-states, with no orbital angular momentum. Zero electron spin suggests an atom from the second column of the periodic table, with two valence electrons forming singlet states for which the spins cancel. It is also fortunate that essentially all the atoms in naturally occurring Ca (99.8%) have spin-zero nuclei. 4) The vapor pressure characteristics of calcium allow for the production of an atomic beam from a suitable oven in a vacuum chamber.

3 Relevant quantum concepts

This section presents, in simplified form, a view of the theoretical background for the entanglement of photon polarization states.

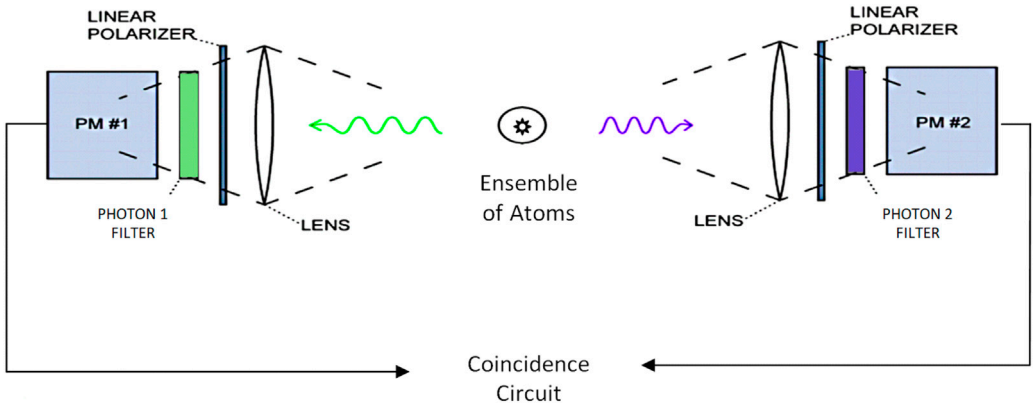

FIGURE 2
Experimental geometry, simplified.

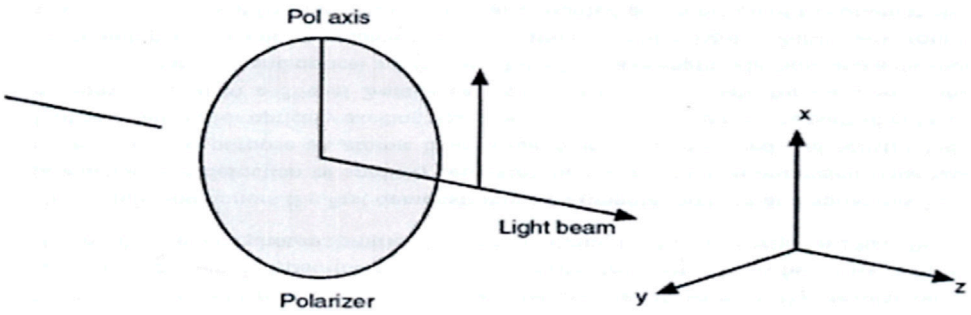

FIGURE 3
Linear polarizer geometry.

3.1 Polarization measurements

A linear polarizer is an anisotropic flat plate with a transmission axis in its plane. In the classical domain, in which light behaves as a transverse electromagnetic wave, linearly polarized light passes undiminished through an ideal polarizer if its axis is parallel to the electric field in the wave. However, no light is transmitted if the electric field and polarizer directions are perpendicular. The meaning of "no light" can be extended to the quantum realm, where it means "no photons" are transmitted. Thus it is possible to regard the polarizer as a filter for quantum states.

In Figure 3, light travels along the experiment's axis of symmetry, shown here as the *z*-axis, with a linear polarizer in the xy plane. Capital letter X will denote the photon state transmitted by a polarizer aligned along the x-axis, and similarly Y for the y-axis. The general polarization state Ψ for a single photon is a linear combination, or coherent mixture, of these states:

$$\Psi = a_x X + a_y Y, \tag{1}$$

where a_x and a_y are amplitudes (in general, complex) that tell how much of each state is present in the admixture.

Quantum theory provides two ways for the state of a system to change in time:

(1) The Time-dependent Schrödinger Equation is central to quantum mechanics. Solving it yields a wave function or state vector Ψ(t) that describes the system and its continuous evolution between measurements.

(2) The Reduction Postulate determines how Ψ changes when a measurement is made. A measurement leads to a sudden collapse, or projection, of Ψ onto the observed state.

The state Ψ for a photon therefore changes discontinuously as a result of a polarization measurement. If the photon described by Eq. 1 is detected after passing through a polarizer with its transmission axis along x, that constitutes a measurement. In this case the reduction postulate requires that the Y term must drop out. Only the observed-state X term remains in Ψ after the measurement.

The experiment in Figure 2 explores the reduction postulate in a two-photon system.

3.2 Polarization states for entangled photons

Photon spin states for light traveling in the *z*-direction can be expressed in terms of linear polarization states X and Y (as above), or in terms of helicity. The two sets of basis states are related as follows (with normalization factors not shown):

Spin parallel to photon momentum:

$$\text{Positive helicity} \quad \Psi^+ = X + iY$$

Spin antiparallel to photon momentum:

$$\text{Negative helicity} \quad \Psi^- = X - iY$$

Conservation laws for angular momentum and parity play a central role in quantum correlation phenomena. For the three-level radiative cascade in Figure 1, the initial atomic state A and final state C both have zero total angular momentum and even parity. Therefore, the two-photon final state Ψ must also satisfy the conditions of zero angular momentum and even parity:

$$\Psi = \Psi_1^+ \cdot \Psi_2^+ + \Psi_1^- \cdot \Psi_2^-. \tag{2}$$

If the same *z*-axis is used for both photons and is directed to the right in Figure 2, the states for Photon 1 require $i \rightarrow -i$. Then

$$\Psi = (X_1 - iY_1) \cdot (X_2 + iY_2) + (X_1 + iY_1) \cdot (X_2 - iY_2), \tag{3}$$

in which the $X_1 \cdot Y_2$ and $Y_1 \cdot X_2$ terms drop out, yielding (without normalization factor) a simple and elegant result

$$\Psi = X_1 \cdot X_2 + Y_1 \cdot Y_2 \tag{4}$$

for the two-photon system, before either photon is detected. The reasoning in Eqs 2, 3, leading to Eq. 4, gives it a sense of universality, as no consideration is given to the internal structure of the source atom or its interaction with a quantized radiation field. Before any measurements have been made, each photon has a potential to pass through a linear polarizer with any orientation.

The two-particle quantum state Ψ is not a simple product, as it would be for photons having no common history. Instead it is a sum of products representing an entangled state. Entanglement of the photons is evident in Eq. 4, where neither photon has an independent identity. In each of the two terms, the amplitude for one of the photons is a wave function for the other.

Since the orientation for the x- and y-axes around z is arbitrary, the form of Eq. 4 will remain unchanged if the xy coordinate system is rotated through any angle about the z-axis.

3.3 Polarization correlation

If the first photon (green) passes through a linear polarizer transmitting the state X_1, the reduction postulate removes the second term, containing Y_1, from Ψ in Eq. 4. Only the first term remains, leaving the second photon (violet) unambiguously in polarization state X_2. More generally, if one of the photons passes through a linear polarizer at any orientation, the remaining photon will then be in the same polarization state, pending future measurements.

Quantum theory makes specific predictions for the experiment shown in Figure 2.

(1) If both polarizers are aligned with their axes parallel, coincidence counts will be observed.
(2) If the polarizer axes are perpendicular, no coincidences will be observed—a conclusion that also follows directly from the absence of cross-terms $X_1 \cdot Y_2$ and $Y_1 \cdot X_2$ in Eq. 4. This signature of entanglement, which has no classical analog, is noteworthy and accessible to experimental observation.

These predictions may seem counterintuitive, bizarre, or weird, especially because there is no known evidence for physical transmission of information from one detector to the other. This question is addressed further in Section 6.

Additional remarks:

(a) Taken separately, the green and violet beams are unpolarized.
(b) If there is a general angle between the polarizer axes, Eq. 4 predicts a coincidence probability (and therefore a counting rate) that varies as the square of the cosine of this angle.
(c) The reduction postulate also enables calculations of the time dependence for the detection of entangled photons emitted by an atom. (Kocher, 1971).

4 Experimental considerations

4.1 Photon detection

A photomultiplier detector is an evacuated and sealed glass tube with a light-sensitive cathode on a window at one end. As Einstein first realized, the energy of a detected photon is conveyed to a single photoelectron from the cathode. This electron is accelerated toward a positively charged metal dynode, where additional electrons are knocked loose. This process is repeated at additional dynodes, producing a negative pulse that can be counted with standard electronics. Quantum efficiencies (output pulse probability per photon) are of order 10% (green) to 20% (violet). Photoelectrons released from different locations on the cathode travel a range of distances in reaching the first dynode, introducing some loss of time resolution, typically several nanoseconds. In addition, thermal processes can release electrons randomly from the cathode, resulting in spurious output pulses, or "dark noise."

4.2 Atomic beam oven

The oven, shown in Figure 4, is 6.5 cm in length and machined from tantalum, a nonreactive refractory metal. It is heated by an electric current through internal resistive coils. A cylinder of calcium metal is loaded into the well. When the oven is installed in a vacuum chamber and heated, monatomic calcium vapor evaporates from the solid and comes out through an opening in the front, forming a beam.

A thermocouple junction, set into a small hole in the oven, reads out the temperature. At 1000 K, an oven load of Ca (12 g) will empty in about 25 h, and a typical beam velocity for a Ca atom is about 10^5 cm/s. Since the radiative cascade requires about 10^{-8} s, the atom moves only about 10^{-3} cm—a negligible distance—while the photons are being emitted.

The oval at the center of Figure 2, labeled "Ensemble of Atoms," represents a cross section of the atomic beam from this oven.

4.3 Excitation strategy

The two-stage cascade, as shown in Figure 1, requires excitation of calcium atoms from the 4S ground state to the 6S excited state. This is a challenging problem, since the direct 4S → 6S transition is "forbidden" for single-photon absorption. (Dipole matrix elements are zero.) An acceptable alternative

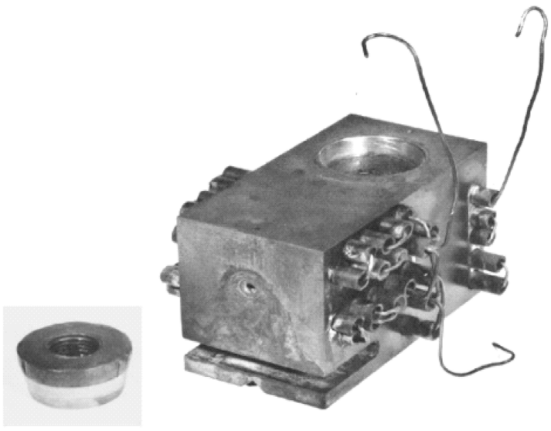

FIGURE 4
Atomic beam oven for calcium.

would be to optically excite the 6P state (also shown in Figure 1) by an allowed transition, 4S → 6P. The 6P can decay to 6S by emitting an infrared photon that is not observed, and then the desired cascade can take place. The 4S → 6P excitation requires a 228 nm ultraviolet light source.

A minor complication is that while the 6P state can decay to 6S, it can also decay to 5S and several D-states (in total about 8 times as likely as 6S). All of these return to the ground state via the 4P state, producing a Photon 2 not time-correlated with a Photon 1. Detector pulses from unpaired violet photons can trigger false coincidences and are a source of noise.

In 1964 it was a major challenge to find an acceptable 228 nm UV excitation source for the 4S → 6P transition. No tunable lasers, UV lasers, or UV LEDs were available. (There were also no pocket calculators and no lab computers. It was still the slide rule era.)

A calcium discharge lamp could not be considered as a 228 nm source, as it would produce intense 423 nm (violet) radiation that could not be effectively blocked from reaching the Photon 2 detector. Electron impact excitation would pose a similar problem. A third possibility was a continuum source of ultraviolet light, in conjunction with a 228 nm bandpass interference filter. A high-pressure mercury lamp was considered, but even this produced far too much visible light.

Then I read about the UV continuum emitted by molecular hydrogen, with wavelengths spanning the range from about 180 nm to 450 nm. No suitable lamps were commercially available, so I designed and built a cylindrical low-voltage high-current H_2 arc lamp in a brass chamber, using a porous tungsten dispenser cathode and a continuous flow of H_2 gas. (Kocher, 1967b). This turned out to be essential to the eventual success of the experiment. The lamp operated at 17 V, 30 amps, with the discharge produced between the cathode and anode in the cross-sectional view of Figure 5. Fused quartz transmits 228 nm radiation, so a quartz focusing lens is mounted between the lamp and the excitation region.

If the broadband UV light were applied perpendicular to the Ca beam, only atoms within the natural linewidth (about 30 MHz) for the 4S → 6P transition could be excited, and all the useful radiation would be absorbed near the edge of the atomic beam. Atoms beyond this edge would not be excited. However, there is a spread in atomic velocities from a thermal oven, and the Doppler-broadened linewidth (1,000 MHz) exceeds the natural linewidth by a factor of about 30. In the experimental plan I therefore introduced the calcium beam at 45° relative to the observation z-axis, from lower left to upper right in Figures 2 and 6. With this configuration the much larger number of atoms in the Doppler-broadened absorption line can potentially be excited to the 6P state. The oblique angle between the atomic beam and the detector axis also effectively eliminates trapping and multiple scattering of the emitted 423 nm violet photons.

4.4 Coincidence rate estimate

It would not be wise to proceed with a complex experiment unless the signal and noise levels can be estimated. Therefore, before

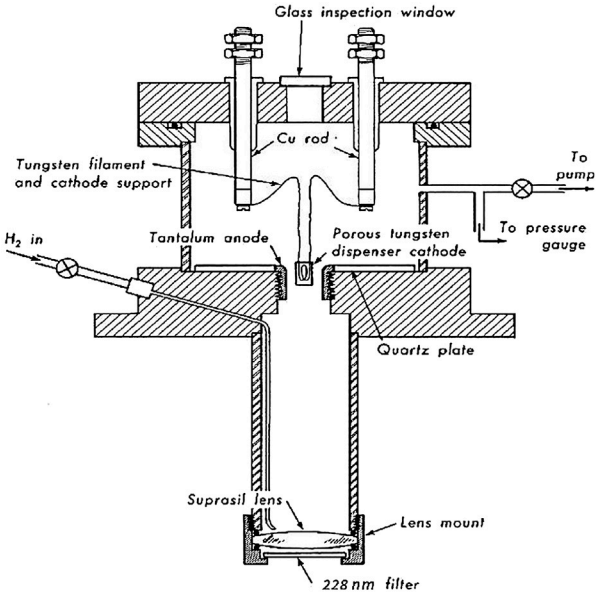

FIGURE 5
500 watt H_2 arc lamp.

the major construction of a vacuum chamber and dealing with pumps, hoses, ion gauges, *etc.*, an effort was made to calculate the coincidence counting rate under reasonable experimental conditions.

For each detector I considered the fractional solid angle of intercept, together with the quantum efficiency and the filter transmission, and found that about 10^6 cascade-emitting atoms are needed for each observable coincidence count—without the polarizers.

The atomic beam oven holds about 10^{23} atoms of Ca, but only 1 atom in 10^3 would pass through the excitation region.

I used a radiation thermopile to measure the intensity of the H_2 arc lamp in conjunction with a 228 nm bandpass filter. I also searched the literature for transition rates in calcium and determined the branching ratios for the transitions.

It was a complex process putting these pieces together, attempting to identify every limitation and concern. In the end I estimated **1 coincidence per second** (with the polarizers removed), with an uncertainty factor of about 5.

Under these conditions, reasonable statistics—and a clear experimental result—might be obtained with a multi-hour observation. It would be a difficult undertaking, requiring considerable care, patience, a long observation time, and some courage.

4.5 Apparatus details

The experimental plan employs a vacuum system with two diffusion-pumped brass chambers and removable flanges for access. A water-cooled source chamber holds the calcium beam oven. The excitation chamber, pumped to a lower pressure (10^{-6} Torr), contains the interaction region, where UV light from the H_2

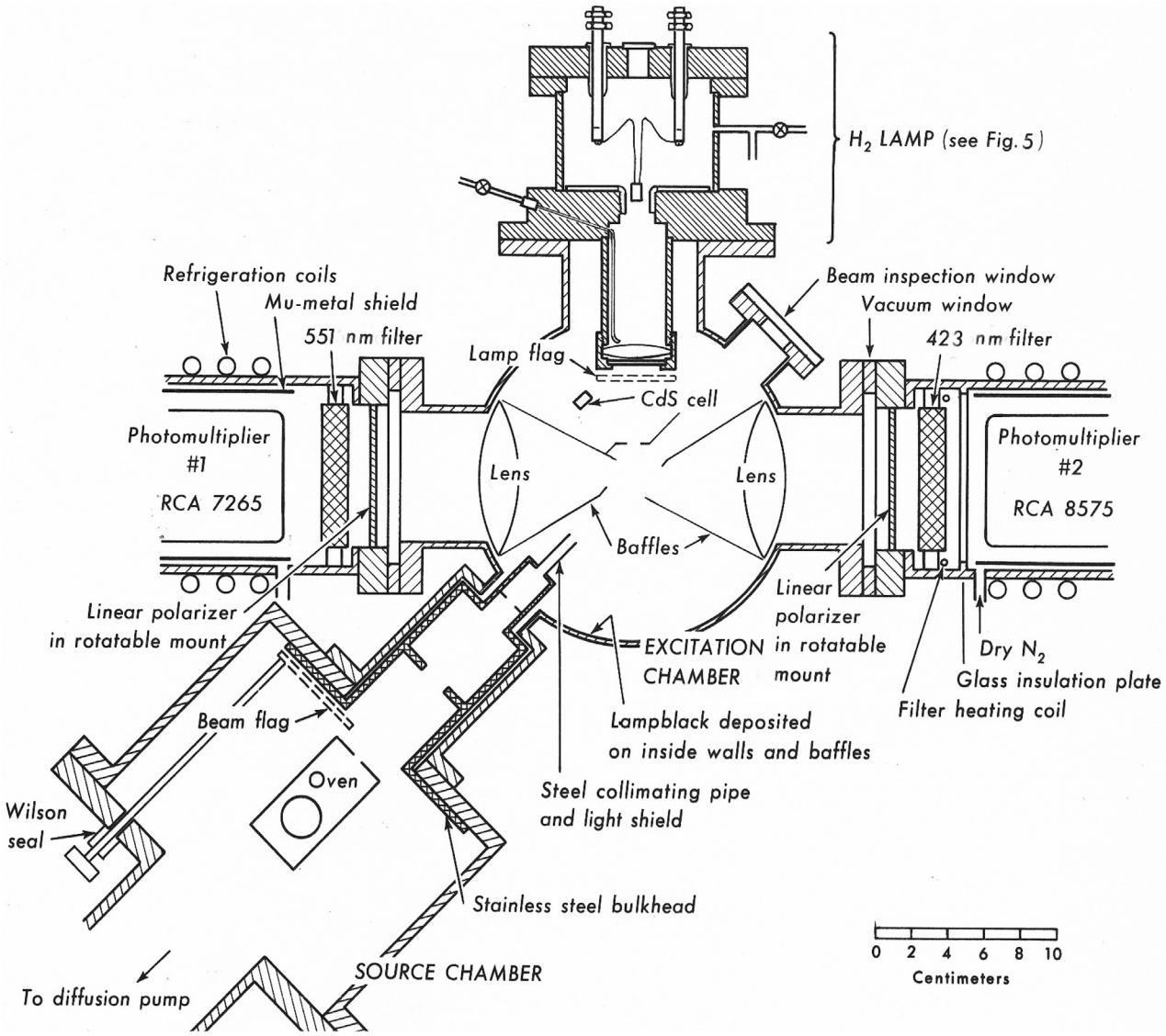

FIGURE 6
Cross section of the apparatus, top view.

lamp would excite Ca atoms in the atomic beam, and from which the green and violet photons would be detected by photomultiplier assemblies outside the chamber.

Details of the experiment are shown in Figure 6 and in a photograph, Figure 7.

It took more than a year to reach the point where all the parts of the experiment could be assembled. The components were tested separately, to the extent possible, and then in tandem.

Two flags, shown in Figure 6, can be controlled from outside the chamber. One can block the calcium beam, and the other can block the UV radiation from the lamp so it cannot reach the beam. This flexibility made it possible to monitor and optimize the counting rate for each detector separately. It was then possible to determine the sources of extraneous coincidence counts, of which there were many, including stray light from the oven heating coils and visible-light fluorescence due to the UV from the lamp. I installed light-blocking baffles and applied lampblack to the chamber walls. The improvements were slow and incremental.

After this was done, photomultiplier "dark noise," which had always been present, became noticeable at room temperature. To address this problem, I cooled the photomultipliers by soldering a helix of copper tubing around each brass photomultiplier enclosure and installing a refrigeration compressor that could circulate refrigerant through the tubing. The photocathode temperatures were cooled to −15°C, reducing the dark noise significantly.

Instead of using a simple coincidence circuit, I recorded coincidence counts versus the time delay between the pulses from the two detectors, using a time-to-pulse-height converter and a multichannel pulse-height analyzer, as in Figure 8.

The time-to-height converter produces an output pulse with an amplitude proportional to the time delay between the "start" pulse (from the Photon 1 detector} and the "stop" pulse (from the

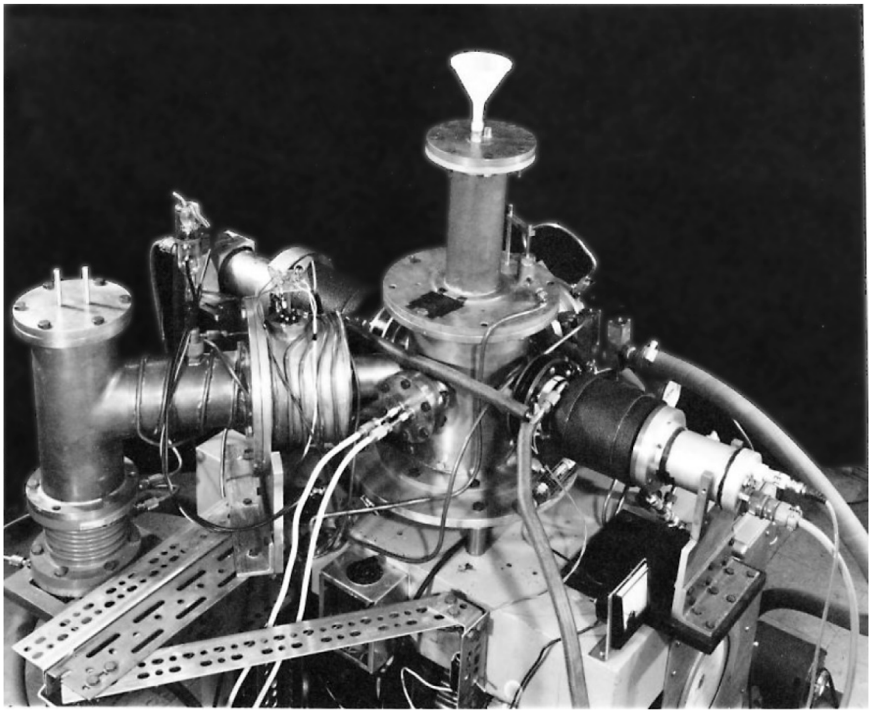

FIGURE 7
Apparatus photograph corresponding to Figure 6.

Photon 2 detector). A pulse-height analyzer stores these counts in an array of magnetic-core memory channels corresponding to a span of delay times. Each memory channel effectively represents a separate coincidence circuit, for which the time spread can be varied by changing the ramp rate. The time offset, corresponding to sliding the distribution to the right or left, can be adjusted by varying a delay line (a length of coaxial cable) on the Photon 2 side.

If the pulse pairs are from the same atom, they contribute to a central peak in the distribution, as viewed on an oscilloscope. Pulse pairs may also be due to photons from different atoms, or to stray light. In these cases the time intervals are random, contributing to a background signal, with fluctuating statistics, along the entire horizontal time scale.

5 Final testing and results

Figure 9 shows the laboratory in 1966. Test runs were attempted with the calcium beam and H_2 lamp running, without the polarizers. As expected, the Photon 2 detector recorded the most photons, and the single-detector counting rates increased encouragingly when the beam and the UV excitation were both on. Unfortunately the rate for coincidence counts was lower than the lower limit I had estimated, by a factor of about 10. Under these conditions the experiment could not yield clear results.

Weeks passed, with considerable frustration, and I went into a deep search for an explanation. All questions had to be asked, and everything rechecked. Then I thought of a possible reason for the low coincidence rate. An interference filter was mounted on each photomultiplier assembly. These were high quality narrow-band filters, made from sets of dielectric plates and built-to-order for the calcium wavelengths. But dielectrics tend to be thermally sensitive, and I now realized that when I installed the refrigeration coils for cooling the photomultipliers, I also ended up cooling the filters. If

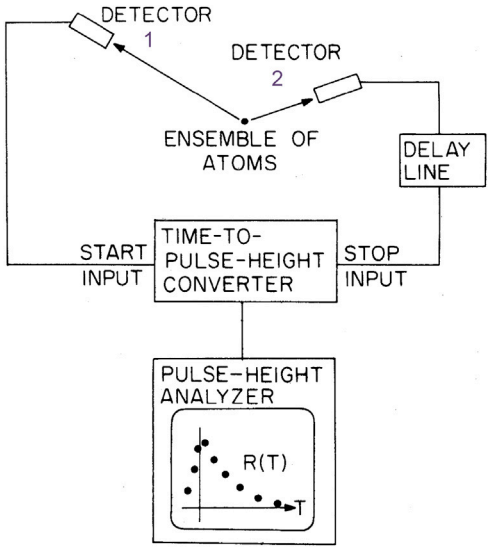

FIGURE 8
Basic electronics for recording and displaying coincidence counts.

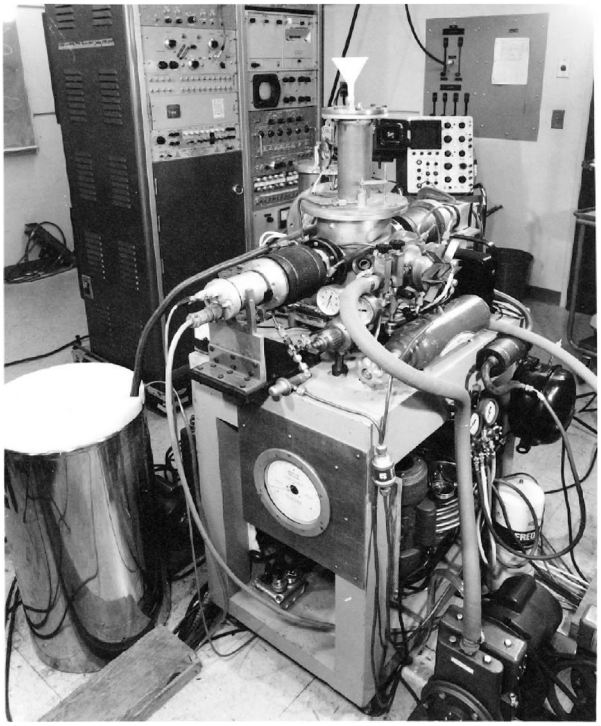

FIGURE 9
Overall view of the experiment.

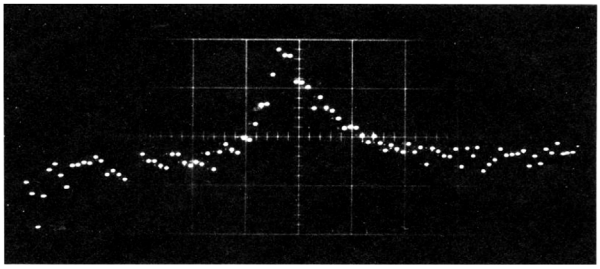

FIGURE 10
Coincidence counts displayed from memory of pulse-height analyzer.

the filters were thermally sensitive, the transmitted wavelength could have shifted. If the shift were large enough, the filter would end up being "tuned off-resonance" and the desired wavelength would be blocked instead of transmitted.

I removed the filters, got a bucket with dry ice, a thermometer, and some clean rags, and scanned the filters using a recording spectrophotometer. I started with the filters at room temperature and printed out the scans. The peak wavelengths were very close to what I had ordered, at 551.3 nm and 422.7 nm. Then I wrapped the filters, cooled them with dry ice to −20°C, and made repeated spectrometer scans as they warmed up. The violet filter, which had the narrower passband, was far off resonance at −20°C and also at −10°C. To correct for this shift I added a small heating coil for the violet filter and adjusted the current through it to bring the filter's transmission peak back onto the wavelength for the violet-light photons. This is shown in Figure 6.

Then I loaded the oven with a full cylinder of calcium and pumped down the vacuum system. A clear, unequivocal coincidence signal was apparent within an hour. That afternoon I obtained the time correlation plot in Figure 10, showing coincidences in the form of a peak.

Here the horizontal separation between channels represents a time interval of 0.8 ns. The exponential decay of the 4P state, which has a mean lifetime of 4.5 ns, shows up as an asymmetry, although each photomultiplier smears out the time resolution by about 3 ns. The counts above the noise baseline are coincidences.

As noted previously, the separate Photon 1 and Photon 2 light beams are expected to be unpolarized. To check this I installed the polarizers and verified that the single-detector counting rates did not vary with the polarizer orientations.

Finally, a 25-h run with the polarizers installed, on December 17 and 18, 1966. The experiment continued through the night, with data recorded during 21 consecutive hours. Parallel and perpendicular polarizer configurations were alternated, with the recording of data switched in cycles between memory banks for horizontal and vertical polarizer combinations xx, yy, xy, and yx. Equal recording periods were allotted to parallel and perpendicular orientations of the polarizers. The results are shown in Figure 11, where each point represents a sum over three adjacent analyzer channels. Upper panel (A) shows a coincidence peak with the polarizer axes parallel. Lower panel (B) shows no peak with the axes perpendicular.

The hint of a peak in (B) can be attributed entirely to the imperfect linear polarizers, which transmitted 6% of unpolarized violet light when crossed at 90°.

Most significantly: **When the polarizer axes are perpendicular, no coincidences are recorded**. This conclusion is in agreement with the predictions of quantum theory for entangled photons.

The photon detectors in this experiment were about 40 cm apart, a macroscopic distance. Each photon is a spherical wave, traveling outward from the atom at the speed of light. Before the photons are detected, their coupled (or entangled) waves occupy the entire space between the atom and the detectors. As a consequence the quantum system is macroscopic, with the two-photon wave function extending over a macroscopic region.

When this work was undertaken it was inconceivable that, decades later, unforeseen and breathtaking developments, including sophisticated lasers and parametric down-conversion, would enable the creation of entangled photons in great numbers, or that they might play a role in practical or useful technology. Yet we now understand that entanglement and quantum correlations can be exploited, leading to an exciting new field of "quantum information."

6 Reflections and overview

In an experiment with non-interacting particles, how can a measurement **here** affect what happens **there**? It may seem profoundly strange that quantum theory—the best we have—does not introduce or incorporate a deterministic "causal mechanism" for correlations in the measurements. Could there be some identifiable process that allows one photon, or one measurement, to communicate with the other?

Einstein famously called these kinds of effects "spooky action at a distance." What is now known as the "Einstein-Podolsky-

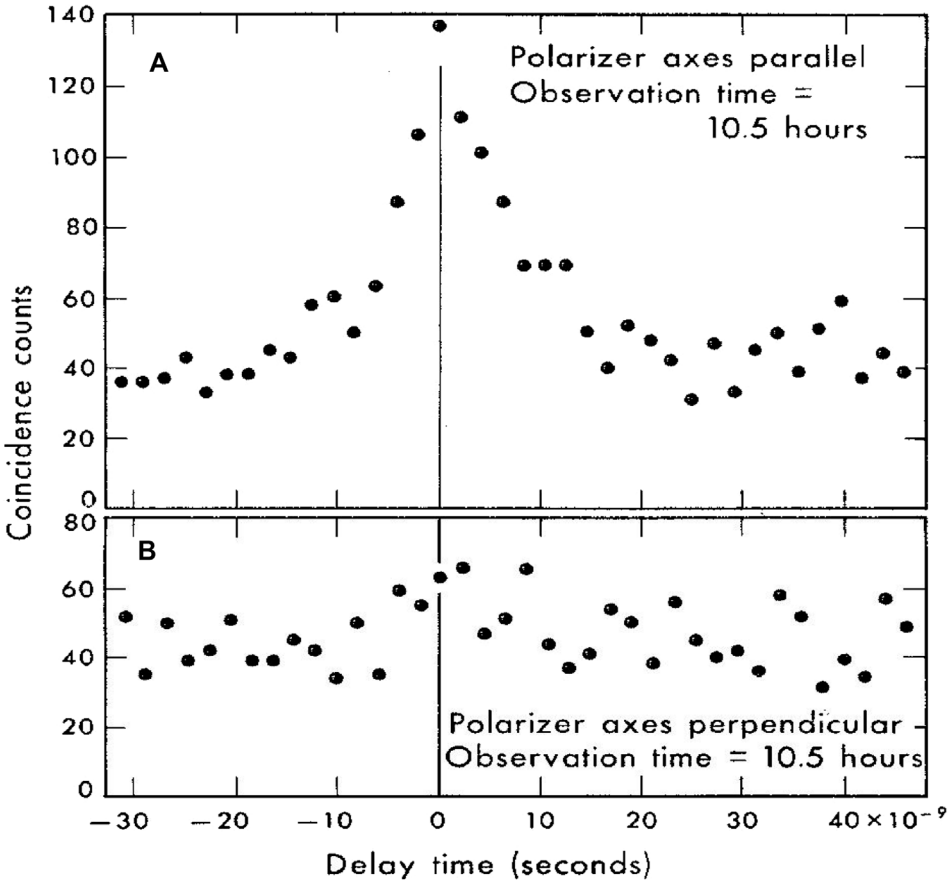

FIGURE 11
Experimental Results: Coincidence counts recorded as a function of delay time: **(A)** With the polarizer axes parallel, a clear coincidence peak is observed, and **(B)** With the polarizer axes perpendicular, no peak is present.

Rosen paradox" led him to suggest that the theory might be "incomplete" in some way. Nevertheless the quantum theory of the 1920s and 30s does accurately predict and describe experimental results, including entanglement phenomena. It is a successful theory that has been tested repeatedly, including by others who used my apparatus years later and confirmed the results presented here. (Freedman and Clauser, 1972).

Could there be situations where quantum theory makes incorrect predictions, or where alternative theories give equally satisfactory explanations? Much effort has been devoted to theories involving hidden variables and to experiments probing the Bell inequalities. Yet none of these, so far, appear to have led to new physics.

Most of us have never lived in an overtly quantum world, and so it is tempting to proclaim a "paradox" when expectations based on classical phenomena are extrapolated into the quantum realm. A corollary might be offered—that credible experiments yielding strange results should be welcomed into our consciousness, celebrated for their insight, and incorporated into the life experience from which intuition derives.

From my perspective, performing an experiment of this kind was a rare opportunity for witnessing a strangely wonderful quantum phenomenon and bringing it into the domain of experience. It is a search for truth, and if the truth changes our outlook on the world, so much the better.

Data availability statement

The original contributions presented in the study are included in the article/Supplementary Material, further inquiries can be directed to the corresponding author.

Author contributions

CK: Conceptualization, Data curation, Investigation, Methodology, Writing–original draft, Writing–review and editing.

Funding

The author declares that no financial support was received for the research, authorship, and/or publication of this article.

Acknowledgments

Eyvind Wichmann, a theoretician, is gratefully acknowledged for inspiring this project. While planning a curriculum in quantum physics for second-year undergraduates, he conceived an original

idea for the instructional laboratory: a "tabletop experiment" for observing the polarizations of atomic cascade photons. I remember his words: "I have one new idea, but I don't know if it can be done."

Eugene Commins, a splendid collaborator and an outstanding teacher, was immediately receptive to this experiment when I proposed that we work on it together. With a unique gift for conveying complex ideas with clarity and humor, Gene offered much encouragement, arranged my access to equipment from LRL, and provided $10,000 to cover all the expenses for the experiment.

John Clauser came to Berkeley several years after this experiment was completed, and used my apparatus, with minor improvements, in a test of the Bell inequalities. In the process, he repeated my experiment and verified the results as presented here. Not every research endeavor has the benefit of independent confirmation.

Conflict of interest

The author declares that the research was conducted in the absence of any commercial or financial relationships that could be construed as a potential conflict of interest.

Publisher's note

References

Einstein, A., Podolsky, B., and Rosen, N. (1935). Can quantum-mechanical description of physical reality be considered complete?. *Phys. Rev.* 47, 777–780. doi:10.1103/PhysRev.47.777

Freedman, S. J., and Clauser, J. F. (1972). Experimental test of local hidden variable theories. *Phys. Rev. Lett.* 28, 938–941. doi:10.1103/PhysRevLett.28.938

Kocher, C. A. (1967a). Polarization correlation of photons emitted in an atomic cascade. UCRL Report 17587, 79. Available at: https://escholarship.org/uc/item/1kb7660q.

Kocher, C. A. (1967b). Metal-cased H_2 arc lamp of simplified design. *Rev. Sci. Instrum.* 38, 1674–1675. doi:10.1063/1.1720643

Kocher, C. A. (1971). Time correlations in the detection of successively emitted photons. *Ann. Phys.* 65, 1–18. doi:10.1016/0003-4916(71)90159-X

Kocher, C. A., and Commins, E. D. (1967). Polarization correlation of photons emitted in an atomic cascade. *Phys. Rev. Lett.* 18, 575–577. doi:10.1103/PhysRevLett.18.575

frontiers | Frontiers in Quantum Science and Technology

TYPE Perspective
PUBLISHED 20 December 2024
DOI 10.3389/frqst.2024.1505593

OPEN ACCESS

EDITED BY
Karl Hess,
University of Illinois at Urbana-Champaign, United States

REVIEWED BY
Christof Wetterich,
Heidelberg University, Germany

*CORRESPONDENCE
Gerard 't Hooft,
g.thooft@uu.nl

RECEIVED 03 October 2024
ACCEPTED 10 October 2024
PUBLISHED 20 December 2024

CITATION
't Hooft G (2024) The hidden ontological variable in quantum harmonic oscillators. *Front. Quantum Sci. Technol.* 3:1505593. doi: 10.3389/frqst.2024.1505593

The hidden ontological variable in quantum harmonic oscillators

Gerard 't Hooft*

Institute for Theoretical Physics, Utrecht University, Utrecht, Netherlands

The standard quantum mechanical harmonic oscillator has an exact, dual relationship with a completely classical system: a classical particle running along a circle. Duality here means that there is a one-to-one relation between all observables in one model, and the observables of the other model. Thus the duality we find, appears to be in conflict with the usual assertion that classical theories can never reproduce quantum effects as observed in many quantum models. We suggest that there must be more of such relationships, but we study only this one as a prototype. It reveals how classical hidden variables may work. The classical states can form the basis of Hilbert space that can be adopted in describing the quantum model. Wave functions in the quantum system generate probability distributions in the classical one. One finds that, where the classical system always obeys the rule probability in = probability out, the same probabilities are quantum probabilities in the quantum system. It is shown how the quantum x and p operators in a quantum oscillator can be given a classical meaning. It is explained how an apparent clash with quantum logic can be rationalized.

KEYWORDS

ontological variable, quantum harmonic oscillator, quantum mechanics, duality, local hidden variable (LHV), classical ontological variable (COV)

1 Introduction

It has become customary to investigate quantum theories by proving that they cannot be represented in terms of ontological variables. These ontological variables, known as "local hidden variables" (LHV), are assumed to reproduce the results of all experiments that can be performed on a given quantum system, which is subsequently shown to lead to logical contradictions.

However, when the outcome of an extensively examined quantum experiment is compared with a classical theory, it is often the classical dynamics that is finished off in one short sentence: "This cannot be the result of a classical theory." One may however suspect that the assumptions made concerning these LHV are too strict, so that there could be loopholes.[1] Many investigations are aimed at closing these loopholes by making further assumptions (Bell, 1964; Bell, 1982; Bell, 1987; Conway and Kochen, 2008; Clauser et al., 1969; Greenberger et al., 1990).

1 A very important loophole, not discussed further in this paper, is that models such as the Standard Model of the elementary particles, require perturbation expansions, which are known to be fundamentally divergent. This procedure introduces uncertainties (Hooft et al., 2021) that can be studied further, under the suspicion that this could be the cause of the tendency of quantum wave functions to spread.

This, we claim, may not be the only way to improve our understanding of quantum mechanics. Here, we approach the question concerning the interpretation of quantum mechanics from the other end: which quantum systems *do* allow for classical variables, and can these models be extended to include physically useful ones? Can these models be demanded to obey (some form of) locality? Can we use them as building blocks? We claim that this is a rich field for further investigation (Brans, 1988; Vervoort, 2013; 't Hooft, 2016; 't Hoofta, 2023).

Here, a very important example is exhibited: the quantum harmonic oscillator. As we shall see, it contains a variable that can explain everything we see in a quantum harmonic oscillator, in terms of completely classical mathematical logic. Our variables are not hidden at all, and completely ontological; therefore we call our variable "COV", standing for "Classical Ontological Variable." The letter L is omitted, since locality may not be guaranteed, and anyway, we do not intend to contradict earlier no-go theorems, but rather search for ways out.[2] Understanding the COV may be an important pathway that could lead us to new insights, perhaps even in model building (Jegerlehner, 2021; 't Hooft, 2022).

The most important part of this paper is Section 2. Here we show how any quantum harmonic oscillator, contains an ontological degree of freedom. Using modern jargon, we observe that the quantum harmonic oscillator is *dual* to a classical particle on a circle.

Questions asked after a talk I presented at the Lindau Meeting, June/July 2024, made me realise that the features discussed below are not very well-known and therefore this short publication may be useful.

2 The harmonic oscillator

In one space-like dimension, consider the Hamiltonian[3] H of an elementary quantum harmonic oscillator in terms of the variables x and p,

$$[x,p]=i\,,\qquad H=\frac{1}{2}\,(p^2+x^2-1). \tag{1}$$

Planck's constant will always be set as $\hbar=1$, and as such it merely relates the units of energy to the units of frequencies. Also the angular frequency ω is set to 1. The operator equations are

$$\frac{\mathrm{d}x}{\mathrm{d}t}=i[H,x]=p\,,\qquad \frac{\mathrm{d}p}{\mathrm{d}t}=i[H,p]=-x. \tag{2}$$

We shall need the annihilation operator a and the creation operator $a^\dagger$, defined by

$$\begin{aligned} a&=\frac{1}{\sqrt{2}}\,(x+ip)\,,\ a^\dagger=\frac{1}{\sqrt{2}}\,(x-ip)\,, && [a,a^\dagger]=1,\\ x&=\frac{1}{\sqrt{2}}\,(a+a^\dagger)\,,\ p=\frac{i}{\sqrt{2}}\,(a^\dagger-a)\,, && [x,p]=i. \end{aligned} \tag{3}$$

(For practical reasons, the signs chosen in our definitions, deviate from the signs chosen in other work). The eigenstates $|n\rangle^E$ of H, and their eigenvalues E_n, are found as usual to obey:

$$H|n\rangle^E=a^\dagger a\,|n\rangle^E=E_n|n\rangle^E\,,\qquad E_n\ =\ n\ =\ 0,1,\cdots \tag{4}$$

This, of course, is a completely standard, quantum mechanical procedure applied to the harmonic oscillator, but now we claim that it is *dually related* to a completely classical model. The classical system we have in mind is *a particle moving on the unit circle*, with fixed velocity $v=1$, and period $=\ 2\pi$. The solution of its e.o.m. is:

$$\varphi(t)=\varphi(0)+t\ \mathrm{mod}\ 2\pi; \tag{5}$$

φ is constrained to the interval $[0\,,\,2\pi)$, where the boundary conditions are periodic.

To make our point, it is important to introduce (temporarily) a large integer N, and a variable $s=0\,,\ldots\,,\ N-1$, discretising the allowed values of φ, as follows:

$$\varphi=2\pi s/N\,,\qquad s=0\,,\ 1\,,\ \cdots\,,\ N-1.$$

This matches with the introduction of small, finite time steps $\delta t=2\pi/N$. The φ states span an N-dimensional vector space $\{|s\rangle^{\mathrm{ont}}\}$, where the superscript "ont" stands for ontological.

The energy eigenstates $|n\rangle^E$, $n=0\,,\ \cdots\ ,\ N-1$, of this rotating particle are superpositions of the ontological states:

$$|n\rangle^E=\frac{1}{\sqrt{N}}\sum_{s=0}^{N-1}e^{\frac{2\pi}{N}ins}\,|s\rangle^{\mathrm{ont}}, \tag{6}$$

with the inverse:

$$|s\rangle^{\mathrm{ont}}=\frac{1}{\sqrt{N}}\sum_{n=0}^{N-1}e^{-\frac{2\pi}{N}ins}\,|n\rangle^E. \tag{7}$$

Note that these equations are merely discrete Fourier transformations. By checking the time dependence of $|n\rangle^E$ and $|s\rangle^{\mathrm{ont}}$, we see that

$$\begin{aligned} &|n\rangle^E\,(t)=e^{-int}\,|n\rangle^E\,(0).\\ \text{and}\qquad &|s\rangle^{\mathrm{ont}}\,(t)=|s-t/2\pi N\rangle^{\mathrm{ont}}\,(0). \end{aligned} \tag{8}$$

We now note that the first N energy eigenstates of the harmonic oscillator, Equation 4, obey exactly the same Equation 8, and therefore Equations 6, 7 define N states, obeying (Equation 5). There is an important reason to start with a finite number N. We see that, in these equations, the energy spectrum not only has a lowest energy state, $|0\rangle^E$, but also a highest energy state, $|N-1\rangle^E$. With strictly continuous angular variables $|\varphi\rangle^{\mathrm{ont}}$, we could postulate an energy spectrum running from $-\infty$ to $+\infty$. This would not dually correspond to a harmonic oscillator.[4] In this paper, we keep the lowest energy to be $E=0$, while the highest energy will be unbounded. This enables us to take the limit $N\to\infty$, where we can write:

$$\varphi=2\pi s\Big/N\,,\qquad \mathrm{d}\varphi=\frac{2\pi}{N}\,,\qquad \text{and}\qquad |\varphi\rangle^{\mathrm{ont}}=|s\rangle^{\mathrm{ont}}\Big/\sqrt{\mathrm{d}\varphi};$$

2 Locality is not a meaningful concept for the single harmonic oscillator.

3 For convenience, we set the ground state energy to zero; ground-state energies can be returned whenever this might be needed.

4 At finite N, there is an exact, dual relationship to the $SU(2)$ algebra, with $N=2\ell+1$.

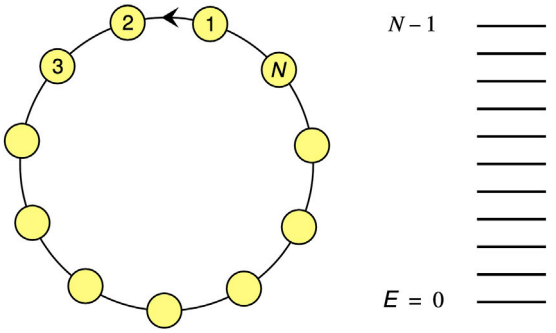

FIGURE 1
The ontological states $|s\rangle^{\rm ont}$ when time is discrete, $\delta t = \frac{2\pi}{N}$. In this picture, the choice $N = 11$ was made. The energy spectrum is shown; the energies form the same sequence as in harmonic oscillators, in particular if we take the limit $N \to \infty$.

This turns Equations 6, 7 into

$$|n\rangle^E = \frac{1}{\sqrt{2\pi}} \oint {\rm d}\varphi\, e^{i\varphi n}\, |\varphi\rangle^{\rm ont}\ , \qquad |\varphi\rangle^{\rm ont} = \frac{1}{\sqrt{2\pi}} \sum_{n=0}^{\infty} e^{-i\varphi n}\, |n\rangle^E .$$

Thus we proved that harmonic oscillators can be described in terms of variables $|\varphi\rangle^{\rm ont}$ that evolve deterministically. It is easy to see that, due to Equation 5, the wave function in terms of the s variable (or the φ variable) does not spread. However, the wave function may not have been chosen to collapse. In that case, the probability distribution $\varrho(\varphi_1) = |\langle\varphi_1|\varphi\rangle^{\rm ont}|^2$ can be seen to rotate along the circle in the same way as φ itself, so that we easily conclude that this probability distribution merely reflects the probabilities of the initial state.

This is a typical feature of the COV in a theory: these variables can be projected on the basis states of any Hilbert space, in which case the theory reproduces the probability distribution of the final states in terms of that of the initial states. It is very important, however, that this identification between Hilbert space and the space of classical probability distributions, only applies to the *ontological basis* of Hilbert space, that is, the basis spanned by all ontological states (the states $|\varphi\rangle^{\rm ont}$ in the case of the harmonic oscillator).

Thus we emphasise: any quantum harmonic oscillator is mathematically equivalent to a periodically moving particle on a unit circle, and the wave function of a quantum harmonic oscillator merely reflects the probability distribution on this circle, if the initial state is not known with infinite precision.

Some useful auxiliary functions are

$$G(z) \equiv \sum_{n=1}^{\infty} \sqrt{n}\, z^n\ , \qquad \text{and} \qquad g(\varphi) = G(e^{i\varphi}). \tag{9}$$

Since the annihilation operator a, defined in Equation 3 obeys

$$a|n\rangle^E = \sqrt{n}|n-1\rangle^E\ ,$$

we can derive the matrix elements

$${}^{\rm ont}\langle\varphi_1|a|\varphi_2\rangle^{\rm ont} = \frac{1}{2\pi} e^{-i\varphi_1}\, g(\varphi_1 - \varphi_2)\ ,$$

$$\text{and} \qquad {}^{\rm ont}\langle\varphi_1|a^\dagger|\varphi_2\rangle^{\rm ont} = \frac{1}{2\pi} e^{i\varphi_2}\ \ g(\varphi_1 - \varphi_2)\ ,$$

and from this, using Equation 3, we find the matrix elements of the operators x and p of the original quantum harmonic oscillator, in terms of the basis states $|\varphi\rangle^{\rm ont}$:

$$\langle\varphi_1|x|\varphi_2\rangle = \frac{1}{2\pi\sqrt{2}} \left(e^{-i\varphi_1} + e^{i\varphi_2}\right) g(\varphi_1 - \varphi_2); \tag{10}$$

$$\langle\varphi_1|p|\varphi_2\rangle = \frac{i}{2\pi\sqrt{2}} \left(e^{-i\varphi_1} - e^{i\varphi_2}\right) g(\varphi_1 - \varphi_2). \tag{11}$$

It is possible to combine N oscillators with different frequencies ω_i, requiring us to generalise Equations 1–4 as

$$H = \sum_{i=i}^{N} H_i\ ; \qquad H_i = \frac{1}{2}\left(\omega_i^2 x_i^2 + p_i^2 - \omega_i\right) \ = \ \omega_i a^\dagger{}_i a_i\ ,$$

$$a_i = \frac{1}{\sqrt{2}}\left(\omega_i^{1/2}\, x + i\omega_i^{-1/2}\, p\right)\ ,$$

$$E_n^i = n_i\, \omega_i.$$

This system of N quantum harmonic oscillators, gives us N variables of the COV type,

$$\varphi_i(t) = \varphi_i(0) + \omega_i t \mod 2\pi\ . \qquad \text{etc.}$$

Ideas of treating quantized field theories as systems in a box with periodic boundary conditions were investigated by Dolce (2023). The wave equation then fixes the timelike component of the periodicities, and systems of this kind may then be regarded as multiple systems of COV variables.

3 On the analytic structure of the auxiliary function $G(z)$

The auxiliary function $G(z)$ is defined by Equation 9, but this only converges for values of z within the unit circle, that is, $|z| < 1$. Also, *on* the unit circle, this definition seems to diverge. Usually, expansions that oscillate wildly at some distance from the origin, can be defined by slightly smearing the coefficients, but here, this procedure is tricky. Indeed, the mathematics needed to show that the probabilities generated by applying $g(\varphi)$ are uniquely defined and real, is rather delicate, an understatement, as shown in this section.

This section is intended only for mathematically minded readers. Their comments would be appreciated.

At finite N the function

$$G_N(z) = \sum_{n=1}^{N} \sqrt{n}\, z^n \tag{12}$$

has N zeros. Most of these will be close to the unit circle, $|z|_n \to 1$. The questions we would like to see answered are:

1. What will be the analytic structure of Equation 12 in the limit $N \to \infty$?
2. Is it possible at all to define and compute an analytic continuation for the function G_N for $|z| > 1$?
3. Where are the zeros and the poles of this analytic function?
4. Can one prove that

$$G^*(z) \stackrel{?}{=} G(z^*)\ , \tag{13}$$

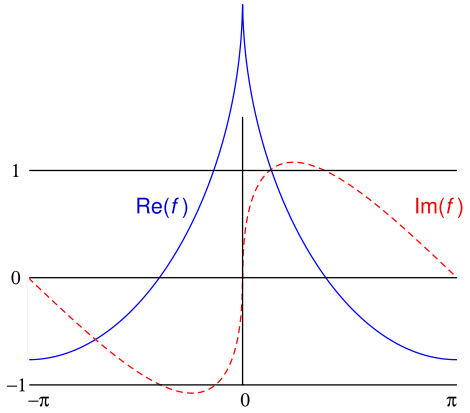

FIGURE 2
An accurate calculation of the function $f(\varphi)$, defined in Equation 14. Blue solid line: its real part, dashed red line: its imaginary part. Both real part and imaginary part have a divergence in their first and second derivatives, apparently only at the origin, $\varphi \to 0$.

so that the operators x and p defined in Equations 10, 11 can be seen to be Hermitian?

The last question is not quite trivial because one must first redefine the limit function $g(\varphi)$, but by careful study of the equations, we found that Equation 13 is true, due to the fact that the coefficients $\sqrt{n}$ are all real, see Figure 2.

First, we find that $G(z)$ is the second derivative of a function $F(z)$ that stays strictly finite on the unit circle (where $|z| = 1$):

$$G(z) = (z\partial_z)^2 F(z)\ , \quad F(z) = \sum_{n=1}^{\infty} z^n \Big/ (n\sqrt{n})\ ;$$
$$g(\varphi) = \frac{-\partial^2}{\partial\varphi^2} f(\varphi)\ , \quad f(\varphi) = F(e^{i\varphi})\ . \tag{14}$$

Therefore, $F(z)$ is also accurately defined *on* the unit circle, but before using it to recuperate $G(z)$, one must carefully choose the order of the limits $N \to \infty$ and $|z| \to 1$. In practice, one encounters no problems, see Figure 2. A useful transformation may be the following:

$$y = \frac{4z}{(1+z)^2}\ , \tag{15}$$

and its inverse:

$$z = -1 + \frac{2}{y}\left(1 - \sqrt{1-y}\right) \ = \ \frac{1}{4}y + \frac{1}{8}y^2 + \ \cdots . \tag{16}$$

This can also be written as

$$\sqrt{y} = \frac{2}{\sqrt{z} \ + \ 1/\sqrt{z}}\ . \tag{17}$$

The second Riemann sheet describes the solution with the opposite sign of the square root on Equation 16. There, we get the solution

$$\tilde{z} = -1 + \frac{2}{y}\left(1 + \sqrt{1-y}\right) = 1/z\ ,$$

which is easiest to see in Equation 17.

$$G_N(z) = \sum_{n=1}^{N} \sqrt{n}\ \tilde{z}^n = \sum_{n=1}^{N} \sqrt{n}\, z^{-n}\ ;$$

Figure 3 shows how the unit circle (Figure 3A) is mapped on the first Riemann sheet (Figure 3B). by the function (Equation 15), and how the branch cut at the right connects the two sheets. The function $G(z)$ does go to infinity where the branch cut begins; the function F stays finite. They are related through Equation 14. By using Cauchy's theorem one may be able to use this branch cut to define faster converging nexpressions for the function $f(\varphi)$, and with that, our auxiliary function $g(\varphi)$. Our attempts to use these observations for obtaining more convergent expressions for $G(z)$ were however unsuccessful; much more work must be done to realise this, but an excessive list of calculations on this matter was not the aim of this paper. The function $G(z)$ does go to infinity where the branch cut begins; the function F stays finite. They are related through Equation 14. Question (4) is now obviously answered in the positive.

4 Epilogue

We showed how one may consider the quantum harmonic oscillator as an ontological theory in disguise. This is important since it appears to contradict theorems claiming that such a behaviour in quantum theories is impossible. Of course those theories were assumed to be far more general than a single harmonic oscillator, or even a simple collection of harmonic oscillators, but this now is a question of principle. Where is the dividing line? Which other quantum systems allow for the definition of COV variables, variables that commute with themselves and others at all times? If for instance one considers the quantum field theory of bosonic free particles in a box of an arbitrary shape in multiple dimensions, one may observe that this is merely a collection of harmonic oscillators.

One would be tempted to conclude that, therefore, bosonic particles in a box should also contain COV states ('t Hooft, 2023), but there is a complication in such systems: it is not easy to restore locality in the COV, since they are defined in momentum space. Turning these into variables that are local in position space appears not to be impossible, but then there is another complication: the operators one obtains that way seem to violate Lorentz invariance. This happens since the box is not Lorentz invariant. It is conceivably possible to restore Lorentz invariance, but we presently do not know how to do this in the Standard Model.

Thus our observations do not imply that text books on quantum mechanics have to be rewritten, except where they state explicitly that classical ontological variables cannot exist. Are *local* ontological variables forbidden? Locality is a meaningless concept in a single quantum harmonic oscillator. In this paper we show exactly what an ontological variable *is*. Emphatically, the ontological variable may be assumed to have a probability distribution as in quantum mechanics *and* in classical theories:

> All uncertainties in the final state merely reflect the uncertainties in the initial state.

As soon as we claim that the initial state is exactly given, the wave function of the final state will collapse. *The harmonic oscillator requires no special axiom for the collapse of the wave function* – provided that we stick to the observables in φ space.

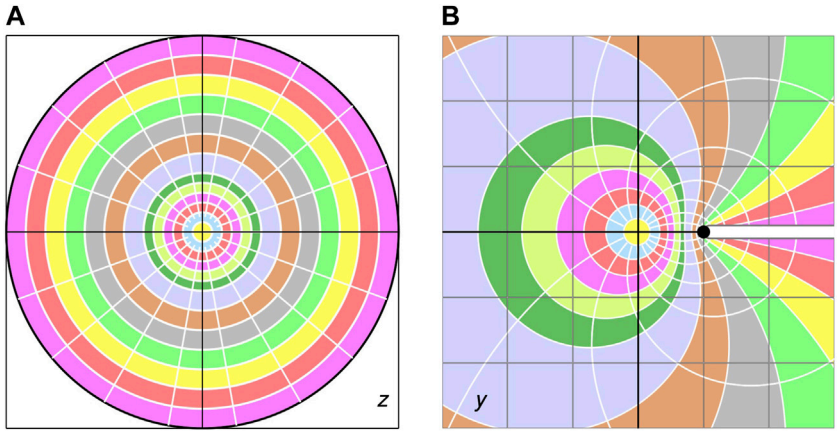

FIGURE 3
(A) y space, regions where the function $G(z)$ converges: domains $|z| \leq .05, .1, \ldots, 1.0$ are shown. **(B)** After the transformation (Equation 15), these domains turn into the regions shown here, that is, the entire z plane up to the branch cut, will be singularity free if expressed in the new y variable.

There, we do not need to assume the existence of many universes. Just one universe, ours, is all we need to understand.

We emphasise that what we found here as a modification of the usual picture of quantum mechanics, is presumably merely the tip of an iceberg. It will not only apply to pure harmonic quantum oscillators, but also to many systems that evolve and interact in more generic ways. It is the fact that harmonic oscillators are periodic that counts. Whenever we consider a simplified model of nature where variables become periodic (for instance if we consider a box with periodic boundary conditions), one may observe that the energy spectrum consists of regular sequences of spectral lines (see Figure 1), so that harmonically oscillating fields enter the picture. Time-periodic motion is always classical. All we then need to talk about is how the probability distributions evolve.

In all classical systems, probability distributions evolve in the same orbits as the classical variables do. Consequently: *probability in = probability out*. If, in φ space, the initial state is defined with infinite precision, the final state will also be infinitely precise. This implies that the "typically quantum feature" of the collapse of the wave function, has its counter part in ontological theories. In the model we presented, the variables φ may be assumed to be infinitely sharply defined, but then also the final states will still be completely sharply defined; they always come in a collapsed form.

The clash with usual findings concerning the "impossible" physical reality of quantum mechanical phenomena and calculations, lies in the fact that the duality transformation is only applicable in *one* basis of Hilbert space: the one consisting of the ontological states. Choosing the conventional basis elements does not modify the results. The fact that we wish to emphasise is that, this "ontological" basis also never needs to be departed from, other than in approximative calculations: both the initial states and the final, observed states of any quantum process will be totally determined by the probabilities in the genuinely ontological basis; therefore, other choices of basis will never be necessary from a strictly logical viewpoint.

And it seems as if this possibility has never been considered before; however, see Refs Brans (1988) and Vervoort (2013). As for the numerous "quantum paradoxes" that have been formulated in the literature, the procedure needed, to formulate the probability patterns in an ontological basis has been worked out in Ref. Hooft et al. (2021). The guiding principle: always stay in the ontological basis.

The author benefitted from many discussions, notably with T. Palmer, C. Wetterich, M. Welling and D. Dolce.

Data availability statement

The original contributions presented in the study are included in the article/supplementary material, further inquiries can be directed to the corresponding author.

Author contributions

G'tH: Writing–review and editing, Writing–original draft.

Funding

The author(s) declare that no financial support was received for the research, authorship, and/or publication of this article.

Conflict of interest

The author declares that the research was conducted in the absence of any commercial or financial relationships that could be construed as a potential conflict of interest.

Generative AI statement

The author(s) declare that no Generative AI was used in the creation of this manuscript.

Publisher's note

References

Bell, J. S. (1964). On the Einstein-Podolsky-Rosen paradox. *Physics* 1, 195–200. doi:10.1103/physicsphysiquefizika.1.195

Bell, J. S. (1982). On the impossible pilot wave. *Found. Phys.* 12, 989–999. doi:10.1007/bf01889272

Bell, J. S. (1987). *Speakable and unspeakable in quantum mechanics*. Cambridge: Cambridge Univ. Press.

Brans, C. H. (1988). Bell's theorem does not eliminate fully causal hidden variables. *Int. J. Theor. Phys.* 27 (2), 219–226. doi:10.1007/bf00670750

Clauser, J. F., Horne, M. A., Shimony, A., and Holt, R. A. (1969). Proposed experiment to test local hidden-variable theories. *Phys. Rev. Lett.* 23 (15), 880–884. doi:10.1103/Phys.Rev.Lett.23.880

Conway, J. H., and Kochen, S. (2008). The strong free will theorem. *arXiv: Quant-Ph* 56 (2), 226.

Dolce, D. (2023). Internal times and how to second-quantize fields by means of periodic boundary conditions. *Ann. Phys.* 457, 169398. doi:10.1016/j.aop.2023.169398

Greenberger, D., Horne, M., Shimony, A., and Zeilinger, A. (1990). Bell's theorem without inequalities. *Am. J. Phys.* 58 (12), 1131–1143. Bibcode:1990AmJPh.58.1131G. doi:10.1119/1.16243

Hooft, G. 't (2021). "Explicit construction of Local Hidden Variables for any quantum theory up to any desired accuracy, arxiv:2103.04335," in: *Quantum mechanics and fundamentality: naturalizing quantum theory between scientific realism and ontological indeterminacy*, Springer Nature, chapt. 13, V. Allori ed arxiv:2103.04335[quant-ph].

Jegerlehner, F. (2021). The Standard Model of particle physics as a conspiracy theory and the possible role of the Higgs boson in the evolution of the Early Universe. *Acta Phys. Pol. B* 52, 575. doi:10.5506/aphyspolb.52.575

't Hooft, G. (2023). An ontological description for relativistic, massive bosons. doi:10.48550/arXiv.2306.09885(quant-ph)09885

't Hooft, G. (2022). Projecting local and global symmetries to the Planck scale, dedicated to Prof. Chen Ning Yang at the occasion of his 100th birthday. *ArXiv*. Available at: http://arxiv.org/abs/2202.05367 (Accessed February 2022).

't Hooft, G. (2016). "The cellular automaton interpretation of quantum mechanics," in *Fundamental theories of physics* (Springer International Publishing), 185. eBook ISBN 978-3-319-41285-6, Hardcover ISBN 978-3- 319-41284-9, Series ISSN 0168-1222, Edition Number 1. doi:10.1007/978-3-319-41285-6

Vervoort, L. (2013). Bell's theorem: two neglected solutions. *Found. Phys.* 43, 769–791. doi:10.1007/s10701-013-9715-7

frontiers | Frontiers in Quantum Science and Technology

TYPE Original Research
PUBLISHED 27 March 2025
DOI 10.3389/frqst.2025.1542466

OPEN ACCESS

EDITED BY
Luca Lepori,
QSTAR, Italy

REVIEWED BY
Andrei Khrennikov,
Linnaeus University, Sweden
Gerard 't Hooft,
Utrecht University, Netherlands
Bengt Norden,
Chalmers University of Technology, Sweden

*CORRESPONDENCE
Jürgen Jakumeit,
jakumeit@uni-koeln.de

RECEIVED 09 December 2024
ACCEPTED 19 March 2025
PUBLISHED 27 March 2025

CITATION
Hess K and Jakumeit J (2025) Explicit mathematical models of multiple polarization-measurements and the Einstein-Bohr debate. *Front. Quantum Sci. Technol.* 4:1542466. doi: 10.3389/frqst.2025.1542466

Explicit mathematical models of multiple polarization-measurements and the Einstein-Bohr debate

Karl Hess[1] and Jürgen Jakumeit[2]*

[1]Center for Advanced Study, University of Illinois, Urbana, IL, United States, [2]Institute of Physics II, University of Cologne, Cologne, Germany

We present mathematical models that also may be formulated as computer models for experiments that feature single photon resolution and multiple pairs of polarizers to determine the sorting into ordinary and extraordinary channels. The models are based on Einstein's hypothesis of elements of physical reality that determine the photon properties and are at first developed for Malus-type experiments. It is then shown that analogous models apply to the well-known Clauser-Aspect-Zeilinger experiments and violate all Bell-type inequalities without violating Einstein's separation principle. The Bell-type inequalities do not apply to the actual experiments, because they cannot obey the physically necessary symmetry with respect to polarizer-pair rotations. We believe that these findings suggest a change of current interpretations of quantum entanglement away from instantaneous influences at a distance, as promoted in the physics Nobel-lectures 2022, and back toward Einstein's ideas as well as the more recent ideas of Gerard 't Hooft.

KEYWORDS

Bell-inequalities, CHSH-inequalities, quantum-entanglement, EPR-experiments, Monte-Carlo simulation

1 Introduction

The well-known debate between Einstein and Bohr can be summarized by the slogan "relativity versus probability". Bohr maintained that, with respect to quanta, probability was a fundamental feature of nature and Pauli explained that in contrast to Bohr ". . . Einstein . . . considered quantum mechanics to be something like statistical gas theory . . . " Einstein resisted indeed the Born-type probability theories that are defined without the involvement of elements of physical reality. At first glance, the differences of the two views appear minor. Probability theorists assume that Tyche, the goddess of fortune choses elements ω of the sample space Ω and a particular ω_{act} that determines the outcome of the measurement of the moment. Einstein in essence insists that in physical experiments we need to deal with physical properties $\lambda \in \Lambda$ and with corresponding λ_{act} that provide the related ω_{act} with a physical meaning. However, Bohr and his school pointed to the fact that the possible physical properties of quanta that determine the actual events, such as the complementary values of location and velocity, cannot even exist before the moment of measurement, owing to the Uncertainty Principle.

It took Einstein years to produce an incisive response to Bohr and the teachings of the Copenhagen school. With Podolsky and Rosen he formulated a manuscript (now called the EPR paper (Einstein et al., 1935)) that offered a possibility to determine complementary

properties of the quanta as follows: create pairs of quanta that are correlated by physical law. Then, if you measure the velocity of one piece of the pair you may deduce the velocity of the other from the physical law. Measuring the position of the other piece gives you, therefore, both properties. The Uncertainty Principle is not violated, because only one measurement is performed on each quantum, to obtain both complementary properties. We may, thus, believe that Tyche's choices also represent elements of physical reality.

The actually performed first direct experiments related to EPR were a variation of a suggestion of Bohm: Kocher and Commins (Kocher and Commins, 1967) used measurements involving photon pairs and the concept of polarization. Judging from their results, Einstein's ideas appeared to be possible. Kocher and Commins found excellent experimental correlations (entanglement) for equal polarizer angles that could be seen as representing a law of nature for the photon-pairs and the corresponding existence of properties.

However, the well-known inequality of J. S. Bell (Bell, 1964) has led to a different explanation of the photon-pair experiments. Note that Bell's original theory was describing spin $\frac{1}{2}$ quantum entities and Stern-Gerlach measurements. His work and its important logical implications concerning such experiments, may be "translated" for photon (spin 1) related experiments by simply including a factor of two in the pertinent equations, which we have done below. We may then imagine that Bell's work has considered experimental sequences, each having different polarizer directions and maintained that the average measurement outcomes must fulfill an inequality. Strangely enough, this inequality was not obeyed by the results of quantum mechanics. It also was convincingly shown by numerous groups related to the 2022 Nobel Laureates Clauser, Aspect and Zeilinger that the actual experiments also contradicted the inequality of Bell and a similar inequality derived by Clauser, Horn Shimony and Holt (CHSH) (Clauser et al., 1969). We assume at this point that the reader is familiar with Bell-CHSH-type inequalities. We will, however, include below a fairly detailed description of the CHSH inequality and its derivations.

The crucial question is why Bell's model does not agree with quantum theory. Bell had an answer to this question. He was convinced that he, CHSH and others had derived the inequalities more or less exclusively based on Einstein's physics and in particular Einstein's separation principle and corresponding "local" properties of physical events (following from the limitations of all velocities to a maximum of the speed of light in vacuum). The violation of their inequalities indicated to Bell and CHSH that a special interpretation of the photon correlation (entanglement) that included "non-local" effects must be in order. As we will show, it is important to distinguish between different forms of "non-localities", in order to understand what indeed the Bell-CHSH inequalities mean. The form that Einstein objected to was any instantaneous influences at a distance, such as a measurement in Tokyo influencing instantly the outcome of a measurement in New York. In contrast to this particular non-locality that Einstein called "spooky", there are physically natural (at least to Einstein) non-localities. For example, any properly relativistic model requires the theoretician's consideration of physical events relative to each other and involves, if these events are spatially separated, non-local theoretical considerations to start with. Such a non-locality may, however, retrospectively be explained without instantaneous influences by use of a space-time system. It is important to distinguish between the permitted global thinking of a theoretician using a space-time system and inappropriate introductions of instantaneous non-local occurrences. These subtle problems related to the physical nature of non-localities are enhanced by the mathematical complications of set theoretic probability that must be the basis of the derivation of the Bell-CHSH inequalities.

We highlight these problems and questions by detailed mathematical- and computer-models for two types of experiments: the Malus-type as explained in the Feynman lectures (Feynman Lectures, 1965) and the EPRB-type, including the experiments of Kocher and Commins (Kocher and Commins, 1967), of Aspect and coworkers (Aspect, 2015) and of Kwiat (Kwiat et al., 1999) and coworkers. Before doing so, however, we discuss what we mean by words like "local" or "measurement" etc. and how to avoid prejudicial conclusions about them.

2 Definitions and prejudices in discussions related to the Bell-CHSH inequalities

Concepts often involved when discussing Bell-CHSH, are those of entanglement, measurement, experiment, local vs. non-local, as well as deterministic vs. probabilistic. We also use these terms but only subject to the following considerations:

It is commonly claimed and believed that the Bell-CHSH inequalities must be valid within Einstein's framework and definitions of physical principles. We put our main emphasis on the refutation of this important point and, therefore, do not involve concepts of quantum mechanics other than those pioneered by Einstein.

As a consequence, we never use any contemporary quantum mechanical meaning of the word "measurement". What we mean by measurement follows from the most elementary explanations such as "a detector clicks", or in another situation "a detector clicks after a photon has passed a polarizer". We agree with the standard definition found on Internet-dictionaries: "Measurement is the quantification of attributes for an object or event, which can be used to compare with other objects and events." It nicely encompasses the importance of the relative comparison of attributes and events. With the expression "experiment" we also refer to the dictionary meaning of "a scientific procedure undertaken to make a discovery, test a hypothesis, or demonstrate a known fact".

When we talk about entanglement, we do mean something related to the quantum-entanglement as defined already by Schrödinger. In our present utilization of the word, we only refer to some basic correlation and hope that a future more detailed interpretation will benefit from our contributions to an understanding of the work of Bell-CHSH.

The concepts of "local" and "deterministic" appear in a vast Bell-CHSH-related literature, often with different meaning. We believe that what is acceptable as "local theory" spans a wide range that is not necessarily accepted by the followers of Bell-CHSH. For example, Einstein's relativity teaches about measurement outcomes relative to each other. If these outcomes have a space-

like distance, then naturally any relativistic thought-process of a theoretician involves non-local factors, as already mentioned. Yet, there are not many physicists who would think of such relativistic thinking as something that is physically undesirable or even forbidden. We, therefore, have limited ourselves to talk about "local" and "non-local" only in connection with specific experiments and measurements that we model also by computers to illustrate the non-local thought processes versus the local causal machinery that mother nature uses (according to Einstein) in a given measurement station.

We dismiss out of hand all definitions of "local" and "deterministic" that use certain conditional probabilities: Bell and followers have frequently used probabilities conditional to one particular element of physical reality (Gisin, 2012). Because the elements of physical reality may involve continua (distances, times, etc.), the Lebesgue measure of the probability that such a particular element of physical reality is actually encountered may be zero. Consequently, such a conditional probability cannot sensibly be defined within the confines of set theory (for additional explanations and problems see (Hess, 2023)).

Regarding the concepts of "deterministic vs. probabilistic", we also adhere to the common-sense definition that: "Deterministic models produce the same exact outcome for any given exact same set of inputs, while probabilistic models do not." However, we have to be cautious with this definition in the following respect. Bell's model contains the symbols of Einstein's elements of physical reality that may be randomly selected out of a continuum and may be modeled, as we will do below, by random real numbers out of the interval [-1, +1]. The subtle point is now that one may not be permitted to use the same real number again for different model-events. While it may be true then that we have the same exact outcome for the same exact input, the probability to encounter the same exact input may be zero. Such a model is, therefore, comparable to models of radioactive decay and must be seen as probabilistic. The consequences of this fact for the interpretation of experiments related to Bell-CHSH were discussed in (Jakumeit and Hess, 2024). Bell's model is, therefore, probabilistic depending on the nature of his variable λ, particularly whenever λ is used just like the general ω of probability theory (as used by many researchers).

We like furthermore to point to the fallacies of the very common Alice and Bob reasoning regarding locality considerations. Alice controls one polarizer angle without knowing anything about Bob, who controls the other polarizer angle. The confusion of the Alice-Bob stories arises from the fact that Alice and Bob are seen as somehow representing mother nature, who must, according to Einstein's views, indeed be local causal. That does not mean however that a theoretician, say Charly, does not know global macroscopic instrument arrangements and designs the local causation of his model by using his global knowledge and the space-time system. For the particular case of EPRB experiments, Charly must know about the ancient principle that events may only be evaluated relative to each other, which Alice and Bob cannot accomplish to start with, because they do not know about each other. Without global physical laws and a space-time system, even the correlation of clocks in distant cities becomes a mystery.

We ask the reader not to abandon our reasoning, because of prejudices regarding the use and meaning of the discussed important terms.

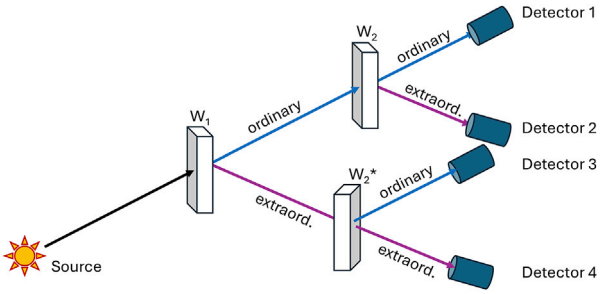

FIGURE 1
Experimental arrangement for single-photon Malus-type experiments. The polarizer is represented by Wollaston prism W_1 and the analyzers by W_2 and W_2^*, respectively.

We also like to point toward other important criticisms involving views more or less different to ours presented here. In particular, the concept of "contextuality" has been used in a number of ways to discuss violations of the Bell-CHSH inequalities. We do not use the loaded word "contextual" at all but only talk about "events being evaluated relative to each other". Of course, in the case of spatially distant experiments relative evaluation encompasses a lot of the meaning of "contextuality". Numerous important works have discussed related violations of Bell-CHSH. Particularly relevant points have been presented in the works of Khrennikov (2009) (see also the well-known Växjö conferences) and Kupczynski (2020) as well as references in their works.

3 Malus-type experiments for single photons with sequential polarizers

3.1 Geometry and measurement-outcomes of the Malus-type experiments

Perhaps the most illuminating experiment, at least with respect to modeling and the Alice-Bob "locality" assumptions by Bell and followers, is the standard Malus-type experiment performed with single photon resolution. Consider two special polarizers, Wollaston prisms, in sequence to the right of a single-photon source S (Wollaston prisms permit a clearer formulation of the arguments, although they have not necessarily been used in all actual experiments). The photons propagate in z- direction and are sorted by the Wollaston prisms into two sets one named ordinary Λ_o and the other extraordinary Λ_e. The properties of these sets depend, in general, on the geometric configuration of the Wollaston prisms. We characterize this configuration throughout this paper by an angle in the x, y plane denoted by the variable $j = a, a', \ldots$ for the primary Wollaston W_1 and by $j' = b, b', \ldots$ for any secondary Wollaston W_2.

Assume now that the source S emanates N photons that behave in the following way. Passing W_1 with a given configuration angle, for example, $j = a$, leads to the sorting of about $\frac{N}{2}$ photons into the ordinary set that we denote now by Λ_o^a and about $\frac{N}{2}$ photons into the extraordinary Λ_e^a . We cannot deduce from such measurements more than the fact that Wollaston prisms, no matter how

configured, lead to binary sorting that may be influenced by the given polarizer direction (angle). This angle is just defined within our rather arbitrary global coordinate system and, therefore, single photon measurements performed with a single polarizer, have only limited significance for distant correlations.

Sequential measurements with two additional Wollaston prisms W_2 and W_2^* (called analyzers), do give us more interesting information. W_2 is arranged to pick up the ordinary channel of W_1 and deals, thus, with the set Λ_o^j, while W_2^* deals with the extraordinary channel of W_1 and the set Λ_e^j. We have illustrated the geometry of the Wollaston prisms including the source S in Figure 1. Note that one cannot have both W_2 and W_2^* precisely perpendicular to the z-axis with their face in the x-y plane, but it is well known how to experimentally approximate this situation and we just assume for the mathematical model that all Wollaston prisms are perpendicular to the z-axis, which is the direction of the photon propagation. The Wollaston's rotation-angle is in the x-y plane starting with zero in the x-direction.

The two sets Λ_o^j and Λ_e^j are now analyzed by Wollaston prisms W_2 and W_2^* that sort these sets into the sets $\Lambda_o^{j,j'}$, $\Lambda_e^{j,j'}$ and $\Lambda_o^{*j,j'}$, $\Lambda_e^{*j,j'}$, respectively.

Einstein's hypothesis is that the photons of these sets have certain properties. We denote these properties of the photons that are contained in the various sets above by the lower-case symbols: $\lambda_o^{j,j'}$, $\lambda_e^{j,j'}$, $\lambda_o^{*j,j'}$ and $\lambda_e^{*j,j'}$ and take them as the basis for our Einstein-type model. This second (relative) sorting follows a law of nature, known for very large numbers $\frac{N}{2}$ of photons as the law of Malus and states:

Of all the photons that transfer into the ordinary channel of W_1, an approximate number of

$$\frac{N}{2}\cos^2(j-j')$$

photons will transfer into the ordinary channel of W_2 for large N. The numbers found in the extraordinary channel of W_2^* follow the same law. As is evident, this law is invariant to rotations of the coordinate system as well as the rotation of the Wollaston prisms around the z-axis. Therefore, we may choose $j = 0$, without restriction of generality, put $j - j' = \theta$ and obtain in this way the Malus law in its usual notation:

$$\frac{N}{2}\cos^2(\theta)$$

The connection of the corresponding expressions in terms of the energy of macroscopic electromagnetic fields (instead of large numbers of photons), has been described in detail in introductory texts and also has been shown to be fully consistent with the laws of quantum mechanics (Feynman Lectures, 1965; Baym, 1973).

In order to provide an Einstein type model for the single photon Malus law we need to develop a model that is in principle described by a set theoretic probability theory that features events ω_{act} that also have a meaning as Einstein's elements of physical reality λ_{act}. We further need to link this element of physical reality to the measurement outcomes for the events of the photons interacting with the Wollaston prisms. This link may be achieved as follows.

3.2 Set theoretic mathematical model for the Malus-type experiments

It has been shown in great detail by David Williams in his textbook on probability theory (Williams, 2001) that experiments describing the possible machineries of our surrounding macroscopic world by using probabilities may be modeled by the set theoretically precise Fundamental Model of Probability Theory. The patient reader must remember that set-theoretic mathematics deals with a "fundamental triple" that includes a sample space Ω, a sigma algebra of subsets of Ω and a unique probability measure P.

The Fundamental Model of probability theory uses the interval $[0,+1]$ of the real numbers for Ω. Every event of actual measurements may be simulated by a real number out of this interval. The events are, as usual, denoted by $\omega \in \Omega$. As mentioned, Tyche, the goddess of fortune, picks one such ω denoted by ω_{act} to instigate a certain actual event. For ω_{act} drawn uniformly from the interval [0,1] the probability that ω_{act} lies in a sub-interval $[0,x]$ is given by x (Williams, 2001).

To simulate the actual polarizer experiments by involving real numbers for the photon properties, it is convenient (as we will see below) to generalize the Fundamental model to include the extended interval $[-1,+1]$ instead of $[0,+1]$, which is straightforward. We introduce now the notation and conventions similar to Bell and denote the measurement outcomes by two-valued functions, A for polarizer W_1 and B for polarizers W_2 as well as W_2^*. We define $A = B = +1$ if the photon is found always in the ordinary channel and $A = B = -1$, if it is always found in the extraordinary channel. Our main postulate is that one can indeed model the photon properties for the particular experiment in question by the real numbers of the Fundamental model. The possibility of mapping the elements of physical reality onto the real interval $[-1,+1]$ is indeed a plausible assumption, because we consider only relative outcomes. For a given polarizer angle j, we may then sort the outcomes of A into two sets that depend only on the sign of the number that models the properties of the photon, because we know that the polarizer accomplishes just such sorting, hereby connecting these sets to the polarizer direction within our arbitrarily chosen coordinate system.

The sorting of the analyzers W_2 and W_2^* into ordinary and extraordinary sets can then be further modeled as follows: the photon stays with the same sorting that W_1 has accomplished (extraordinary or ordinary), meaning $B = A$ if and only if:

$$\left|\lambda_{e,o}^j\right| \le \cos^2(\theta). \tag{1}$$

According to the Fundamental Model, the probability measure that we indeed encounter such $|\lambda_{e,o}^j|$ equals precisely $\cos^2(\theta)$, which leads to the law of Malus-type for large N. The absolute value is now used because we have extended the Fundamental interval to $[-1,+1]$.

Notice that the use of the relative polarizer angles θ in Equation 1 appears completely natural, because the photon has passed both polarizers and may be sorted into the appropriate sets due to its properties that are recognized by both polarizers. No "forbidden" non-locality has ever been attributed to the use of $(j' - j = \theta)$ for that particular experiment in contrast to the EPRB-type experiments. We

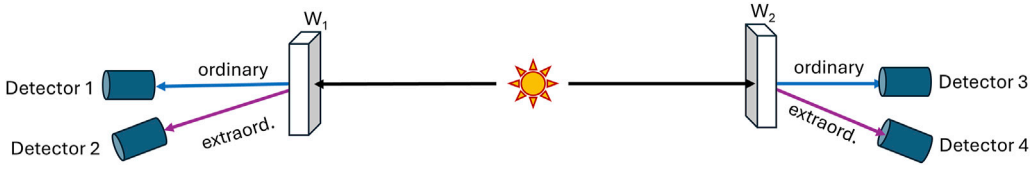

FIGURE 2
Experimental arrangement for entangled-photon for EPRB-Kocher-Commins-type experiments.

note in passing that mathematically there exists almost no difference between this Malus-type experiment and the EPRB-type as soon as Einstein's hypothesis of elements of physical reality is made. One of the reasons for this fact is that we do not need to assume that the Wollaston polarizers change the properties of the photons. It is sufficient to assume that the photon properties are recognized by the polarizers and used for the sorting. In this connection it is important to realize the difference between the properties described by λ immediately after the emission of the photons and the properties (actual or model) that mark the photons and λ after passing the polarizers. It is these properties that may be represented by markers related to the law of nature that determines the outcomes. We will return to this important point below.

4 Polarizers on opposite sides of a source

We now turn to the configuration with the polarizers on opposite sides of the source as illustrated in Figure 2, which shows the experimental arrangement along the lines of the EPR ideas with the modifications by Bohm and first implementation using photon-pairs and a stretched film of poly-vinyl alcohol containing oriented anisotropic molecules instead of a Wollaston prism, by Kocher and Commins (Kocher and Commins, 1967).

Unlike the Malus-type single-photon experiment, this experiment has been performed by many researchers starting with Kocher and Commins and continuing with significant extensions by groups around Clauser et al. (1969), Aspect (2015), Giustina et al. (2015), Kwiat et al. (1999) and others.

We use the same notation that we have used in the previous section, in order to highlight the important similarities and differences with respect to the modeling of the Malus-type. Wollaston W_1 is now arranged to the left of the source S and Wollaston W_2 to the right as shown in Figure 2. Wollaston W_2^* is being merged with W_2.

The source emanates now correlated photon-pairs (see explanations by Kocher and Commins (1967)). We assume in the following theoretical discussions that the correlation of the photon-pair is ideal and such that each photon is being recognized according to its properties in identical fashion by W_1 and W_2. In other words, the photons are identical twins as viewed with W_1 or W_2.

As for the case of the Malus-type experiments, we need to maintain the principle that the measurements of events have only physical meaning relative to each other. Alice and Bob, knowing nothing about each other, may only judge their local measurements relative to their own previous measurements and thus conclude that the clicks of their detectors are random, corresponding to the detections for ordinary and extraordinary channels of W_1 and W_2, respectively. If we wish to probe into the distant relative measurement-outcomes, we need to employ a theoretician, Charly, who must involve global factors into his thinking, while still admitting only local causes for the interactions and measurement-outcomes on a given side. As Einstein told Heisenberg: "it is the theory that determines what we can measure" and it is historically true that great experimentalists have also had a deep grasp of theory and *vice versa*.

Therefore, if we wish to proceed to the understanding of the non-local distant correlations, we need to clearly distinguish on one hand between the theoretical knowledge that Charly must have about the global situation and on the other hand the local causality that must apply according to Einstein for the events in the respective stations.

The natural local interactions involve the polarizer angles j and j' at the time of interaction, which is measured by local synchronized clocks. Charly describes the local configurations by use of his global coordinate system. Therefore, the local configurations of the polarizers at the time t_n^1 for polarizer W_1 and t_n^2 for polarizer W_2 may both assumed to be available to Charly within the space-time system, while Nature has available just the single local configurations. Charly, of course, can only find out later what the actual polarizer configurations were, by checking the records of measurement at the registered clock-times.

Note, that the experimenters must, as Charly does, involve more than their local knowledge of equipment configurations if they wish to consider relative outcomes. They too must have a global coordinate system and synchronized clocks (a space-time system), whenever they attempt to compare the outcomes A, B and determine whether $A = B$ (Aspect, 2015). They also have worked with fixed polarizers and without clocks during the whole sequence of measurements (see, for example, some of the measurements in (Kwiat et al., 1999)).

What is it then that can be measured, while the global rules of relative evaluation as well as the rules of local causes are strictly obeyed? Consider the case of registered detector clicks $A = \pm 1$ and $B = \pm 1$. Relatively speaking, we have then four possibilities of interesting physical outcomes and we collapse them by symmetry onto two: we either have $A = B$ or $A \neq B$. All relative physics must, therefore, be contained in the numbers of equal versus not-equal outcomes of the experimental runs. Importantly, it turns out that the results of $A = B$ vs $A \neq B$ are also the only results used to obtain the Bell-CHSH inequalities. Charly needs to model, therefore, only the number N_{eq} of equal outcomes $A = B$ that contains all interesting

physics. The number of not equal outcomes N_{neq} is given by $N_{neq} = N - N_{eq}$. Thus, Charly is not interested in modeling natures outcomes for A and B separately but is satisfied to obtain a correct model for the product $A \cdot B$, which also happens to be all that Bell-CHSH have needed and used in their work.

We now apply the methods that we have developed for the Malus-type experiment in the previous section: W_1 is thought to establish the connection of the actual experiment to the global coordinate system and sorts the incoming photon of the pair into two sets, while W_2 analyzes the incoming twin-photon corresponding to its properties and "markers" that are for all practical purposes assumed identical for the twins. Because we treat W_2 as the analyzer we have a situation which is completely analogous to the Malus-type experiments. To see this fact, imagine the measurement of the W_1 detector to be performed slightly earlier, exactly as it is for the Malus type measurements. This analogy permits us to sorting the identical twins as we did in the Malus-type experiments and as is described next. Of course, we may also exchange the roles of W_1 and W_2. Imagining that the measurement involving W_1 happens before that involving W_2, is only used to illustrate the analogy to the Malus type experiment.

There exists one big difference of the EPRB-type experiments to the Malus-type. For these latter, we could use W_2 and W_2^* to further process the ordinary and extraordinary channels. Without this possibility we must employ very careful procedures that avoid the introduction and appearance of instantaneous distant influences.

We still use Einstein's elements of physical reality that may be imagined as "markers" of the single photons that are the causes for W_1 to guide the incoming photon of the pair toward the +1 or the −1 detector and thus makes it a member of the sets Λ_o^j or Λ_e^j, respectively, after being detected. Note that we must postulate that these sets depend on the angle j, because otherwise the polarizer-geometry would have no influence. We have denoted their elements by λ_o^j or λ_e^j for the Malus-type experiments, but add now an index n for the measurement number in order to obtain the notation of λ_{on}^j or λ_{en}^j, respectively.

In our opinion, this approach synthesizes the views of Einstein and Bohr. The properties of the photons and photon pairs are only known after at least one measurement (with say j = a) was performed, relative to which other measurements are evaluated and analyzed.

We turn now to our model in which all of Einstein's elements of physical reality are simulated by real numbers out of [-1, +1]. Each of the randomly selected numbers signifies different properties and is denoted by λ_n with $n = 1, 2, 3, \ldots, N$. We postulate further that there exists a one-to-one correspondence of the Einsteinian elements (that occur in the actual measurements for a given polarizer angle, e.g., $j = a$) and our model-numbers λ_n. Each λ_n is, therefore being mapped to represent one of the specific elements λ_{on}^j or λ_{en}^j arising from the measurements involving W_1 and belonging to the sets Λ_o^j or Λ_e^j for the selected value $j = a$. The source has sent a twin element toward the analyzer W_2, and that analyzer is being represented by the function $B(j' = b, \lambda_n = \lambda_{on}^{j=a})$. The evaluation of that function may, thus, depend on both $j = a$ and $j' = b$, because both angles appear in the entirely local domain of the function B. The concrete form of the function is not known for certain and may not even exist. Nevertheless, Charly may guess the value of j and base his model on this guess, while validating the model later on when the information about the value of j is available to him (as in the model of (Jakumeit and Hess, 2024)).

Based on all these facts, Charly lets:

$$A(j, \lambda_n) = sign\,(\lambda_n) \tag{2a}$$

and

$$B(j', \lambda_n) = sign(\lambda_n) \text{ if and only if } |\lambda_n| \leq \cos^2(j' - j)$$

in order to model the law of nature that determines the equal and not-equal relative outcomes $(A = B)$.

We do admit that our multiple assumptions, although very plausible, do not let us prove with certainty that quantum-non-localities are not involved in any way. Such proof can probably never be achieved. One simply cannot prove that "spooky" influences (in Einstein's sense) do not exist.

There is just one minor modification necessary in order to fully compare this model with the experiments of Kocher, Clauser, Aspect and others. All these well-known actual experiments use complete anti-correlation instead of correlation. To obtain the results for anti-correlation, we just need to put

$$Bj', \lambda_n = sign(\lambda_n) \tag{2b}$$

If and only if:

$$|\lambda_n| > cos^2(j' - j). \tag{2c}$$

Equations 2a-c permit us to derive the well-known measured averages by our model. For any given polarizer-angle pair (j, j'), we denote the normalized sum of N measurements by $D(j, j')$:

$$D(j, j') = \frac{1}{N}\sum_{n=1}^{N} A(j, \lambda_n)\, B(j', \lambda_n) \tag{3}$$

In the limit of $N \to \infty$, we obtain from expressions (Equations 2a-c) of our model:

$$D(j, j') = -\cos(2(j' - j)) \tag{4}$$

This latter result agrees with the results of quantum mechanics, which appears entirely natural, because it represents in essence a Malus-type law and is very closely connected to the measurement-outcomes for single photon Malus type experiments.

This very result is, however, incompatible with the Bell-CHSH inequalities derived in (Clauser et al., 1969). How can that be? The obvious reason is that Bell-CHSH and followers have used the same measurement number n for different polarizer setting pairs. As long as one considers only one polarizer-angle pair (no matter which), this is correct. However, as soon as one calculates the four sums $D(j, j')$ that are the basis for the Bell-CHSH inequality, one needs to realize that different polarizer-angle pairs must have, in general, a different measurement number. As we show next, this lack of precise mathematical labeling still permits the correct derivation of the Bell-CHSH-type inequalities if (and only if) Einstein's elements of physical reality are countable (see also (Jakumeit and Hess, 2024)). However, just in this very case of countability, the so derived Bell-CHSH inequalities are not invariant under rotations of the polarizers around the z-axis and, therefore, physically speaking, unacceptable

5 Bell-type inequalities as derived in the terms of the Fundamental Model

Bell-CHSH deduced by elementary manipulations that one expects:

$$CHSH =: |D(a,b) - D(a,b') + D(a',b) + D(a',b')| \leq 2 \quad (5)$$

Key to this finding is that they used identical λ_n in all the sums of Equation 3 for all values of (j, j'), meaning for (a,b), (a,b'), (a',b) and (a',b').

Notice that identical λ_n permit the derivation of Equation 5 from Equation 3, because then all $4N$ measurement-outcomes may be described by N quadruples of the form:

$$A(a,\lambda_n)\cdot B(b,\lambda_n) - A(a,\lambda_n)\cdot B(b',\lambda_n) + A(a',\lambda_n)\cdot B(b,\lambda_n) + A(a',\lambda_n)\cdot B(b',\lambda_n) \quad (6)$$

which are now each cyclically connected (with three products known, the fourth is fully determined) and, therefore, all quadruples are equal to +2 or −2. However, for our Fundamental model, the λ_n are represented by real numbers chosen randomly out of $[-1, +1]$. The probability to obtain the same λ_n for any different model-measurement is zero and this applies also to any actual measurement if Einstein's elements of physical reality indeed correspond to a continuum that can be mapped onto (or modeled by) the interval [-1, +1] of real numbers.

As mentioned, Bell-CHSH have deduced their use of the identical λ_n in each of the four sums from the fact that the emitted elements of physical reality may not depend on the polarizer angles, because these may be chosen in the last moment just before the actual measurement and indeed have been so chosen in all Aspect-type (Aspect, 2015) experiments. As mentioned, however, that fact does not mean that the λ_n of Equation 6 must be identical for all polarizer angle pairs. In strict mathematical terms, the λ_n are only identical in approximately all quadruples if their number M is countable (finite) and if the number of measurements $N \gg M$. (We do not include the case of countable infinite into our discussions in spite of the fact that similar situations can be constructed with countable infinite sets such as rational numbers.)

The astounding conundrum of the Bell-CHSH inequalities arose from the conviction of Bell and followers that their derivations followed mostly from Einstein's separation principle. They did not realize that their derivation required additional mathematical conditions regarding the cardinality of Einstein's elements of physical reality and a certain cyclicity of the polarizer angles. They also did not realize that these mathematical conditions have the consequence that the inequalities are physically not acceptable, because they are not invariant under rotations of the polarizer angle-pair around the z-axis. We show these facts in form of two theorems in the following section. We formulate these theorems in terms of the Fundamental Model that we have used all along. It is important to note that the theorems are derived without a direct use of Einstein's separation principle (although it is indirectly guaranteed by the random draws of real numbers). All the above facts and following Theorems are also consistent with Gerard 't Hooft's widely published ideas ('t Hooft, 2020) regarding the Einstein-Bohr debate and his recent additional important findings with regard to "hidden ontological variables" ('t Hooft, 2024).

6 Physical inconsistency of mathematically correct Bell-CHSH inequality: two theorems

6.1 Theorem 1

Given the polarizer geometry of Section 4, a cyclical arrangement of the polarizer angle pairs such as (a,b); (a,b'); (a',b); (a',b') and a mathematical representation of Einstein's elements of physical reality by real numbers of the interval $[-1, +1]$ encompassing two possible cases: (i) Each real number of the interval $[-1, +1]$ represents an element of physical reality, which is drawn randomly and uniformly for each different model-measurement. (ii) Einstein's elements consist of a countable finite number M of reals randomly and uniformly chosen from the interval $[-1, +1]$. In this case, the draws of the model-measurements are random choices from these finite subsets with given number M independent of the polarizer angles. Given further the Bell-CHSH functions (of these drawn numbers and polarizer angles) with values $A = \pm 1, B = \pm 1$, the following holds:

The Bell-CHSH-type inequalities may be validated if and only if the cardinality of the number of draws N significantly exceeds the cardinality of the number M of Einstein's elements of physical reality (which can never be true for case (i)).

6.2 Proof

6.2.1 Necessity

If Einstein's elements are not countable and modeled by numbers selected randomly and uniformly from the interval [-1, +1] of the reals, all the chosen numbers are different with probability 1. We may, therefore, choose function-values A, B that model the N quadruples of Equation 6 such that the Bell-CHSH inequalities are violated, because the necessary cyclicity of (Equation 6) may now be eliminated for all the quadruples in a suitable way.

6.2.2 Sufficiency

Given are the cyclical arrangement of polarizer angles from above and an arbitrary finite number M of Einstein's elements as well as a number of measurements (draws) $N \gg M$. One can then build about $\frac{N}{M}$ stacks of the M elements for each of the four pairs of polarizer angles that lead to the validity of Equation 6 and thus to the inequalities for $N \to \infty$. Q. E. D.

The facts of this theorem with regard to the cardinality of Einstein's elements vs. the number of draws were unknown to Bell and followers. They believed that it was rather "locality" that was the virtually sole non-trivial basis for their inequalities, while, in fact, it is only locality together with cardinality. The locality requirement that, at the source, Einstein's elements are independent of the polarizer angles, is automatically fulfilled by the randomness of the draws. Note that our proof above has not assumed any probability measure for the possible function-outcomes of A, B. As a consequence, Theorem 1 (and also Theorem two below) do not give us any actual degree of violation they only tell us that Bell-CHSH cannot be regarded as impossibility-proofs. To obtain the violations that correspond to the quantum results, we need the additional assumptions of our model

as described above and also below in the computer model. In particular, we need to assume the evaluation of the model results relative to each other.

Some may wish to indeed accept a finite number of Einstein's elements as a physical fact and, thus, have the physical validity of the Bell-CHSH inequalities guaranteed. There is, however, another important factor to be considered. The results of quantum mechanics for the data averages of the above experiments (Equation 3) are invariant under rotations of the polarizer-pairs around the z-axis and this invariance has also been proven experimentally for the photon-pair experiments beyond reasonable doubt [see 2, 4, 6, 7, 15]. Consequently, the sum of three (Bell) or four (CHSH) such data averages of experimental runs should be invariant with respect to rotations of the polarizer pairs around the z-axis for one or more such experimental runs. However, we prove in Theorem two below that for a finite number M of elements of physical reality and, thus, valid Bell-CHSH inequalities, these inequalities are not rotationally invariant. The Bell-CHSH inequalities lead, therefore, to a contradiction: their mathematical proof of using finite numbers M requires also that they are physically unacceptable, because they violate invariance to rotations of the polarizer pairs around the z-axis.

6.3 Theorem 2

Given the premises of Theorem 1 and a finite number M for Einstein's elements of physical reality, the following holds:

The Bell-CHSH inequalities are not invariant to rotations of the polarizer pairs around the z-axis.

6.4 Proof

Take the four polarizer angles used by CHSH. Then, the Bell-CHSH inequalities are valid according to Theorem 1.

Now rotate the two polarizers for each of the separate experimental runs with polarizer angle pairs (a,b); (a,b'); (a',b); (a',b') such that the left polarizer has always the angle 0 (zero) in a given coordinate system. We have in this way removed the cyclicity, which is a necessary condition to arrive at the Bell-CHSH inequality as shown by expression (6) (and in much greater mathematical generality by the work of Vorob'ev for topological-combinatorial cyclicities (Vorob'ev, 1962)). Consequently, the inequality must no longer be fulfilled. Q. E. D.

The Bell-CHSH inequality is, therefore, not invariant with respect to rotations of the polarizer angles around the z-axis and violates, thus, both the results of quantum mechanics and of actual measurements. We emphasize again that we have not made the specific model assumptions of Equations 2a–c to derive the theorems. Theorem two does not tell us, for this reason, how large the violations of the Bell-CHSH inequalities are. The numerical experiment discussed in the next section shows that with the additional assumptions of our model, the violation is major and approximates the quantum results.

The above theorems leave us then with a very reasonable and physically acceptable corollary: the Bell-CHSH inequalities do simply not apply to the Clauser-Aspect-Zeilinger experiments. Furthermore, if we are willing to accept that Einstein's elements of physical reality have the cardinality of a continuum, we can find a model that violates Bell-CHSH and is rotationally invariant. This model may also be implemented on two distant computers.

7 Two-computer model for EPRB experiments and application to actual experiments

We present now a numerical EPRB experiment, executed by two computers C_1 and C_2 precisely in the same way as done by the experimenters equipped with polarizer W_1 and analyzer W_2 as well as photon detectors. The detection of photons and the correlation of events related to entangled photon pairs by the time stamp are assumed to be ideal. Therefore, every measurement is marked by an index n of the photon pair property λ_n. The measurement times, meaning the times of the detector clicks, are also often recorded by synchronized clocks and denoted by t_n^1 and t_n^2, respectively. Also recorded at these times are polarizer angles j and j', which are available and used on the computers. Note that time-dependences innate in the experiments as explained by Kocher (Kocher and Commins, 1967) may be included into our computer simulation.

Overall, we use precisely the same model that we have developed above and Equations 2a–c with two exceptions: We use a computer random number instead of a mathematical real number for λ_n. The random numbers for computers are naturally countable and of number M. They can be, however, made large enough so that for any simulated experiment $M \gg N$, which is all that is needed to show the important points. As we will see, Bell-CHSH is not valid anyway, because we do not use the cyclicity by involving the rotational invariance. Furthermore, in order to highlight the role of the cyclicity assumptions, we remove the cyclicity by the physically permitted and necessary rotational invariance with respect to rotations around the z-axis to obtain $j = 0$ for all cases. Thus, we have:

$$A = sign\,(\lambda_n) \tag{7a}$$

And we guess the law of nature that

$$B = sign\,(\lambda_n) \tag{7b}$$

if and only if

$$|\lambda_n| \geq cos^2\,(j') \tag{7c}$$

Remember that the subscript n denotes the number of measurement and must be different for different polarizer-angle pairs and now for different j' .

The computer-model outcomes compare well with the results of quantum mechanics. Of course, we have included a fair number of definitions and theoretical assumptions and have used global space and time coordinates as well as rotational invariance, in order to develop this "theory laden" computer experiment.

Notice that any fast changes of j' do not cause any differences in our computer-model. It is not Bell's "locality" or spooky influences that play any role, it is our inclusion of rotational invariance that removes the cyclicity and, therefore, the validity of Bell-CHSH.

The necessary special and relative treatment of the W_1 polarizer in contrast to the W_2 analyzer (or *vice versa*), becomes totally acceptable, as soon as one notices the absolute need of a global

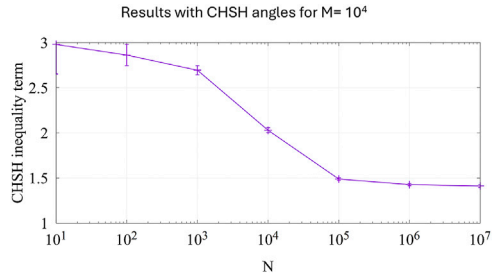

FIGURE 3
Model results for the values of CHSH (defined by Equation 4) plotted versus the number of measurements N. Note the validity of the CHSH inequality for $N \gg M$.

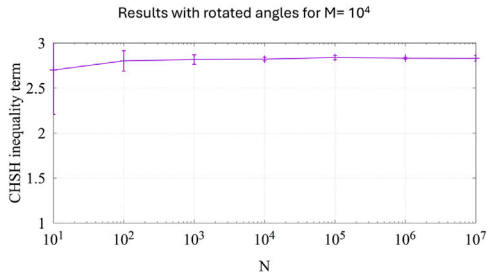

FIGURE 4
The CHSH values for a system of coordinates rotated such that we have $j = 0$ for all four terms of the CHSH inequality and j' rotated appropriately to obtain the angle differences $j' - j$ as used in Aspect-type experiments. Note that the CHSH inequality is always significantly violated, with a value close to the quantum result.

measure in order to consider correlations. For example, if we were to measure instead of polarization some kind of "length", one clearly needs to agree globally on a length-measure. If Alice measures in units that she switches rapidly between Inches, Parsec and Angstrom and without telling Bob, clearly Bob cannot guess the correlations in the length of the identical twins that they investigate.

As a corollary, the Bell-CHSH inequalities should have never been considered as a staple of physical theory related to EPRB, because they violate rotational invariance that is a hallmark of quantum theory and the Malus law, and has been experimentally proven by countless single photon EPRB-type measurements.

7.1 Computer simulations illustrating Theorem 2

The just described computer model can be used in a straightforward way to simulate the results that are expected for a countable number of elements of physical reality. We just select randomly a set of M numbers, for example, $= 10,000$, out of the interval $[-1, +1]$ and compute a consistent set of outcomes $A \cdot B$ for all possible polarizer setting pairs by using expressions (7a-c) within a Monte Carlo framework, meaning that we determine and store the outcomes for the M random numbers in a consistent way for $4N$ measurements; N for every one of the four different polarizer angle-pairs. We have used the CHSH polarizer orientations that lead to the largest violation of the CHSH inequality for the polarizer angle differences: $a = 0°, a' = 45°, b = 22.5°$ and $b' = 67.5°$. We have published the precise procedure in (Jakumeit and Hess, 2024).

We have performed this calculation for the polarizer angles used by CHSH (Clauser et al., 1969) and Aspect (Aspect, 2015) for the given M and varying N. The results are shown in Figure 3., which shows the values of CHSH as defined in Equation 4 (note that these are absolute values) as a function of the number N of measurements for a value of $M = 10,000$. As expected from Theorem 1, the CHSH inequality must be fulfilled for $N \gg M$ and begins to be fulfilled approximately for $M = N$. Big violations are clearly visible for $N \leq M$, simply because then most of the λ_n are different and we are free to choose outcomes A, B commensurate with a Malus-type law.

We then have rotated the four polarizer-angle-pairs in such a way around the z-axis that the angle j of W_1 is always 0, while j' of W_2 is chosen to obtain the desired differences $j - j'$ that CHSH and Aspect have used. For the concrete selection of CHSH angles mentioned above, this means to rotate D (a', b) to D (a'-a', b-a') = D (0°, −22.5°) (previously D (45°,22,5°) and D (a', b') to D (a'-a', b'-a') = D (0°,22.5°) (previously D (45°,67.5°), by just using the rotational symmetry. The results of this procedure are shown in Figure 4.

As clearly seen in Figure 4, the rotation of the polarizer angle-pairs has completely destroyed the validity of the CHSH inequality. Therefore, the CHSH inequality is not invariant to rotations of the polarizer angle-pairs and the coordinate system as is required by the results of quantum mechanics and by a world of experimental evidence including the classical limit for very large numbers of photons.

8 Conclusion

We have used the Fundamental Model of probability theory (Williams, 2001) for experiments using single photons or photon-pairs and polarizers in two very different configurations, one corresponding to Malus-type measurements, the other to EPRB-type measurements such as performed by Kocher and Commins (1967) and groups related to Aspect (2015), Clauser et al. (1969) and Kwiat et al. (1999); Giustina et al., 2015).

Our model shows a pronounced violation of the Bell-CHSH inequalities and agreement with the quantum result. We have shown that this unexpected violation of the highly respected inequalities arises, within the confines of the Fundamental Model (Williams, 2001), from the fact that there are precise premises that guarantee the mathematical validity of the inequalities. However, these mathematical premises lead to a mathematical-physical problem: The correctly derived Bell-CHSH inequalities are physically not acceptable, because they are not invariant to rotations of the polarizer-angle pairs. This lack of invariance makes Bell-CHSH physically unacceptable as a model for the actual experiments such as (Kocher and Commins, 1967; Clauser et al., 1969; Aspect, 2015; Kwiat et al., 1999; Giustina et al., 2015), which are invariant to such rotations. The paradox created by the work of Bell is, thus, resolved and proven to be no reason to suspect any failure of Einstein's separation principle as well as the ideas of Einstein and 't Hooft ('t Hooft, 2020; 't Hooft, 2024) regarding the existence of ontological hidden variables and their local-causal nature.

Data availability statement

The original contributions presented in the study are included in the article/supplementary material, further inquiries can be directed to the corresponding author.

Author contributions

KH: Writing–original draft, Writing–review and editing, Conceptualization, Formal Analysis, Methodology, Visualization. JK: Writing–review and editing, Methodology, Software, Validation, Visualization.

Funding

The author(s) declare that no financial support was received for the research and/or publication of this article.

Acknowledgments

Recent correspondence with Anthony J. Leggett has been a very valuable motivation for us to derive Theorems 1 and 2. While we agree on the importance of the cardinality, the Theorems may explain at least some of the differences of our views mentioned in (Leggett, 2024). Comments of Colin Naturman regarding finite subsets and subtleties for a countable-infinite number of elements of physical reality were helpful for our formulation of the Theorems. We also thank the referees for their important contributions to the clarity of the explanations.

Conflict of interest

The authors declare that the research was conducted in the absence of any commercial or financial relationships that could be construed as a potential conflict of interest.

The author(s) declared that they were an editorial board member of Frontiers, at the time of submission. This had no impact on the peer review process and the final decision.

Generative AI statement

The author(s) declare that no Generative AI was used in the creation of this manuscript.

Publisher's note

References

Aspect, A. (2015). Closing the door on Einstein and bohr's quantum debate. *Physics* 8, 123. doi:10.1103/physics.8.123

Baym, G. (1973). *Lectures on quantum mechanics*. Redwood City: Adison-Wesley Publishing Company Inc., 1–8.

Bell, J. S. (1964). On the Einstein podolsky rosen paradox. *Physics* 1, 195–200. doi:10.1103/physicsphysiquefizika.1.195

Clauser, J. F., Horne, M. A., Shimony, A., and Holt, R. A. (1969). Proposed experiment to test local hidden-variable theories. *Phys. Rev. Lett.* 23, 880–884. doi:10.1103/physrevlett.23.880

Einstein, A., Podolsky, B., and Rosen, N. (1935). Can quantum mechanical description of physical reality be considered complete? *Phys. Rev.* 16, 777–780. doi:10.1103/physrev.47.777

Feynman Lectures (1965). *Physics* 11–14.

Gisin, N. (2012). Non-realism: deep thought or a soft option? *Found. Phys.* 42, 80–85. doi:10.1007/s10701-010-9508-1

Giustina, M., Versteegh, M. A., Wengerowsky, S., Handsteiner, J., Hochrainer, A., Phelan, K., et al. (2015). Significant-loophole-free test of bell's theorem with entangled photons. *Phys. Rev. Lett.* 115, 250401–250407. doi:10.1103/physrevlett.115.250401

Hess, K. (2023). Logical conflict between Bell's locality and probability theory. *J. Mod. Phys.* 14, 1762–1770. doi:10.4236/jmp.2023.1413105

't Hooft, G. (2024). The hidden ontological variable in quantum harmonic oscillators. *Front. Quantum Sci. Technol.* 3, 1505593.

Jakumeit, J., and Hess, K. (2024). Breaking a combinatorial symmetry resolves the paradox of einstein-podolsky-rosen and Bell. *Symmetry* 16, 255–265. doi:10.3390/sym16030255

Khrennikov, A. (2009). "Contextual approach to quantum formalism," in *Fundamental theories of physics*. Springer Nature.

Kocher, C. A., and Commins, E. D. (1967). Polarization correlation of photons emitted in an atomic cascade. *Phys. Rev. Lett.* 18, 575–577. doi:10.1103/physrevlett.18.575

Kupczynski, M. (2020). Is the moon there if nobody looks: Bell inequalities and physical reality. *Front. Phys.* 8, 1–13. doi:10.3389/fphy.2020.00273

Kwiat, P. G., Waks, E., White, E. G., Appelbaum, I., and Eberhard, P. H. (1999). Ultrabright source of polarization-entangled photons. *Phys. Rev. A* 60, 773–776. doi:10.1103/physreva.60.r773

Leggett, A. J. (2024). The EPR-bell experiments: the role of counterfactuality and probability in the context of actually conducted experiments. *Philosophies* 9.5, 133. doi:10.3390/philosophies9050133

't Hooft, G. (2020). Deterministic quantum mechanics: the mathematical equations. *Front. Phys.* 8. doi:10.3389/fphy.2020.00253

Vorob'ev, N. N. (1962). Consistent families of measures and their extension. *Theory Probab. Its Appl.* 7, 147–163.

Williams, D. (2001). 44. Cambridge: Cambridge University Press, 73–110.

frontiers | Frontiers in Quantum Science and Technology

TYPE Review
PUBLISHED 01 May 2025
DOI 10.3389/frqst.2025.1569496

OPEN ACCESS

EDITED BY
Karl Hess,
University of Illinois at Urbana-Champaign,
United States

REVIEWED BY
Juergen Jakumeit,
Access e.V., Germany
Andrei Khrennikov,
Linnaeus University, Sweden

*CORRESPONDENCE
Marian Kupczynski,
marian.kupczynski@uqo.ca

RECEIVED 31 January 2025
ACCEPTED 24 March 2025
PUBLISHED 01 May 2025

CITATION
Kupczynski M (2025) Statistical contextual explanation of quantum paradoxes.
Front. Quantum Sci. Technol. 4:1569496.
doi: 10.3389/frqst.2025.1569496

Statistical contextual explanation of quantum paradoxes

Marian Kupczynski*

Département de l'Informatique et d'Ingénierie, UQO, Gatineau, QC, Canada

This year we celebrate 100 years of quantum mechanics (QM). Incorrect interpretations of QM and incorrect mental models of the invisible details of quantum phenomena lead to paradoxes. To explain these, we advocate the statistical contextual interpretation (SCI) of quantum mechanics. State vectors (wave functions) and various operators are purely mathematical entities that permit quantitative probabilistic predictions. "State vector" describes an ensemble of identically prepared physical systems, and a specific "operator" represents a class of equivalent measurements of a physical observable. A collapse of wavefunction is not a mysterious and instantaneous physical process; a collapsed quantum state describes a new ensemble of physical systems prepared in a particular way. A value of a physical observable, such as a spin projection, associated with a pure quantum ensemble is a characteristic of this ensemble created by its interaction with measuring instruments. Probabilities are objective properties of random experiments in which empirical frequencies stabilize. Following Einstein, SCI rejects the claim that QM provides a complete description of individual physical systems, but it remains agnostic about whether a more detailed subquantum description can be found or is necessary. In conformity with Bohr contextuality, SCI rejects Bell-local and Bell-causal hidden variable models. Nevertheless, by incorporating into a probabilistic model contextual hidden variable measuring instruments, long distance quantum correlations studied in Bell tests can be explained without evoking quantum nonlocality or retro-causality. SCI allows the explanation of several quantum phenomena without evoking quantum magic. SCI does not claim to provide a complete description of quantum phenomena; in fact, it is unknown whether quantum probabilities even provide a complete description of existing experimental data. Time series of experimental data may contain much more information than is obtained using empirical frequencies and histograms. Therefore, predictable completeness of QM must be tested and not taken for granted.

KEYWORDS

EPR paradox, Bell-CHSH inequalities, Bell tests, entanglement, quantum nonlocality, contextuality, completeness of quantum mechanics

1 Introduction

In 1925, Werner Heisenberg, Max Born, and Pascual Jordan developed matrix mechanics (Heisenberg, 1925; Born and Jordan, 1925; Author anonymous, 2024a), the first consistent formulation of quantum mechanics (QM). To commemorate this achievement, 2025 has been declared the International Year of Quantum Science and Technology (IYQ) by the United Nations.

Despite the incredible advances made in quantum science and technology over the past century, there is still no consensus regarding its interpretation and limitations (Author

anonymous, 2024b; Schlosshauer et al., 2013; Kupczynski, 2018a; Kupczynski, 2024a). Incorrect interpretations of QM and incorrect mental models of invisible details of quantum phenomena lead to paradoxes and speculations about quantum weirdness and quantum magic. Most of these paradoxes are due to the "individual" interpretation, according to which an instantaneous collapse of wave function describing individual physical system(s) is triggered by a single measurement performed on one of these systems.

We here review and advocate a statistical contextual interpretation (SCI) which is free of paradoxes (Einstein and Schilpp, 1949; Einstein, 1936; Ballentine, 1989; Ballentine, 1998; Kupczynski, 2007; Kupczynski, 1973; Kupczynski, 1987a; Kupczynski, 2005; Kupczynski, 2006; Kupczynski, 2015a; Kupczynski, 2016a; Kupczynski, 2017a; Khrennikov, 1999; Khrennikov, 2024; Khrennikov, 2009; Khrennikov, 2016; Allahverdyan et al., 2013). According to this interpretation, a quantum state is not an attribute of an individual physical system which can be changed instantaneously. The so-called collapse of the wavefunction is not a mysterious physical process. Quantum state/wavefunction is a mathematical entity representing an equivalence class of subsequent preparations of the physical systems. Quantum states together with specific operators representing physical observables are used to make probabilistic predictions for a statistical scatter of measured values of these observables in well-defined experimental contexts. A value of a physical observable, such as a spin projection, associated with a pure quantum ensemble is a characteristic of this ensemble created by its interaction with measuring instruments. Probabilities are objective properties of random experiments in which empirical frequencies stabilize. SCI rejects the claim that quantum mechanics provides a complete description of individual physical systems, but it remains agnostic on whether a more detailed subquantum description can be found or is necessary. In conformity with Bohr contextuality, SCI rejects Bell-local and Bell-causal hidden variable models. Nevertheless, by incorporation into probabilistic model contextual hidden variables measuring instruments, the quantum correlations studied in Bell tests can be explained without evoking quantum nonlocality. SCI does not claim to provide a complete description of quantum phenomena. In fact, it is not even known whether quantum probabilities provide a complete description of existing experimental data. Time series of experimental data may contain much more information than is obtained using empirical frequencies and histograms.

SCI (Kupczynski, 2006; Kupczynski, 2007; Kupczynski, 2016a; Kupczynski, 2017a) is similar but not identical to Ballentine's statistical (Ballentine, 1989; Ballentine, 1998) and Khrennikov's Växjö interpretation (Khrennikov, 1999; Khrennikov, 2024; Khrennikov, 2009; Khrennikov, 2016). In Ballentine's statistical interpretation, the quantum state also describes an ensemble of similarly prepared systems, not individual systems. This interpretation avoids the need for wave function collapse. It is compatible with hidden variable theories but contrary to SCI and Växjö interpretation it acknowledges that such theories must be non-local to comply with Bell's theorem (Ballentine, 1998). Växjö interpretation combines realism at the subquantum level with the contextuality of quantum observables. The value of an observable depends on the measurement context, in conformity with Bohr's complementarity and contextuality. The quantum probabilities are conditional probabilities. In contrast to SCI, it introduces the concept of a "prespace," suggesting that both classical and quantum spaces are reductions of a more fundamental reality.

A probability can have a different meaning (Khrennikov, 1999; Author anonymous, 2024c). In SCI, it is an objective property of a random experiment in which empirical frequencies stabilize. Thus, a probabilistic description of quantum phenomena can hardly be considered a complete description of individual physical systems (Einstein, 1936; Ballentine, 1989; Ballentine, 1998; Kupczynski, 2006).

Therefore, Einstein believed that QM is an emergent theory and that a more detailed description of quantum phenomena should be found (Einstein and Schilpp, 1949; Einstein, 1936; Ballentine, 1989). Bohr insisted that quantum probabilities were irreducible and that QM provided a complete description of quantum phenomena and experiments (Bohr, 1963; Bohr, 1987; Plotnitsky, 2009; Plotnitsky, 2012).

Heisenberg (1927) demonstrated the uncertainty principle according to which one may not measure simultaneously, with arbitrary accuracy, a linear momentum p and a position x of a sub-atomic particle, $\Delta x \Delta p \leq h$, where h is a Planck constant. The principle was generalized by Robertson (1929) and its precise statistical meaning was given by Kennard (1927). We have two experiments performed on two identically prepared beams/ensembles of "particles". In one experiment, we measure their linear momenta and, in another, their positions. A statistical scatter of experimental data is described by respective standard deviations and $\sigma_x \sigma_p \leq \hbar/2$ where $\hbar = h/2\pi$. This interpretation only refers to a statistical scatter of measurement outcomes and not to positions and linear momenta of "particles" if no measurements are performed. According to the Copenhagen interpretation (CI), all speculations about the sharp unmeasured values of linear momenta and positions of sub-atomic particles are meaningless, and QM does not imply that an electron can be here and a meter away at the same time (Kupczynski, 2024a; Kupczynski, 2024b), as incorrectly claimed by several authors.

In 1935, Einstein, Podolsky and Rosen (Einstein et al., 1935) proposed a thought experiment—the "EPR paradox"—intended to demonstrate the incompleteness of quantum mechanics. They considered two entangled particles which interacted in the past moving away from each other in distant locations. According to the Copenhagen interpretation (CI), measuring the position or momentum of one particle would instantly give information about the position or momentum of its distant partner without disturbing it in any way. Thus, physical properties of objects exist independently of measurement, contrary to CI. Bohr (1935) explained that EPR inference requires different incompatible but complementary experiments and that it could not provide more information about an individual physical system than was allowed by QM.

The EPR paradox was rephrased by Bohm (1951) in terms of measurements of a particle's spin. If you measure the spin of one particle, you instantly know the spin of the other. According to QM, outcomes are produced in irreducibly random ways, but in an ideal EPR-B experiment they are perfectly correlated or anti-correlated in specific randomly chosen experimental settings. This is called the

"EPR-B paradox", since a pair of fair dice cannot always produce correlated outcomes (Mermin, 1985; Mermim, 1993; Kupczynski, 2017b; Kupczynski, 2020).

(Bell, 1965, 2004) abandoned irreducible randomness and proposed the Local Realistic Hidden Variable Model (LRHVM) in which outcomes are predetermined at a source. Clauser and Horne (1974) abandoned predetermination and proposed the Stochastic Hidden Variable Model (SHVM). LRHVM describes entangled pairs/qubits as pairs of socks and SHVM as pairs of dice. In these models, correlations between distant outcomes coded ±1 must obey Bell–CHSH inequalities (Clauser et al., 1969).

Later, hidden variables were assumed to represent all common causes of events in distant laboratories, and the Local Hidden Variable Model (LHVM) (Mermin, 1993; Bell, 2004; Valdenebro, 2002; Wiseman, 2014) could be rejected in several Bell tests (Hensen et al., 2015; Giustina et al., 2015; Shalm et al., 2015; Handsteiner et al., 2017; The BIG Bell Test Collaboration, 2018; Rosenfeld et al., 2017; Zhang et al., 2022; Storz et al., 2023).

Since Bell–CHSH inequalities are violated by some quantum predictions and by experimental data, the majority of the physics community believes that no other locally causal explanation of quantum correlation is possible. Therefore, nature does exhibit non-locality, and entangled particles can influence each other instantaneously across huge distances. This is a source of extraordinary metaphysical speculation about experimenters' freedom of choice, retro-causality, quantum nonlocality, and quantum magic.

It has been widely explained that such speculations are unfounded (Kupczynski, 2006; Kupczynski, 2007; Kupczynski, 2016a; Kupczynski, 2017a; Kupczynski, 2018a; Khrennikov, 1999; Khrennikov, 2024; Khrennikov, 2009; Khrennikov, 2016; Allahverdyan et al., 2013; Kupczynski, 1973; Kupczynski, 1987a; Kupczynski, 2005; Kupczynski, 2015a; Accardi, 1981; Accardi et al., 2002; Accardi, 2005; Accardi and Uchiyama, 2007; Aerts, 1982; Aerts, 1986; Aerts et al., 2000; Boughn, 2022; Czahor, 1988; Dzhafarov, 2021; Fine, 1982; Hance and Hossenfelder, 2022; Hess and Philipp, 2005; Hess, 2014; Hess et al., 2009; Hess et al., 2016; Hess, 2022; Jaynes and Skilling, 1989; Jung, 2017; Khrennikov, 2007; Khrennikov, 2008; Khrennikov, 2019; Khrennikov, 2020a; Khrennikov, 2022; Kupczynski, 1987b; Khrennikov, 1986; Khrennikov, 2012; Khrennikov, 2014; Khrennikov, 2018b; Khrennikov, 2021; Khrennikov, 2023a; Khrennikov, 2024a; Khrennikov, 2024b; De Muynck et al., 1994; De Muynck, 2002; Nieuwenhuizen, 2009; Nieuwenhuizen, 2011; Nieuwenhuizen and Kupczynski, 2017; Peres, 1978; Pitovsky, 1983; Pitovsky, 1994; De la Peña et al., 1972; Zhao et al., 2008).

- In spin polarization correlation experiments (SPCE) and other Bell tests, we have four incompatible random experiments for different pairs of settings. LRHVM use a unique probability space and a joint probability distribution to describe these experiments, what is only possible in rare circumstances, and what is clearly incompatible with experimental protocols in Bell Tests (Kupczynski, 2007; Kupczynski, 2016a; Kupczynski, 2017a; Khrennikov, 1999; Kupczynski, 1987a; Kupczynski, 2005; Kupczynski, 2015a; Kupczynski, 2017b; Accardi et al., 2002; Accardi, 2005; Accardi et al., 2007; Accardi and Uchiyama, 2007; Aerts, 1982; Aerts, 1986; Czahor, 1988; Fine, 1982; Hess and Philipp, 2005; Hess, 2014; Hess et al., 2009; Hess et al., 2016; Hess, 2022; Khrennikov, 2007; Khrennikov, 2008; Khrennikov, 2019; Khrennikov, 2020a; Khrennikov, 2022; Kupczynski, 2024c; Pitovsky, 1994; De la Peña et al., 1972).
- In 1982, Arthur Fine was the first to clearly demonstrate that the following statements are mutually equivalent (Fine, 1982). 1) There is a deterministic hidden-variables model for the experiment. 2) There is a factorizable, stochastic model. 3) There is one joint distribution for all observables of the experiment, returning the experimental probabilities. 4) There are well-defined, compatible joint distributions for all pairs and triples of commuting and non-commuting observables. 5) The Bell inequalities hold.
- Bell and CHSH inequalities are trivial algebraic properties of experimental spreadsheets (Kupczynski, 2020; Hess and Philipp, 2005; Kupczynski, 2018b; De Raedt et al., 2017; De Raedt et al., 2023; De Raedt et al., 2024) containing quadruplets of ±1 which are, in fact, samples drawn from a statistical population described by some joint probability distribution of four compatible random variables. The outcomes of Bell tests are displayed using four spreadsheets each containing only couples ±1. The violation of Bell–CHSH inequalities only provides the evidence that the data in these four spreadsheets cannot be reshuffled to form quadruples (De Raedt et al., 2023; De Raedt et al., 2024).
- In QM, interactions of instruments with physical systems during the measurement process may not be neglected, and outcomes are not passively registered pre-existing values of the physical observables. Therefore, the Bell-causal hidden variable model suffers from a theoretical "contextuality loophole" (Kupczynski, 2015a; Kupczynski, 2017b; Kupczynski, 2020; Kupczynski, 2021; Kupczynski, 2023a; Kupczynski, 2024e; Kupczynski, 2024a; Nieuwenhuizen, 2009; Nieuwenhuizen, 2011; Nieuwenhuizen and Kupczynski, 2017) because it fails to correctly include setting-dependent variables that describe measuring instruments at the moment of measurement.

A detailed discussion of EPR-type paradoxes and Bell Tests in the spirit of SCI may be found in Kupczynski (2006), Kupczynski et al. (2007), Kupczynski (2016a), and in a dedicated section of this study. As we conclude in Kupczynski (2024b) and Kupczynski (2024c), Bell tests allow only the rejection of probabilistic couplings provided by Bell-local and Bell-causal hidden variable models. If contextual variables, describing varying experimental contexts, are correctly incorporated into a probabilistic model, then Bell–CHSH inequalities cannot be proven, and *nonlocal quantum correlations* may be explained intuitively.

This study is organized as follows. Section 2 recalls different definitions of probability and Bertrand`s paradox. We explain that in physics, probabilities are objective properties of random experiments in which empirical frequencies stabilize. Section 3 compares classical and quantum observables and filters. Section 4 recalls EPR-B paradoxes and explains them using SCI. In Section 5, quantum predictions for an ideal EPR-B experiment are derived. Section 6 gives an explanation of how Bell–CHSH inequalities are trivial arithmetic properties of N×4 spreadsheets

containing ±1 entries and can be rigorously derived only for random experiments described by four binary jointly-distributed random variables. Section 7 discusses hidden variable models proposed to explain EPR-B experiments. Section 8 is about loophole free Bell Tests, their interpretation, and their implications. Section 9 presents a contextual hidden variable model, which allows an explanation of long-range correlations observed in Bell tests. A more detailed analysis of existing time-series of data in order to elucidate the problem of completeness of quantum mechanics is advocated in Section 10. Additional conclusions are presented in Section 11.

2 Probability and Bertrand paradox

Probability and randomness are subtle notions long debated by mathematicians and philosophers. There are several definitions of probability (Khrennikov, 1999; Author anonymous, 2024a; Author anonymous, 2024b).

Classical probability is the ratio of the number of favorable outcomes to the total number of possible outcomes. For example, the probability of drawing a black king from a deck of 52 cards is 2/52 = 1/26. *Geometric probability* is the probability that a point chosen at random within a certain geometric figure will satisfy a given condition, and it is calculated as the ratio of the area (or length, volume, etc.) of the favorable region to the area of the entire region. For example, the probability of hitting a specific region on the dartboard can be calculated by dividing the area of that region by the total area of the dartboard.

Frequentist probability is the relative frequency of occurrence of an experiment's *outcome* "in the long run" of outcomes (theoretically if the experiment could be repeated an infinite number of times). It is an objective property of a random experiment. Another objective probability is *propensity*, which is defined as the tendency of some experiments to yield a certain outcome, even if they are performed only once. A *subjective probability* is based on the personal judgment of an agent and quantifies her degree of belief of how likely an event is to occur.

The limitations of the classical and geometric probabilities became evident due to Bertrand's paradox. This demonstrates how different methods of defining "randomness" can lead to different probabilities for the same event. In 1889, Bertrand posed the following problem. Consider an equilateral triangle inscribed in a circle. What is the probability that a randomly chosen chord of the circle is longer than a side of the triangle? He provided three different methods to choose a random chord, each yielding a different probability (Bertrand, 1889; Author anonymous, 2024c).

Bertrand's paradox can be rephrased in a more intuitive way (Kupczynski, 1987a). If we consider two concentric circles on a plane with radii R and R/2 respectively, we can ask what the probability P is that a chord of the larger circle chosen at random cuts the smaller one at least one point? The various answers seem to be equally reasonable. If we divide the ensemble of all chords into sub-ensembles of parallel chords, we find that P = ½. If we consider sub-ensembles of chords having the same beginning, we find that P = ⅓. Finally, if we choose midpoints of chords lying in small circle, we find that P = ¼.

The solution of Bertrand's paradox is simple. Different probabilistic models leading to different answers correspond to random experiments performed using different specific experimental protocols. It proves the contextual character of probabilities and their intimate relation to specific random experiments (Kupczynski, 2015a). Therefore, the probability of obtaining "heads" in a coin flipping experiment using a specific coin and a specific flipping device is neither a property of the coin nor of the flipping device. It is only a property of the whole experiment: "flipping this particular coin with that particular flipping device." This is why in physics, probabilities are objective properties of phenomena and random experiments in which empirical frequencies stabilize.

3 Classical *versus* quantum: properties, filters, and observables

In classical physics, measurement outcomes may contain experimental errors, but measurements are assumed to be non-invasive, meaning that they do not change the properties they measure. Therefore, macroscopic physical systems are described by properties p_i (i = 1, . . . ,n) quantified by the values of classical compatible observables which can be measured in any order.

If we have a mixed statistical ensemble (a beam) B of macroscopic systems, we can choose systems having particular properties using classical filters. *A classical filter F_i or a macro selector is a device which passes only through systems having a property p_i. Classical filters operate according to Boolean yes-or-no logic. If we have n different properties, we have n filters corresponding to them. A lattice of classical filters have simple properties: $F_i F_j = F_j F_i F_j = F_j F_i$. There also exists a maximal filter $F = F_1 F_2 \ldots F_n$ which transforms a mixed statistical ensemble into a pure statistical ensemble in which all the systems have exactly the same properties* (Kupczynski, 2015a). Mixed statistical ensembles of physical systems can be described by a joint probability distribution of random variables associated with measured physical observables.

In quantum experiments, the information obtained about invisible physical systems is indirect and obtained from their interactions with macroscopic measuring instruments. As Bohr correctly insisted, the atomic phenomena are characterized by "...the impossibility of any sharp separation between the behaviour of atomic objects and the interaction with the measuring instruments which serve to define the conditions under which the phenomena appear" (Bohr, 1987, v. 2, pp. 40–41). Quantum observables have the following properties of Bohr-contextuality (Khrennikov, 2020b; Kupczynski, 2021): *the output of any quantum observable is indivisibly composed of the contributions of the system and the measurement apparatus.*

The formalism of QM was inspired by optical experiments with polarized light. Linearly polarized light passes without noticeable attenuation by a subsequent identical polarizer. The intensity of linearly polarized light after a passage through another polarizer is reduced according to Malus law $= I_0 \cos^2 \theta$, where I_0 is the initial intensity and θ is the angle between the light's initial polarization direction and the axis of the polarizer.

Discrete atomic spectral lines and the photoelectric effect proved that exchanges of energy between electromagnetic field and matter are quantized, and "carriers" of quantized exchanged energy are called

"photons." Therefore, linearly polarized monochromatic light is usually represented as a beam of linearly polarized photons carrying energy $h\nu$. This mental picture is misleading because we cannot see photons—they are not point-like objects. When a sophisticated photon detector, after several steps of signal enhancement, produces a click, we conclude that a photon was detected. The intensity of light is now measured by counting clicks on detectors. We say that each linearly polarized photon has a probability (propensity) = $\cos^2\theta$ to pass through a polarizer if θ is the angle between the direction of the photon's initial polarization and the axis of the polarizer.

After passing through a quantum filter, the linear polarization of light becomes a contextual property of photons. *A quantum filter F_i is a device which creates a contextual property "i": passing by F_i. A physical system having a property " i" has a probability (propensity) p_{ij} to pass through another filter F_j, acquiring after the passage a new property"* j." *Quantum filters are idempotent, $F_i F_i = F_i$, but in general they do not commute Fi Fj ≠Fj Fi, and the lattice of quantum filters is isomorphic to the lattice of projectors on subspaces of a Hilbert space. Quantum filters are not selectors of pre-existing attributes of physical systems but are creators of the contextual properties defined above* (Kupczynski, 2015a).

Incompatible filters, such as polarizers with non-parallel axes, create incompatible contextual properties which cannot be measured simultaneously and, if measured in a sequence a previous contextual property, is destroyed in a new measurement. As explained in the preceding section, the probabilities are objective properties of phenomena and random experiments, and thus considering propensity as the property of individual physical systems (here, invisible photons) is in fact unfounded. This is why vectors in SCI quantum state are not considered to be properties of the individual physical systems. Treating a wavefunction as an attribute of the individual physical system leads to the EPR paradox, which is discussed in the next section.

4 EPR paradox and statistical contextual interpretation

Resumed here is the discussion of the EPR paradox in Kupczynski (2016a). Before the publication of the EPR paper, it was believed that:

A1: Any pure state of a physical system is described by a specific unique wavefunction Ψ.

A2: Any measurement causes a physical system to jump instantaneously into an eigenstate of the dynamical variable being measured. This eigenstate becomes a new wavefunction describing a state of the system.

A3: A wave function Ψ provides a complete description of a pure state of an individual physical system.

EPR considers two particular individual systems, I + II, in a pure quantum state; they interacted in the past, separated, and evolved freely afterward (Einstein et al., 1935). Using A2, they concluded that

- A single measurement performed on one of the systems—for example, on system I—gives instantaneous knowledge of the wave function of system II moving freely far away.
- By choosing two different incompatible observables to be measured on system I, it is possible to assign two different wave functions to system II (the same physical reality: the second system after the interaction with the first).

Since a measurement performed in a distant location on system I does not disturb system II in any way, according to A1 and A3 system II should be described by a unique wavefunction and not by two different wave functions. Moreover, these wave functions are eigenstates of two non-commuting operators that represent incompatible physical observables which allow indirect deduction of the values of these incompatible physical observables for the same system II without disturbing it in any way which contradicts Heisenberg uncertainty relations and CI.

EPR discussed particle positions and momenta, and Bohm discussed an experiment in which a source produces pairs of particles prepared in a spin singlet state (Bohm, 1951). One of a pair (photon or electron) is sent to Alice and another to Bob in distant laboratories. According to A1, each pair of photons is described by a state vector:

$$\Psi = \left(|+\rangle_P|-\rangle_P - |-\rangle_P|+\rangle_P\right)/\sqrt{2}. \quad (1)$$

—where $|+\rangle_P$ and $|-\rangle_P$ are state vectors corresponding to photon states in which their spin is "up" or "down" in direction **P**, respectively**.** If we measure a spin projection of a photon I on direction **P**, we have an equal probability of obtaining result "1" or "–1". If we obtain "1," a reduced state vector of the photon II is $|-\rangle_P$; if we obtain "-1," a reduced state vector of the photon II is $|+\rangle_P$. By choosing direction **P** for the measurement to be performed on photon I, when "photons are in flight and far apart" we can assign different incompatible reduced state vectors to the same photon II. In other words, we can predict with certainty and without in any way disturbing the second photon that the **P**-component of the spin of photon II must have the opposite value to the value of the measured **P**- component of the spin of photon I (Ballentine, 1998). Therefore, for any direction **P**, the **P**-component of the spin of photon II has unknown but predetermined value which contradicts QM and is called the "EPR-B paradox".

Bohr (1935) promptly replied to the EPR paper and explained that two different wave functions could be assigned to system II only in two different incompatible experiments in which both systems were exposed to different influences before the measurement on system I was performed. In order to make predictions concerning the individual physical systems in EPR scenario 1, much more detailed knowledge of how a particular pair was prepared in each of these incompatible experiments is necessary (Kupczynski, 2006).

In 1936, Einstein advocated a purely statistical interpretation of QM and explained that the EPR paradox disappears because "...Ψ function does not, in any sense, describe the state of one single physical system and reduced wave functions describe different sub-ensembles of systems" (Einstein, 1936). This statistical interpretation has been generalized and promoted with success by Ballentine 1989 and Ballentine 1998: "...the habit of considering an individual particle to have its own wave function is hard to break ... though it has been demonstrated strictly incorrect".

According to the statistical contextual interpretation of QM (SCI) (Ballentine, 1998; Kupczynski, 2006; Kupczynski, 2007; Kupczynski, 2016a; Khrennikov, 2009; Allahverdyan et al., 2013):

1. A state vector Ψ is not an attribute of a single electron, photon, trapped ion, quantum dot, *etc.* A state vector Ψ or a density matrix ρ describe only an ensemble of identical state preparations of some physical systems.
2. A wave function reduction is neither instantaneous nor non-local. In an EPR experiment, a state vector describing system II obtained by reduction of an entangled state (Equation 1) of two physical systems I + II describes only a sub-ensemble of systems II being partners of those systems I for which a measurement of some observable gave the same specific outcome. Different sub-ensembles are described by different reduced state vectors.
3. A value of a physical observable, such as a spin projection, is not a predetermined attribute of a system but is a property of a pure ensemble of identically prepared physical systems created in the interaction with a measuring instrument (Kupczynski, 1987b, 2015a).

The solution of the EPR-B paradox given by SCI is simple: the wave function reduction is not instantaneous, and a reduced one-particle state $|+\rangle_P$ "describes" only an ensemble of partners of the particles I which were detected to have "spin down" in the direction **P.** For different directions **P,** we perform specific experiments, and we obtain a different sub-ensemble of particles II. Strong correlations between distant outcomes in EPR experiments are due to contextuality and various conservation laws. More detailed discussion of EPR and EPR-B paradoxes may be found, for example, in (Kupczynski, 2009).

5 Kolmogorov and quantum probabilistic models

Outcomes of any random experiment are described by a specific probability space Ω, σ-algebra of its all sub-ensembles F, and a probabilistic measure μ. A sub-ensemble $E \in F$ is an event corresponding to a subset of possible outcomes of a random experiment. A probability of observing this event is given by $0 \le \mu(E) \le 1$. In statistics, instead of Ω we use a sample space S which contains only the possible outcomes of a studied random experiment.

Every random experiment is defined by its experimental context C (Kupczynski, 2017a; Kupczynski, 2015a; Khrennikov, 1999; Khrennikov, 2024; Khrennikov, 2009; Khrennikov, 2016; Khrennikov, 2022). If its outcomes are discrete, it may be described by a random variable A and a probability distribution

$$P(a|C) = P(A = a \,|\, C) \tag{2}$$

and its expectation value

$$E(A|C) = \sum_a aP(a|C). \tag{3}$$

In quantum experiments, the context of an experiment is determined by a preparation of an ensemble of physical systems represented by a density operator ρ (or a state vector ψ) and by a Hermitian operator $\hat{A}$ representing the experimental set-up used to measure a physical observable A. Instead of (Equations 2, 3), we have

$$P\left(a\middle|\psi, \hat{A}\right) = \left|\langle a|\psi\rangle\right|^2, \tag{4}$$

—where $|a\rangle$ is a corresponding eigenvector of the operator $\hat{A}$ and

$$E\left(A|\psi, \hat{A}\right) = \langle\psi|\hat{A}|\psi\rangle. \tag{5}$$

If a density matrix ρ is used to describe a pure or mixed prepared ensemble, then

$$E\left(A|\rho, \hat{A}\right) = Tr\left(\rho\hat{A}\right). \tag{6}$$

In an idealized EPR-B experiment (Equation 1), which is impossible to implement, a source sends two correlated signals which arrive to distant laboratories, pass by polarization analyzers, and produce coincident counts on detectors. The experimental situation is much more complicated since clicks are not registered at the same time and one has to decide which clicks are correlated by introducing specific time windows and deciding how to use them in order to define coincident clicks (Kupczynski, 2017b; 2021).

An idealized EPR-B experiment is described by the following probabilistic model (Kupczynski, 2020, 2023a, 2024a; Cetto et al., 2020). Randomly chosen polarization measurement settings are (x, y), prepared ensemble E is described by $\rho = |\psi\rangle\langle\psi|$, $\hat{A}_x = \vec{\sigma}\cdot\vec{n}_x$ and $\hat{B}_y = \vec{\sigma}\cdot\vec{n}_y$ represent spin projections on the corresponding unit vectors, and

$$E\left(A_xB_y\right) = Tr\left(\rho\hat{A}_x\otimes\hat{B}_y\right) = \langle\psi\,|\,\hat{A}_x\otimes\hat{B}_y|\psi\rangle = \sum_{\alpha\beta}\alpha\beta p_{xy}(\alpha,\beta)$$
$$= -\vec{n}_x\cdot\vec{n}_y = -\cos\left(\theta_{xy}\right), \tag{7}$$

—where $\hat{A}_x\otimes\hat{B}_y|\alpha\beta\rangle_{xy} = \alpha\beta|\alpha\beta\rangle_{xy}$, $p_{xy}(\alpha,\beta) = |\langle\psi|\alpha\beta\rangle_{xy}|^2$ and α = ±1 and β = ±1 (Kupczynski, 2024b; Cetto et al., 2020).

The model is contextual because a triplet $\left\{\rho, \hat{A}_x, \hat{B}_y\right\}$ changes if a preparation or defined by Equations 4-7 experimental settings change. For each choice of settings (x, y), QM provides a specific Kolmogorov model.

Since $E(A_xB_y) = -1$ for $\theta_{xy} = (\theta_x - \theta_y) = 0$, it has been incorrectly claimed that QM predicts strict anti-correlations of two space-like events produced in an irreducibly random way. Since two space-like events produced randomly cannot be correlated $(E(A_xB_y) = 0)$, irreducible randomness was abandoned, and several hidden variable models were proposed to explain the correlations predicted by QM. In fact, QM does not predict strict correlations for EPRB-type experiments. Directions can only be defined by some small intervals I_x and I_y containing angles close to θ_x and θ_y respectively. Therefore, the correct quantum prediction for expectation values is (Kupczynski, 2016a, 1987b)

$$E\left(A_xB_y\right) = -\iint_{I_xI_y}\cos(\theta_1-\theta_2)\,d\rho_x(\theta_1)\,d\rho_y(\theta_2). \tag{8}$$

After defining in the next section Bell–CHSH inequalities, we will discuss several hidden variable models proposed to explain quantum correlations Equations 7, 8.

6 Experimental spreadsheets and Bell–CHSH inequalities

Let us consider a random experiment described by four jointly distributed binary random variables (A, A', B, B') taking the values ± 1. In each trial of this experiment, four outcomes (a. a, b, b') are obtained and displayed in an N×4 experimental spreadsheet (Kupczynski, 2020). Since b = b' or b = -b' thus

$$|s| = |ab - ab' + a'b + a'b'| = |a(b - b')| + |a'(b + b')| \le 2. \quad (9)$$

From Equation 9 we obtain CHSH inequality:

$$|S| \le \sum_{a,a',b,b'} |ab - ab' + a'b + a'b'| p(a, a', b, b') \le |E(AB)\text{-}E(AB')| + |E(A'B) + E(A'B')| \le 2, \quad (10)$$

—where p(a, a′, b, b') is a joint probability distribution of (A, A′, B, B'), and $E(AB) = \sum_{a,b} ab\,p(a, b)$ is a pairwise expectation of A and B obtained using a marginal probability distribution $p(a, b) = \sum_{a',b'} p(a, a', b, b')$ (Kupczynski, 2020).

If all pair-wise expectation values in Equation 10 are estimated using the same N×4 experimental spreadsheet, then the inequality (Equation 10) is strictly obeyed by all finite samples. The inequalities (Equation 10) are in fact necessary and sufficient conditions for the existence of a joint probability distribution of only pairwise measurable ±1-valued random variables (Fine, 1982). The inequalities (Equation 10) are also valid if |A|≤1, |A'|≤1|, |B|≤1, and |B'|≤1. It is now well known that cyclic combinations of pairwise marginal expectations of jointly distributed binary random variables must obey non-contextuality inequalities (NCI) (Araujo et al., 2013). Bell–CHSH inequalities are a special case of NCI.

If we have four N×4 spreadsheets containing outcomes from four runs of the same random experiment, as discussed above, but we use each of these spreadsheets to estimate only one pairwise expectation E (A, B), E(A,B′), E (A'. B), and E(A'. B') respectively, then 50% of the time, these estimates violate the inequality (Equation 10) (Kupczynski, 2016a; Kupczynski, 2023a; Gill, 2014), Only if N increases to infinity the probability of the violation of the inequality (Equation 10) tends to 0. Therefore, the violation of CHSH-inequality by experimental data in EPR-type experiments allows only the evaluation of the plausibility of particular probabilistic models (Kupczynski, 2024c). The next section will discuss such models.

7 Local realistic models for the EPR–Bohm experiment

7.1 Local realistic hidden variable model (LRHVM)

In an attempt to explain correlations in an ideal EPR-B experiment, (Bell, 1965, 2004; Kupczynski, 2015a, 2024d) proposed a probabilistic model in which outcomes registered in distant laboratories are predetermined at a source:

$$E(A_x B_y) = \sum_{\lambda \in \Lambda} A_x(\lambda) B_y(\lambda) P(\lambda), \quad (11)$$

—where $A_x(\lambda) = \pm 1$ and. $B_y(\lambda) = \pm 1$. In LRHVM, we have four jointly distributed random variables (A_x(L), B_y(L), $A_{x'}$(L), $B_{y'}$ (L)) being functions of the same random variable L. The random variable L describes a classical random experiment in which λ is sampled with replacement from a probability space Λ. For each value of λ, all outcomes can be calculated. LRHVM describes *entangled pairs* as pairs of socks, which can have different sizes and colors; for example, Harry draws a pair of socks, sends one sock to Alice and another to Bob, who in function of (x, y) record corresponding properties of color or size.

Since (A_x(L), B_y(L), $A_{x'}$(L), $B_{y'}$ (L)) are jointly distributed, they thus obey CHSH inequality:

$$|S| = |E(A_x B_y) + E(A_x B_{y'}) + E(A_{x'} B_y) - E(A_{x'} B_{y'})| \le 2. \quad (12)$$

Bell knew that in the EPR-B experiment, (A_x, B_y, $A_{x'}$, $B_{y'}$) are not jointly measurable and that their joint probability distribution does not exist. He did not notice that to prove his inequalities, he was tacitly using the existence of a joint probability distribution of (A_x(L), B_y(L), $A_{x'}$(L), $B_{y'}$ (L)). As explained in the preceding section, the inequalities (Equations 10 and 12) can be rigorously proven for a random experiment outputting in each trial four ±1 outcomes.

7.2 Stochastic hidden variable model (SHVM)

(Clauser and Horne, 1974; Kupczynski, 2024e) proposed a stochastic hidden variable model (SHVM) in which λ does not determine outcomes in a given trial but only their probability.

Using the notation of Big Bell Test collaboration (The BIG Bell Test Collaboration, 2018):

$$P(a, b|x, y) = \sum_{\lambda} P(a|x, \lambda) P(b|y, \lambda) P(\lambda), \quad (13)$$

—where P(-|-) denotes a conditional probability. Equation 13 for a fixed setting (x, y) describes a family of independent random experiments labelled by λ and

$$E(A_x B_y) = \sum_{\lambda} E(A|x, \lambda) E(B|y, \lambda) P(\lambda). \quad (14)$$

Pair-wise expectations defined by Equation 13 are also constrained by CHSH inequalities Equation 12. In SHVM, entangled photon pairs are described as pairs of dice, and the correlations which can be created in this model are quite limited.

7.3 Local causal hidden variable model (LHVM)

LHVM is a generalization of the preceding two models, where λ represents all possible common causes of events happening in distant laboratories, and "...they may include the usual quantum state; they may also include all the information about the past of both Alice and Bob. Actually, the λ′s may even include the state of the entire universe" (The BIG Bell Test Collaboration, 2018; Kupczynski, 2024a) —except that inputs (x, y) cannot depend on them.

$$P(a,b,x,y) = \sum_{\lambda} P(a|x,\lambda)P(b|y,\lambda)P(x,y|\lambda)P(\lambda) \quad (15)$$

and

$$P(x,y|\lambda) = P(x,y). \quad (16)$$

The condition (Equation 16) is called "measurement independence," experimenters' "freedom-of-choice" (FoC) or "no conspiracy" (The BIG Bell Test Collaboration, 2018; Hall, 2010; Myrvold et al., 2020; Blasiak et al., 2021; Kupczynski, 2024b, 2022). Since correlation does not mean causation, this terminology is based on the incorrect causal interpretation of conditional probabilities (Kupczynski, 2017a, 2021, 2023a, 2024a, 2024b, 2024c, 2022). In a probabilistic model, $P(x,y|\lambda) \neq P(x,y)$ does not imply that FoC is constrained by causal influences.

If λ represents ontic properties of entangled pairs or common causes, it thus cannot not depend in any sense on chosen settings:

$$P(\lambda,x,y) = P(\lambda)P(x,y) \Rightarrow P(\lambda|x,y) = P(\lambda). \quad (17)$$

However, hidden variables can also describe measuring instruments, so they can depend on the chosen settings (Kupczynski, 2006; Kupczynski, 2016a; Kupczynski et al., 2007). As Theo Nieuwenhuizen explained, the model (Equations 13–16) suffers from a theoretical *contextuality loophole* because the hidden variables describing measuring instruments had not been included (Nieuwenhuizen, 2009; Nieuwenhuizen, 2011; Nieuwenhuizen and Kupczynski, 2017).

There is no doubt that experimenters can freely choose binary random labels of their setting (x, y), and this is what they do (Hensen et al., 2015; Giustina et al., 2015; Shalm et al., 2015; Handsteiner et al., 2017; The BIG Bell Test Collaboration, 2018; Rosenfeld et al., 2017; Zhang et al., 2022; Storz et al., 2023). However, this random choice of labels (x, y) is followed by a choice of corresponding specific instruments and setting-dependent measuring procedures. Since measuring instruments play an active role in quantum experiments, it is reasonable to assume that outcomes depend not only on setting-independent hidden variables that describe prepared physical systems but also on setting-dependent hidden variables that describe local instruments and measuring procedures; and thus *statistical independence* (Equation 17) is violated:

$$P(\lambda|x,y) \neq P(\lambda). \quad (18)$$

Bell was the first to notice that if hidden variables depend on settings; then Bell–CHSH inequalities could not be derived. However, since Equation 18 implied the violation of Equation 16, this option was rejected as violating FoC (Kupczynski, 2017a; The BIG Bell Test Collaboration, 2018; Myrvold et al., 2020; Kupczynski, 2023a, 2024a, 2024b). As explained above, the violation of Equation 16 does not constraint FoC.

Bell clearly demonstrated that LRHVM is inconsistent with QM because there exist four particular experimental settings for which, using Equation 7, one obtains $|S| \leq 2\sqrt{2}$, which significantly violates Equation 12. Various Bell Tests (Hensen et al., 2015; Giustina et al., 2015; Shalm et al., 2015; Handsteiner et al., 2017; The BIG Bell Test Collaboration, 2018; Rosenfeld et al., 2017; Zhang et al., 2022; Storz et al., 2023) were performed in order to check the plausibility of local hidden variable models. Before explaining a contextual hidden variable model in which hidden variables depend on settings, the next section discusses recent Bell tests and their implications.

8 Bell tests and what they have proven

Bell tests are inspired by an ideal EPR experiment. Entangled pairs are created at a source and sent to distant locations or are created directly in distant laboratories using specific synchronized preparations/treatments such as entanglement swapping or entanglement transfer protocols (Kupczynski, 2024a). Despite differences, experimental protocols are subdivided into three steps:

1) Preparation of an ensemble E of pairs of entangled physical systems.
2) Random local choice of labels/inputs (x, y) using random number generators (RNG), and signals coming from distant stars (Handsteiner et al., 2017; The BIG Bell Test Collaboration, 2018) or/and human choices (The BIG Bell Test Collaboration, 2018; Rosenfeld et al., 2017; Zhang et al., 2022; Storz et al., 2023). This study uses four pairs of labels/inputs—(x, y), (x, y'), (x', y), and (x', y') —which denote four incompatible experimental settings/contexts.
3) Implementation of correlated and synchronized measurements in distant locations and readout of binary outcomes (a, b) (called outputs), which are the coded information corresponding to clicks on different distant detectors, *etc.*

In Bell Tests to each randomly chosen input (x,y) corresponds a specific pair of correlated distant experiments. Outcomes of these experiments are described by four pairs of binary random variables: (A_{xy}, B_{xy}), $(A_{xy'}, B_{xy'})$, $(A_{x'y}, B_{x'y})$, and $(A_{x'y'}, B_{x'y'})$ (Kupczynski, 2024a). Our notation is inspired by the contextuality-by-default approach (CbD) (Kupczynski, 2021; Dzhafarov and Kujala, 2014; Dzhafarov et al., 2015; Kujala et al., 2015) in which random variables measuring the same content in a different context are *a priori* stochastically unrelated, such as A_{xy} and $A_{x'y}$. It is evident that in Bell tests, a joint probability distribution of these eight random variables does not exist, and Bell– CHSH inequalities cannot be derived without additional assumptions (Khrennikov, 2022).

A pair of random empirical variables (A_{xy}, B_{xy}) describes a scatter of outputs in the experiment using settings (x, y). We have four random experiments described by specific empirical probability distributions. Using these distributions, we may test the plausibility of quantum and local hidden variable models proposed to explain a statistical scatter of outcomes in an ideal EPR-B experiment. If random variables in probabilistic models are denoted (A'_{xy}, B'_{xy}) in order to not be confounded with empirical random variables (A_{xy}, B_{xy}), then we say that a probabilistic model provides a *probabilistic coupling* if:

$$E(A_{xy}) = E(A'_{xy}), E(B_{xy}) = E(B'_{xy}), E(A_{xy}B_{xy}) = E(A'_{xy}B'_{xy}). \quad (19)$$

Therefore, in Bell tests, we are testing the plausibility of different probabilistic couplings, in particular for LRHVM:

$$\mathrm{E}\left(\mathrm{A'_{xy}}\right)=\mathrm{E}\left(\mathrm{A'_{xy'}}\right)=\mathrm{E}\left(\mathrm{A_x}\right),\mathrm{E}\left(\mathrm{B'_{xy}}\right)=\mathrm{E}\left(\mathrm{B'_{x'y}}\right)$$
$$=\mathrm{E}\left(\mathrm{B_y}\right),\mathrm{E}\left(\mathrm{A'_{xy}B'_{xy}}\right)=\mathrm{E}\left(\mathrm{A_xB_y}\right), \quad (20)$$

where (A_x, B_y, $A_{x'}$, $B_{y'}$) are jointly distributed Equation 11. More detailed discussion may be found in Kupczynski (2024a).

There is still much confusion in journals, books, and in social media concerning the metaphysical implications of the results of Bell tests (The BIG Bell Test Collaboration, 2018; Rosenfeld et al., 2017; Zhang et al., 2022; Storz et al., 2023), so it is beneficial to explain it here. Using LHVM Equations 15–17, one derives inequalities which must be satisfied by specific combinations of probabilities of events to be observed in the experiments performed using different experimental settings. These combinations are denoted "S," "J," or "T," which are called in brief "Bell parameters". If the observed parameter violates inequality, one can conclude that measured systems were not governed by any LHVM. It should be noted that this conclusion is always statistical and typically takes a form of a hypothesis test, leading to a conclusion of the form: "...assuming nature is governed by local realism, the probability to produce the observed Bell inequality violation ... is P(observed or stronger | local realism)≤ p. This p-value is a key indicator of statistical significance in Bell Tests" (The BIG Bell Test Collaboration, 2018)

Since p-values in several experiments are very small, one concludes: *Local realism, i.e., realism plus relativistic limits on causation, was debated by Einstein and Bohr using metaphysical arguments, and recently has been rejected by Bell tests*. Such a conclusion is imprecise and misleading. As correctly observed by Wiseman (2014), "*the usual* philosophical meaning of 'realism' is the belief that entities exist independent of the mind, a worldview one might expect to be foundational for scientists." It is also claimed that Bell tests allow the rejection of *local causality*, where *Bell-local causality* is defined: *Alice's output* a *depends only on her input* x *and on* λ *describing all possible common causes included in the intersection of the of the backward light cones of* a *and* b *and independent of inputs* x *and* y.

It is true that tested probabilistic models have been motivated by various metaphysical assumptions. Nevertheless, Bell tests allow only the rejection of a statistical hypothesis that says that LHVM Equations 15–17 provides a probabilistic coupling (Equation 20) consistent with experimental data. Therefore, the violation of Bell–CHSH inequalities does not allow for far reaching metaphysical speculations. We agree also with De Raedt et al., (2023):

...all EPRB experiments which have been performed and may be performed in the future and which only focus on demonstrating a violation BI-CHSH merely provide evidence that not all contributions to the correlations can be reshuffled to form quadruples ... These violations do not provide a clue about the nature of the physical processes that produce the data...

Similar conclusions have been drawn (Kupczynski, 1987a, 2018b, 2020; Dzhafarov, 2021; Hess and Philipp, 2005; Khrennikov, 2007, 2008, 2019, 2020a, 2022; De Raedt et al., 2024).

Bell tests confirm the existence of long range correlations between outcomes of experiments performed in space-like locations. If additional context-dependent variables that describe measuring instruments and procedures are correctly incorporated into a probabilistic model (Equation 11), then Bell–CHSH inequalities cannot be derived and "nonlocal "correlations can be explained without evoking quantum magic. Such a model is discussed in the next section.

9 Contextual hidden variable model and the violation of statistical independence

We incorporate into the model (Equation 11) additional variables that describe distant measuring contexts (Kupczynski, 2024a).

- $\lambda_1 \in \Lambda_1$ and $\lambda_2 \in \Lambda_2$ describe correlated physical systems and do not depend on measurement settings (x, y).
- $\mu_x \in M_x$ and $\mu_y \in M_y$ describe measurement procedures and instruments at the moment of measurement when settings (x, y) were chosen.
- Inputs/labels (x, y) are randomly chosen in separate random experiments.
- Outputs are created locally: $a = A'_x(\lambda_1, \mu_x) = \pm 1$ and $b = B'_y(\lambda_2, \mu_y) = \pm 1$

The resulting contextual model (CHVM) is defined by three equations

$$E\left(A_xB_y\right)=\sum_{\lambda\in\Lambda_{xy}} A_x(\lambda_1,\mu_x)B_y\left(\lambda_2,\mu_y\right)\mathrm{P}(\lambda_1,\lambda_2)\mathrm{P}_{xy}\left(\mu_x,\mu_y\right), \quad (21)$$

—where $\Lambda_{xy}=\Lambda_1\times\Lambda_2\times M_x\times M_y$,

$$\mathrm{P}(\mathrm{a},\mathrm{b},\mathrm{x},\mathrm{y})=\sum_{\lambda\in\Lambda_{xy}}\mathrm{P}(\mathrm{a}\,|\,\lambda_1,\mu_x)\mathrm{P}(\mathrm{b}\big|\lambda_2,\mu_y)\mathrm{P}(\mu_x,\mu_y\big|\mathrm{x},\mathrm{y})\mathrm{P}(\mathrm{x},\mathrm{y})\mathrm{P}(\lambda_1,\lambda_2) \quad (22)$$

and

$$\mathrm{P}\left(\mu_x,\mu_y\,|\,\mathrm{x},\mathrm{y}\right)=\mathrm{P}_{xy}\left(\mu_x,\mu_y\right)\neq P\left(\mu_x,\mu_y\right) \quad (23)$$

In Bell tests, P(x, y) = P(x) P(y), but in the contextual model Equation 21 and in QM, it does not matter how labels (x, y) are chosen. In general, spaces Λ_{xy} for different settings (x, y) do not overlap and, as Larsson and Gill (2004) demonstrated, Bell–CHSH inequalities cannot be derived and $|S|\leq 4$.

The model (Equations 21–23) violates statistical independence, and $P(x,y|\mu_x,\mu_y)\neq P(x,y)$:

$$\mathrm{P}\left(\mu_x,\mu_y,\mathrm{x},\mathrm{y}\right)=P_{xy}\left(\mu_x,\mu_y\right)\mathrm{P}(\mathrm{x},\mathrm{y})=P\left(\mu_x,\mu_y\right)\rightarrow P\left(\mathrm{x},\mathrm{y}\,|\,\mu_x,\mu_y\right)$$
$$=\frac{P\left(\mu_x,\mu_y\right)}{P\left(\mu_x,\mu_y\right)}=1. \quad (24)$$

The Equation 24: $P(\mathrm{x},\mathrm{y}\,|\,\mu_x,\mu_y)=1$ only "says" that if a hidden event $\{\mu_x,\mu_y\}$ "happened", then the settings (x,y) were used (Kupczynski, 2017a, 2021, 2023a, 2024a, 2022). It has nothing to do with *conspiracy* or FoC.

Since inputs (x,y) were chosen using signals from distant stars (Handsteiner et al., 2017), random number generators or random

human choices were made during online computer games (The BIG Bell Test Collaboration, 2018), and thus the *freedom-of-choice loophole* was successfully closed, but it did not prove *statistical independence*. As I proposed in preceding papers, a violation of *statistical independence* should be called "Bohr-contextuality"—not to be cofounded with *CbD contextuality* (Dzhafarov and Kujala, 2014; Dzhafarov et al., 2015; Kujala et al., 2015) or simply *contextuality*.

CHVM violates Bell-locality and Bell-causality, but outputs are created in a locally causal way. Hidden variables describing physical systems and measuring contexts in space-like separated laboratories can be statistically correlated, but the violation of statistical independence and apparently non-local correlations may be explained without evoking spooky influences. It may be the effect of setting dependent post-selection of data (Kupczynski, 2017b, 2021, 2024a), or it may be due to the global space-time symmetries (Kupczynski, 2023a, 2024a, 2023b).

The model (Equation 21) can be further simplified. For example, μ_x can be a fixed set of variables describing experimental procedures labeled by x. If in a distant laboratory, a setting labeled by y is used, then a measuring instrument and/or laser beam are rotated by angle $\theta_{xy} = \theta_x - \theta_y$. Therefore, due to global rotational symmetry, $\mu_y = f(\mu_x, \cos(\theta_{xy}))$, and:

$$E(A_x B_y) = \sum_{\lambda \in \Lambda_{xy}} A_x(\lambda_1, \mu_x) B_y(\lambda_2, \mathrm{f}(\mu_x, \cos(\theta_{xy}))\mathrm{P}(\lambda_1, \lambda_2). \quad (25)$$

The model (Equation 25) seems to have enough flexibility in order to explain long range correlations in Bell tests depending on $\theta_{xy} = \theta_x - \theta_y$. The model (Equation 25) does not allow the derivation of any Bell-type inequalities.

10 Can a quantum-mechanical description of physical reality be considered complete?

This question asked by Einstein, Podolsky, and Rosen (EPR) (Einstein et al., 1935) and answered by Bohr (1935) has been debated for 90 years. Many incorrectly believe that the results of recent Bell tests prove that if we reconcile QM with general relativity, we will obtain a complete description of physical reality. In fact, we should be much more humble (Kupczynski, 2024c) because we even do not know whether QM is predictably complete.

QM gives probabilistic predictions for distributions of the results obtained in long runs of one experiment or in several repetitions of the same experiment on a single physical system. It is unclear how and in what sense a claim can be made that QM provides a complete description of individual physical systems. This is why (Einstein, 1936; Einstein and Schilpp, 1949) never accepted that a statistical theory may provide a complete description of individual physical systems and believed that QM should be completed by some microscopic theory of sub-phenomena that enable the reproduction of quantum probabilistic predictions.

According to Bohr, quantum probabilities describe completely quantum phenomena and experiments, and no more detailed sub-quantum description is possible or necessary. Quantum probabilities are thus irreducible, and QM is not an emergent theory. In statistical mechanics, probabilities reflect a lack of knowledge about the properties of physical systems. In SCI, quantum probabilities reflect a lack of knowledge about the interactions of physical systems with measuring instruments in well-defined experimental contexts. The Bertrand paradox teaches that probabilities are not properties of individual physical systems but are only properties of random phenomena and experiments as a whole. In this sense, they do not provide a complete description of individual physical systems.

Whether a more detailed description of quantum phenomena does exist is an open question, and several hidden variable models have been proposed and discussed. Bell tests permit the rejection of several hidden variable models but neither prove the completeness nor non-locality of QM. Several years ago, we pointed out that the question about the completeness of QM cannot be answered by constructing *ad hoc* sub-quantum hidden variable models. It can only be answered by a different and a more detailed analysis of experimental data (Kupczynski, 2006; Kupczynski et al., 2007; Kupczynski, 2016a, 1986, 1984).

In quantum experiments, outcomes are registered by online computers as finite time series of data. It can be a laser beam which, after passing by a PBS (polarization beam splitter), produces clicks on detectors coded ±1. It can be a physical system in a trap, a physical observable is measured, an outcome is recorded, and initial conditions in the trap are reset.

No single result is predictable in all these experiments. Empirical frequency distributions are obtained from long-term series of counts and compared with probabilistic predictions of QT. In this way, *predictable completeness* of QT is taken for granted, and any fine structure of time-series, if it existed, would be averaged.

Let us consider two experiments repeated N times each. In the first experiment, we obtain a time series of the results, 1,-1,1,-1, . . . 1,-1 . . ., and in the second, 1,-1,-1,1,1,1,-1,-1, 1,-1,-1,1,1,1,1,-1 . . . By increasing the value of N, the relative frequency of achieving 1 can approach ½ as close as we wish. However, it is not a complete description of these time series. By searching for reproducible fine structures in experimental time series, we can investigate whether QM is emergent without constructing specific hidden variable models.

In any more detailed description of quantum phenomena, pure quantum ensembles become mixed statistical ensembles with respect to additional uncontrollable parameters that describe physical systems and measuring instruments. There is a principal difference between a pure statistical ensemble and a mixed one. For a pure ensemble, any sub-ensemble has the same properties. Sub-ensembles of a mixed statistical ensemble may differ from one to another if mixing is not perfect. These differences can be, in principle, detected by using so called purity tests (Kupczynski, 2006, 1986, 1984; Kupczynski et al., 2007), which I introduced in a different context (Kupczynski, 1974, 1977).

Let us consider time series of outcomes T(S, E, i) obtained in an i^{th} run of an experiment E performed on physical system(s) S. Since we do not control the distribution of hidden variables, time-series T(S, E, i) may differ from run to run of the same experiment. Using the language of mathematical statistics, T(S, E, i) represents a random sample drawn from some statistical population. A pure ensemble is one characterized by such empirical distributions of various counting rates, which remain approximately unchanged for any rich sub-ensembles drawn from this ensemble in a random way

(Kupczynski et al., 2007; Kupczynski, 1973, 1986). Therefore, we must test the null hypothesis H_0:

Samples T(S, E, i) for different values of i are drawn from the same statistical population.

Various statistical non-parametric compatibility tests can be used to test H_0.

Purity tests are not sufficient. To prove that QM is not *predictably complete*, it is necessary to study in more detail time series of data, detect some temporal fine structure, and find a stochastic model to explain it. Several methods are used to study and compare empirical time-series: frequency or harmonic analysis, periodograms, autocorrelation and partial autocorrelation functions, *etc.* (Kupczynski, 2009, 2011). The aim of most physical experiments is to compare empirical probability distributions with quantum probabilistic predictions. Therefore, all fine structures in time-series of data, if they exist, are averaged out and are not discovered.

Completeness of QM has been discussed for nearly 100 years, but a detailed study of experimental time series of existing experimental data is still to be done. As demonstrated recently with Hans de Raedt, sample inhomogeneity invalidates dramatically significance tests (Kupczynski and De Raedt, 2016); therefore, if sample homogeneity is not tested carefully enough, then the *sample homogeneity loophole* is not closed and statistical inference cannot be trusted (Kupczynski and De Raedt, 2016; Kupczynski, 2015b, 2016b).

11 Conclusion

This review article has explained why speculations about quantum nonlocality and quantum magic are rooted in incorrect interpretations of QM and/or in incorrect "mental pictures" and models that try to explain invisible details of quantum phenomena. In particular, it is not true that in Bell tests, entangled qubits behave as "a pair of dice showing always perfectly correlated outcomes."

We advocate an abstract statistical contextual interpretation (SCI) of QM which is free of paradoxes. SCI rejects the existence of a universal wave function. Quantum probabilities are objective properties of quantum phenomena. Whether these probabilities can be explained as emergent is an open question which cannot be settled by philosophical discussions and no-go theorems; it can be only elucidated by more detailed study of experimental time series of data than is usual.

Bell tests are subtle experiments that are imperfect implementations of an ideal EPRB experiment. It is often claimed that the violation of Bell–CHSH inequalities in these tests allow the rejection with great confidence of *local realism* and *local causality*. Such conclusions, though, are misleading.

Bell–CHSH are trivial properties of N×4 spreadsheets on which the outcomes of measurements of four jointly distributed random variables (e.g., A_x, B_y, $A_{x'}$, $B_{y'}$) are displayed. In Bell tests, such experimental spreadsheets do not exist because there are four pairs of distant random experiments performed using four incompatible experimental settings (x, y). These experiments are described by empirical probability distributions of four pairs of random variables (A_{xy}, B_{xy}). Bell–CHSH inequalities cannot be derived, and estimated pairwise expectations $E(A_{xy}\, B_{xy})$ are not constrained by these inequalities.

Probabilistic couplings can be postulated in order to explain statistical regularities in experimental data, such as $E(A_{xy}B_{xy}) = E(A_xB_y)$. The quantum probabilistic model and Bell-causal hidden variable model can only be tested as plausible probabilistic couplings (Kupczynski, 2024a). Quantum coupling (Equation 7) is constrained by quantum–CHSH inequalities: $|S| \leq 2\sqrt{2}$ (Kupczynski, 2020; Kupczynski, 2024a; Khrennikov, 2019; Cirel'son, 1980; Landau, 1987). Local hidden variable couplings (Equations 11,13, 15–17) are constrained by Bell–CHSH inequalities: $|S| \leq 2$.

It was incorrectly believed that if the *freedom-of-choice* loophole was closed then hidden variables could not statistically depend on randomly chosen binary inputs (settings' labels). This is untrue because variables describing distant measuring instruments used in different settings can depend on inputs and may be correlated due to global rotational symmetry. Therefore, closing the *freedom-of-choice* loophole does not close the *contextuality loophole*.

In contextual hidden variable models (Equations 21–23) and (Equation 25), which are neither Bell-local nor Bell-causal, distant outcomes are locally determined by setting independent hidden variables that describe prepared qubits and setting dependent hidden variables that describe distant measuring instruments and procedures. This model is only constrained by $|S| \leq 4$. Due to global rotational symmetry, the pairwise expectation values of distant random variables (describing Alice's and Bob's outcomes) have to depend on angle $\theta_{xy} = \theta_x - \theta_y$, where (θ_x, θ_y) are the respective angles by which distant qubits are rotated before local read-outs.

We can intuitively explain how parameters describing measuring devices in space-like locations may obey the equation $\mu_y = f(\mu_x, \cos(\theta_{xy}))$, even if (θ_x, θ_y) are chosen perfectly randomly. We imagine two observers in front of two screens on which two identical triangles are projected. They record their observations by six coordinates $\mu=(x_1, y_1; x_2, y_2; x_3, y_3)$. Next, (θ_x, θ_y) are chosen randomly, and rotated triangles are projected onto respective screens. Now the observers' recordings differ: $\mu_x = R(\theta_x)\mu$, $\mu_y = R(\theta_y)\mu$ and $\mu_x = R(\theta_{xy})\mu_y$. Variables describing distant measuring devices and procedures can be strongly correlated without any spooky influences. We used a shortened notation according to which the rotation 2 x 2 matrices are applied at the same time to coordinates of three triangle's vertices.

Therefore, Bell tests prove only that the probabilistic coupling LHVM is inconsistent with the experimental data. They allow the rejection of Bell-locality and Bell-causality assumptions but have little to say about the completeness of QM or *local causality* in nature. As has been observed, *quantum nonlocality* is a misleading notion (Boughn, 2022; Czahor, 1988; Dzhafarov, 2021; Fine, 1982; Hance and Hossenfelder, 2022; Hess and Philipp, 2005; Hess, 2022; Jaynes and Skilling, 1989; Jung, 2017; Khrennikov, 2007; Khrennikov, 2008; Khrennikov, 2019; Khrennikov, 2020a; Khrennikov, 2022; Kupczynski, 2018b; Kupczynski, 2023a; Kupczynski, 2024a; Kupczynski, 2024b; Peres, 1978; Pitovsky, 1983; Pitovsky, 1994; Żukowski and Brukner, 2014; De Raedt et al., 2017; De Raedt et al., 2023; De Raedt et al., 2024; Żukowski and Brukner, 2014; Jung, 2020; Boughn, 2017), and extraordinary metaphysical speculations based on the results of Bell tests are unfounded.

Correlation does not mean causation. Alice's and Bob's experimental outcomes may be correlated, but a probabilistic scatter of Alice's outcomes cannot depend on what Bob is measuring in his distant laboratory. This is called "no-signaling."

No-signaling was verified and confirmed for raw experimental data in all Bell tests. Nevertheless, to study correlations in some experiments involves rejecting single clicks and combining coincident clicks in pairs on Alice's and Bob's detectors. This has created an apparent signaling in some experiments (Hensen et al., 2015; Weihs et al., 2024; Adenier and Khrennikov, 2007; Adenier and Khrennikov, 2017; Bednorz, 2017) which could be explained without evoking spooky influences (Kupczynski, 2017b; Kupczynski, 2021; Kupczynski, 2024a; Khrennikov, 2022). The presence of signaling patterns in the experimental data means that these data have to be described by random variables labelled by both the content and context of the experiment, and of course a joint probability distribution of such variables does not exist.

An external world certainly does exist and it does not depend on whether it is observed or not. Our mathematical models describe only imperfectly its different layers (Kupczynski, 2024c). Quantum phenomena under investigation depend on the detailed contexts of our experiments. The information obtained is contextual and complementary, but quantum probabilities are objective properties of quantum phenomena.

Questions about the completeness of quantum mechanics can only be answered by a search of reproducible fine structures in time series of experimental data which were not predicted by QM. It would not only demonstrate that QM may not provide the most complete description of the individual physical systems but also that QM is not *predictably complete* (Kupczynski, 2006; Kupczynski, 2009; Kupczynski, 2011).

We finish this article with words of Einstein (1936):

Is there really any physicist who believes that we shall never get any insight into these important changes in the single systems, in their structure and their causal connections ... To believe this is logically possible without contradiction; but it is so very contrary to my scientific instinct that I cannot forego the search for a more complete description.

Author contributions

MK: writing – original draft and writing – review and editing.

Funding

The author(s) declare that no financial support was received for the research and/or publication of this article.

Acknowledgments

I express my gratitude to Andrei Khrennikov for his kind hospitality extended to me during several Växjö conferences on the Foundations of Quantum Mechanics and for many stimulating discussions.

Conflict of interest

The author declares that the research was conducted in the absence of any commercial or financial relationships that could be construed as a potential conflict of interest.

The author declares that they were an editorial board member of Frontiers at the time of submission. This had no impact on the peer review process and the final decision.

Generative AI statement

The author(s) declare that no generative AI was used in the creation of this manuscript.

Publisher's note

References

Accardi, L. (1981). Topics in quantum probability. *Phys. Rep.* 77, 169–192. doi:10.1016/0370-1573(81)90070-3

Accardi, L. (2005). Some loopholes to save quantum nonlocality. *AIP Conf. Proc.* 750, 1–19.

Accardi, L., and Regoli, M. (2002). "Locality and Bell's inequality," in *QP-XIII, Foundations of probability and physics*. Editor A. Khrennikov (Singapore: World Scientific), 1–28.

Accardi, L., and Uchiyama, S. (2007). "Universality of the EPR-chameleon model," in *Quantum theory reconsideration of Foundations-4. AIP Conf. Editor G. Adenier*, (NY: Melville: Proc.), 962, 15–27. doi:10.1063/1.2827299

Adenier, G., and Khrennikov, A. (2007). Is the fair sampling assumption supported by EPR experiments? *J. Phys. B At. Mol. Opt. Phys.* 40, 131–141. doi:10.1088/0953-4075/40/1/012

Adenier, G., and Khrennikov, A. (2017). Test of the no-signaling principle in the Hensen loophole-free CHSH experiment. *Fortschr. Der Phys.* 65. doi:10.1002/prop.201600096

Aerts, D. (1982). Example of a macroscopical classical situation that violates Bell inequalities. *Lett. Nuovo Cimento* 34, 107–111. doi:10.1007/bf02817207

Aerts, D. (1986). A possible explanation for the probabilities of quantum mechanics. *J. Math. Phys.* 27, 202–210. doi:10.1063/1.527362

Aerts, D., Aerts, S., Broekaert, J., and Gabora, L. (2000). The violation of Bell inequalities in the Macroworld. *Found. Phys.* 30, 1387.

Allahverdyan, A. E., Balian, R., and Nieuwenhuizen, T. M. (2013). Understanding quantum measurement from the solution of dynamical models. *Phys. Rep.* 525, 1–166. doi:10.1016/j.physrep.2012.11.001

Araujo, M., Quintino, M. T., Budroni, C., Cunha, M. T., and Cabello, A. (2013). All noncontextuality inequalities for the n-cycle scenario. *Phys. Rev. A* 88, 022118. doi:10.1103/physreva.88.022118

Author anonymous Bertrand's paradox (2024a). Accessed January 30, 2025 Available online at: https://en.wikipedia.org/wiki/Bertrand_paradox_.

Author anonymous Matrix mechanics (2024b). Accessed January 30, 25 Available online at: https://en.wikipedia.org/wiki/Matrix_mechanics.

Author anonymous Probability (2024c). Accessed January 30, 2025 Available online at: https://en.wikipedia.org/wiki/Probability.

Ballentine, L. E. (1989). The statistical interpretation of quantum mechanics. *Rev. Mod. Phys.* 42, 358–381. doi:10.1103/revmodphys.42.358

Ballentine, L. E. (1998). *Quantum mechanics: a modern Development*. Singapore: World Scientific.

Bednorz, A. (2017). Analysis of assumptions of recent tests of local realism. *Phys. Rev. A* 95, 042118. doi:10.1103/physreva.95.042118

Bell, J. S. (1965). On the Einstein-Podolsky-Rosen paradox. *Physics* 1, 195–200. doi:10.1103/physicsphysiquefizika.1.195

Bell, J. S. (2004). *Speakable and Unspeakable in quantum mechanics*. Cambridge UP, Cambridge.

Bertrand, J. (1889). "Calcul des probabilités," in *Gauthier-villars*, 5–6.

Blasiak, P., Pothos, E. M., Yearsley, J. M., Gallus, C., and Borsuk, E. (2021). Violations of locality and free choice are equivalent resources in Bell experiments. *Proc. Natl. Acad. Sci. U. S. A.* 118, e2020569118. doi:10.1073/pnas.2020569118

Bohm, D. (1951). *Quantum theory*. New York: Prentice-Hall.

Bohr, N. (1935). Can quantum-mechanical description of physical reality Be considered complete. *Phys. Rev.* 48, 696–702. doi:10.1103/physrev.48.696

Bohr, N. (1963). *Essays 1958-1962 on atomic physics and human knowledge*. NY: Wiley.

Bohr, N. (1987). *The philosophical Writings of Niels Bohr*. Woodbridge, UK: Ox Bow Press.

Born, M., and Jordan, P. (1925). Zur Quantenmechanik. *Z. für Phys.* 34, 858–888. English translation in: B. L. van der Waerden, editor, Sources of Quantum Mechanics (Dover Publications, 1968) ISBN 0-486-61881-1 (English title: On Quantum Mechanics). doi:10.1007/bf01328531

Boughn, S. (2017). Making sense of Bell's theorem and quantum nonlocality. *Found. Phys.* 47, 640–657. doi:10.1007/s10701-017-0083-6

Boughn, S. (2022). There is No spooky action at a distance in quantum mechanics. *Entropy* 24, 560. doi:10.3390/e24040560

Cetto, A. M., Valdes-Hernandez, A., and de la Pena, L. (2020). On the spin projection operator and the probabilistic meaning of the bipartite correlation function. *Found. Phys.* 50, 27–39. doi:10.1007/s10701-019-00313-8

Cirel'son, B. S. (1980). Quantum generalizations of Bell's inequality. *Lett. Math. Phys.* 4 (2), 93–100. doi:10.1007/bf00417500

Clauser, J. F., and Horne, M. A. (1974). Experimental consequences of objective local theories. *Phys. Rev. D.* 10, 526–535. doi:10.1103/physrevd.10.526

Clauser, J. F., Horne, M. A., Shimony, A., and Holt, R. A. (1969). Proposed experiment to test local hidden-variable theories. *Phys. Rev. Lett.* 23, 880–884. doi:10.1103/physrevlett.23.880

Czahor, M. (1988). On some class of random variables leading to violations of Bell inequality. *Phys. Lett.* A129, 6.

De la Peña, L., Cetto, A. M., and Brody, T. A. (1972). On hidden variable theories and Bell's inequality. *Lett. Nuovo Cimento* 5, 177–181. doi:10.1007/bf02815921

De Muynck, V. M., De Baere, W., and Martens, H. (1994). Interpretations of quantum mechanics, joint measurement of incompatible observables and counterfactual definiteness. *Found. Phys.* 24, 1589–1664. doi:10.1007/bf02054787

De Muynck, W. M. (2002). *Foundations of quantum mechanics*. Dordrecht: Kluver Academic.

De Raedt, H., Hess, K., and Michielsen, K. (2011). Extended Boole-Bell inequalities applicable to quantum theory. *J. Comp. Theor. Nanosci.* 8, 1011–1039. doi:10.1166/jctn.2011.1781

De Raedt, H., Katsnelson, M. I., Jattana, M. S., Mehta, V., Willsch, M., Willsch, D., et al. (2023). Einstein–Podolsky–Rosen–Bohm experiments: a discrete data driven approach. *Ann. Phys.* 453, 169314. doi:10.1016/j.aop.2023.169314

De Raedt, H., Katsnelson, M. I., Jattana, M. S., Mehta, V., Willsch, M., Willsch, D., et al. (2024). Can foreign exchange rates violate Bell inequalities? *Ann. Phys.* 469, 169742. doi:10.1016/j.aop.2024.169742

De Raedt, H., Michielsen, K., and Hess, K. (2017). The photon identification loophole in EPRB experiments:computer models with single-wing selection. *Open Phys.* 15, 713–733. doi:10.1515/phys-2017-0085

Dzhafarov, E. N. (2021). Assumption-free derivation of the Bell-type Criteria of contextuality/nonlocality. *Entropy* 23, 1543. doi:10.3390/e23111543

Dzhafarov, E. N., and Kujala, J. V. (2014). Contextuality is about identity of random variables. *PhysicaScripta* T163, 014009. doi:10.1088/0031-8949/2014/t163/014009

Dzhafarov, E. N., &Kujala, J. V., and Larsson, J.-Å. (2015). Contextuality in three types ofquantum-mechanical systems. *Found. Phys.* 7, 762–782. doi:10.1007/s10701-015-9882-9

Einstein, A. (1936). Physics and reality. *J. Frankl. Inst.* 221, 349–382. doi:10.1016/s0016-0032(36)91047-5

Einstein, A. (1949). in *Albert Einstein: Philosopher–Scientist*. Editor P. A. Schilpp (NY: Harper & Row).

Einstein, A., Podolsky, B., and Rosen, N. (1935). Can quantum-mechanical description of physical reality Be considered complete. *Phys. Rev.* 47, 777–780. doi:10.1103/physrev.47.777

Fine, A. (1982). Hidden variables, joint probability and the Bell inequalities. *Phys. Rev. Lett.* 48, 291–295. doi:10.1103/physrevlett.48.291

Gill, R. D. (2014). Statistics, causality and Bell's theorem *Stat. Science. Stat. Sci.* 29, 512. doi:10.1214/14-sts490

Giustina, M., Versteegh, M., Wengerowsky, S., Handsteiner, J., Hochrainer, A., Phelan, K., et al. (2015). Significant-loophole-free test of Bell's theorem with entangled photons. *Phys. Rev. Lett.* 115, 250401. doi:10.1103/physrevlett.115.250401

Hall, M. J. W. (2010). Local deterministic model of singlet state correlations based on Relaxing measurement independence. *Phys. Rev. Lett.* 105, 250404. doi:10.1103/physrevlett.105.250404

Hance, J. R., and Hossenfelder, S. (2022). Bell's theorem allows local theories of quantum mechanics. *Nat. Phys.* 18, 1382. doi:10.1038/s41567-022-01831-5

Handsteiner, J., Friedman, A. S., Rauch, D., Gallicchio, J., Liu, B., Hosp, H., et al. (2017). Cosmic Bell test measurement settings from Milky Way stars. *Phys. Rev. Lett.* 118, 060401. doi:10.1103/physrevlett.118.060401

Heisenberg, W. (1925). Über quantentheoretische Umdeutung kinematischer und mechanischer Beziehungen. *Z. für Phys.* 33, 879–893. English translation in: B. L. van der Waerden, editor, Sources of Quantum Mechanics (Dover Publications, 1968) ISBN 0-486-61881-1 (English title: "Quantum-Theoretical Re-interpretation of Kinematic and Mechanical Relations". doi:10.1007/bf01328377

Heisenberg, W. (1927). Über den anschaulichen Inhalt der quantentheoretischen Kinematik und Mechanik. *Z. für Phys.* 43 (3–4), 172–198. (in German). doi:10.1007/BF01397280

Hensen, B., Bernien, H., Dreau, A. E., Reiserer, A., Kalb, N., Blok, M. S., et al. (2015). Loopholefree Bell inequality violation using electron spins separated by 1.3 kilometres. *Nature* 526, 682–686. doi:10.1038/nature15759

Hess, K. (2014). *Einstein was Right*. Stanford: Pan.

Hess, K. (2022). A Critical review of Works Pertinent to the Einstein-Bohr debate and Bell's theorem. *Symmetry* 14, 163. doi:10.3390/sym14010163

Hess, K., Michielsen, K., and De Raedt, H. (2009). Possible experience: from Boole to Bell. *Europhys. Lett.* 87, 60007. doi:10.1209/0295-5075/87/60007

Hess, K., Michielsen, K., and De Raedt, H. (2016). From Boole to Leggett-Garg: Epistemology of Bell-type inequalities. *Adv. Math. Phys.* 2016, 1–7. doi:10.1155/2016/4623040

Hess, K., and Philipp, W. (2005). Bell's theorem: critique of proofs with and without inequalities. *AIP Conf. Proc.* 750, 150–157. doi:10.1063/1.1874568

Jaynes, E. T. (1989). "Clearing up mysteries - the original goal," *Maximum Entropy and Bayesian methods*. Editor J. Skilling (Dordrecht: Kluwer Academic Publishers), 36, 1–27. doi:10.1007/978-94-015-7860-8_1

Jung, K. (2020). Polarization correlation of entangled photons derived without using non-local interactions ,*Front. Phys.*, 8. doi:10.3389/fphy.2020.00170

Jung, K. (2017). Violation of Bell's inequality: must the Einstein locality really be abandoned? *J. Phys. Conf. Ser.* 880, 012065. doi:10.1088/1742-6596/880/1/012065

Kennard, E. H. (1927). Zur Quantenmechanik einfacher Bewegungstypen. *Z. für Phys.* 44 (4–5), 326–352. doi:10.1007/BF01391200

Khrennikov, A. (2009). *Contextual approach to quantum formalism*. Dordrecht, Netherlands: Springer.

Khrennikov, A. (2016). *Probability and randomness: quantum versus classical*. London, UK: Imperial College Press.

Khrennikov, A. (2019). Get rid of nonlocality from quantum physics. *Entropy* 21, 806. doi:10.3390/e21080806

Khrennikov, A. (2020a). Two faced Janus of quantum nonlocality. *Entropy* 22 (3), 303. doi:10.3390/e22030303

Khrennikov, A. (2020b). Can there be given any meaning to contextuality without incompatibility? *Int. J. Theor. Phys.* 60, 106–114. doi:10.1007/s10773-020-04666-z

Khrennikov, A. (2022). Contextuality, complementarity, signaling, and Bell tests. *Entropy* 24, 1380. doi:10.3390/e24101380

Khrennikov, A. (2024). Växjö interpretation-2003: realism of contexts. Available online at: https://arxiv.org/abs/quant-ph/0401072.

Khrennikov, A. Y. (1999). "Växjö interpretation-2003: realism of contexts," in Interpretations of probability; *VSP Int. Sc. Publishers: Utrecht, The Netherlands*. Tokyo, Japan.

Khrennikov, A. Y. (2007). Bell's inequality: nonlocality, "death of reality", or incompatibility of random variables. *AIP Conf. Proc.* 962, 121–131. doi:10.1063/1.2827294

Khrennikov, A. Y. (2008). Bell-boole inequality: nonlocality or probabilistic incompatibility of random variables? *Entropy* 10, 19–32. doi:10.3390/entropy-e10020019

Kujala, J. V., Dzhafarov, E. N., and Larsson, J.-Å. (2015). Necessary and sufficient conditions for an extended noncontextuality in a Broad class of quantum mechanical systems. *Phys. Rev. Lett.* 115, 150401. doi:10.1103/physrevlett.115.150401

Kupczynski, New test of completeness of quantum mechanics, (1984). ICTP preprint IC/84/242.

Kupczynski, M. (1973). Is Hilbert space language too rich. *Int. J. Theor. Phys.*, 79, 319–343. reprinted in: Hooker, C.A (ed). Physical Theory as Logico-Operational Structure, 89-113. Reidel, Dordrecht, 1978. doi:10.1007/BF01808040

Kupczynski, M. (1974). Tests for the purity of the initial ensemble of states in scattering experiments. *Lett. Nuovo Cimento* 11, 121–124. doi:10.1007/bf02752787

Kupczynski, M. (1977). On some important statistical tests, Riv. *Nuovo Cimento* 7, 215–227.

Kupczynski, M. (1986). On some new tests of completeness of quantum mechanics. *Phys.Lett. A* 116, 417–419. doi:10.1016/0375-9601(86)90372-5

Kupczynski, M. (1987a). Bertrand's paradox and Bell's inequalities. *Phys.Lett. A* 121, 205–207. doi:10.1016/0375-9601(87)90002-8

Kupczynski, M. (1987b). Pitovsky model and complementarity. *Phys.Lett. A* 121, 51–53. doi:10.1016/0375-9601(87)90263-5

Kupczynski, M. (2005). Entanglement and Bell inequalities. *J.Russ.Laser Res.* 26, 514–523. doi:10.1007/s10946-005-0048-7

Kupczynski, M. (2006). Seventy years of the EPR paradox. *AIP Conf. Proc.* 861, 516–523. doi:10.1063/1.2399618

Kupczynski, M. (2009). Is quantum theory predictably complete? *Phys. Scr.* T135, 014005. doi:10.1088/0031-8949/2009/T135/014005

Kupczynski, M. (2011). "Time series, stochastic processes and completeness of quantum theory," in *Time series, stochastic processes and completeness of quantum theory*, 1327. AIP. Conf. Proc., 394–400. doi:10.1063/1.3567465

Kupczynski, M. (2012). Entanglement and quantum nonlocality demystified. *AIP Conf. Proc.* 1508, 253–264. doi:10.1063/1.4773137

Kupczynski, M. (2014). Causality and local determinism versus quantum nonlocality. *J. Phys.Conf. Ser.* 504, 012015. doi:10.1088/1742-6596/504/1/012015

Kupczynski, M. (2015a). Bell inequalities, experimental protocols and contextuality. *Found. Phys.* 45, 735–753. doi:10.1007/s10701-014-9863-4

Kupczynski, M. (2015b). Significance tests and sample homogeneity loophole. arXiv: 1505.06349 [quant-ph]. doi:10.48550/arXiv.1505.06349

Kupczynski, M. (2016a). EPR paradox, quantum nonlocality and physical reality. *J. Phys. Conf. Ser.* 701, 012021. doi:10.1088/1742-6596/701/1/012021

Kupczynski, M. (2016b). Operational approach to entanglement and how to certify it. *Int. J. Quantum Inf.* 14 (4), 1640003. doi:10.1142/S0219749916400037

Kupczynski, M. (2017a). Can we close the Bohr-Einstein quantum debate? *Phil. Trans. R. Soc. A* 375, 20160392. doi:10.1098/rsta.2016,0392

Kupczynski, M. (2017b). Is Einsteinian no-signalling violated in Bell tests? *Open Phys.* 15, 739–753. doi:10.1515/phys-2017-0087

Kupczynski, M. (2018a). Quantum mechanics and modeling of physical reality. *Phys. Scr.* 93 (10pp), 123001. doi:10.1088/1402-4896/aae212

Kupczynski, M. (2018b). Closing the door on quantum nonlocality. *Entropy* 20, 877. doi:10.3390/e20110877

Kupczynski, M. (2020). Is the moon there if nobody looks: Bell inequalities and physical reality. *Front. Phys.* 8, 273. doi:10.3389/fphy.2020.00273

Kupczynski, M. (2021). Contextuality-by-default description of Bell tests: contextuality as the rule and not as an exception. *Entropy* 23, 1104. doi:10.3390/e23091104

Kupczynski, M. (2022). Comment on causal Networks and freedom of choice in Bell's theorem. *Int. J. Quantum Found.* 8 (2), 117–124. doi:10.48550/arXiv.2201.08483

Kupczynski, M. (2023a). Contextuality or nonlocality: what would John Bell choose Today? *Entropy* 25, 280. doi:10.3390/e25020280

Kupczynski, M. (2023b). Response:"Commentary: is the moon there if nobody looks? Bell inequalities and physical reality". *Front. Phys.* 11, 1117843. doi:10.3389/fphy.2023.1117843

Kupczynski, M. (2024a). Quantum nonlocality: how does nature do it? *Entropy* 26, 191. doi:10.3390/e26030191

Kupczynski, M. (2024b). My discussions of quantum Foundations with John Stewart Bell. *Found. Sci.*, 1–20. doi:10.1007/s10699-024-09946-z

Kupczynski, M. (2024c). Mathematical modeling of physical reality: from numbers to Fractals, quantum mechanics and the standard model. *Entropy* 26, 991. doi:10.3390/e26110991

Kupczynski, M. (2007). EPR paradox, locality and completeness of quantum. *AIP Conf. Proc.* 962: 274–285.

Kupczynski, M. (2024d). A comment on: the violations of locality and free choice are equivalent resources in Bell experiments. *arXiv:2105*, 14279. doi:10.48550/arXiv.2105.14279

Kupczynski, M. (2024e). Contextuality as the key to understand quantum paradoxes, *arXiv:2202.09639*. doi:10.48550/arXiv.2202.09639

Kupczynski, M., and De Raedt, H. (2016). Breakdown of statistical inference from some random experiments. *Comput. Phys. Commun.* 200, 168–175. doi:10.1016/j.cpc.2015.11.010

Landau, L. J. (1987). On the violation of Bell's inequality in quantum theory. *Phys. Lett. A* 1 (20)–54.

Larsson, J.-A., and Gill, R. D. (2004). Bell's inequality and the coincidence-time loophole. *Europhys. Lett.* 67, 707–713. doi:10.1209/epl/i2004-10124-7

Mermin, D. (1985). Is the moon there when nobody looks? Reality and the quantum theory. *Phys. Today* 38, 38–47. doi:10.1063/1.880968

Mermin, N. D. (1993). Hidden variables and the two theorems of John Bell. *Rev. Mod. Phys.* 65, 803–815. doi:10.1103/revmodphys.65.803

Michielsen, K., and De Raedt, H. (2014). Event-based simulation of quantum physics experiments. *Int. J. Mod. Phys. C* 25, 1430003–1430066. doi:10.1142/s0129183114300036

Myrvold, W., Genovese, M., and Shimony, A. (2020). in *Bell's theorem. The Stanford Encyclopedia of philosophy. Editor N.Z. Edward*. Fall 2020 Edition. Available online at: https://plato.stanford.edu/archives/fall2020/entries/bell-theorem/(Accessed January 30, 2025).

Nieuwenhuizen, T. M. (2011). Is the contextuality loophole fatal for the derivation of Bell inequalities, Found. *Phys.* 41, 580–591. doi:10.1007/s10701-010-9461-z

Nieuwenhuizen, T. M. (2009). Where Bell went wrong. *AIP Conf. Proc.* 1101, 127–133. doi:10.1063/1.3109932

Nieuwenhuizen, T. M., and Kupczynski, M. (2017). The contextuality loophole is fatal for the derivation of Bell inequalities: Reply to a comment by I. Schmelzer. *Schmelzer. Found. Phys.* 47, 316–319. doi:10.1007/s10701-017-0062-y

Peres, A. (1978). Unperformed experiments have no results. *Am. J. Phys.* 46, 745–747. doi:10.1119/1.11393

Pitovsky, I. (1983). Deterministic model of spin and statistics. *Phys. Rev. D.* 27, 2316–2326. doi:10.1103/physrevd.27.2316

Pitovsky, I. (1994). George Boole's conditions of possible experience and the quantum puzzle, Brit. *J. Phil. Sci.* 45, 95–125.

Plotnitsky, A. (2009). *Epistemology and probability: Bohr, Heisenberg, Schrödinger and the nature of quantum-theoretical Thinking*. Berlin, Germany; New York, NY, USA: Springer.

Plotnitsky, A. (2012). *Niels Bohr and complementarity: an introduction*. Berlin, Germany; New York, NY, USA: Springer.

Robertson, H. P. (1929). The uncertainty principle. *Phys. Rev.* 34 (1), 163–164. doi:10.1103/PhysRev.34.163

Rosenfeld, W., Burchardt, D., Garthoff, R., Redeker, K., Ortegel, N., Rau, M., et al. (2017). Event-ready Bell test using entangled atoms simultaneously closing detection and locality loopholes. *Phys. Rev. Lett.* 119, 010402. doi:10.1103/physrevlett.119.010402

Schlosshauer, M., Kofler, J., and Zeilinger, A. (2013). *A snapshot of foundational attitudes toward quantum mechanics Studies in History and Philosophy of Modern Physics*, 44, 222–230.

Shalm, L. K., Meyer-Scott, E., Christensen, B. G., Bierhorst, P., Wayne, M. A., Stevens, M. J., et al. (2015). Strong loophole-free test of local realism. *Phys. Rev. Lett.* 115, 250402. doi:10.1103/physrevlett.115.250402

Storz, S., Schär, J., Kulikov, A., Magnard, P., Kurpiers, P., Lütolf, J., et al. (2023). Loophole-free Bell inequality violation with superconducting circuits. *Nature* 615, 265–270. doi:10.1038/s41586-023-05885-0

The BIG Bell Test Collaboration (2018). Challenging local realism with human choices. *Nature* 557, 212–216. doi:10.1038/s41586-018-0085-3

Valdenebro, A. (2002). Assumptions underlying Bell's inequalities. *Eur. Jour. Phys.* 23, 569–577. doi:10.1088/0143-0807/23/5/313

Weihs, G., Jennewein, T., Simon, C., Weinfurther, H., and Zeilinger, A. (2024). Violation of Bell's.

Wiseman, H. (2014). The two Bell's theorems of John Bell. *J. Phys. A Math. Theor.* 47, 424001. doi:10.1088/1751-8113/47/42/424001

Zhang, W., van Leent, T., Redeker, K., Garthoff, R., Schwonnek, R., Fertig, F., et al. (2022). A device-independent quantum key distribution system for distant users. *Nature* 607, 687–691. doi:10.1038/s41586-022-04891-y

Zhao, S., De Raedt, H., and Michielsen, K. (2008). Event-by-Event simulation of Einstein-Podolsky-Rosen-Bohm experiments. *Found. Phys.* 38, 322–347. doi:10.1007/s10701-008-9205-5

Żukowski, M., and Brukner, Č. (2014). Quantum non-locality—it ain't necessarily so. *J. Phys. A Math. Theor.* 47, 424009. doi:10.1088/1751-8113/47/42/424009

frontiers | Frontiers in Quantum Science and Technology

TYPE Original Research
PUBLISHED 20 June 2025
DOI 10.3389/frqst.2025.1554763

OPEN ACCESS

EDITED BY
Karl Hess,
University of Illinois at Urbana-Champaign, United States

REVIEWED BY
Juergen Jakumeit,
Access e.V., Germany
Omar Magana-Loaiza,
Louisiana State University, United States

*CORRESPONDENCE
Ana María Cetto,
ana@fisica.unam.mx

†These authors have contributed equally to this work

RECEIVED 02 January 2025
ACCEPTED 09 May 2025
PUBLISHED 20 June 2025

CITATION
Cetto AM and de la Peña L (2025) Signature of matter–field coupling in quantum–mechanical statistics.
Front. Quantum Sci. Technol. 4:1554763.
doi: 10.3389/frqst.2025.1554763

Signature of matter–field coupling in quantum–mechanical statistics

Ana María Cetto*† and Luis de la Peña†

Instituto de Física, Universidad Autónoma de México, Mexico City, Mexico

The connection between the intrinsic angular momentum (spin) of particles and quantum statistics is established by considering the response of identical particles to a common background radiation field. For this purpose, the Hamiltonian analysis previously performed in stochastic electrodynamics to derive the quantum description of a one-particle system is extended to a system of two identical bound particles subject to the same field. Depending on the relative phase of the response of the particles to a common field mode, two types of particles are distinguished by their symmetry or antisymmetry with respect to particle exchange. While any number of identical particles responding in phase can occupy the same energy state, there can only be two particles responding in antiphase. The calculation of bipartite correlations between the response functions reveals maximum entanglement as a consequence of the parallel response of the particles to the common field. The introduction of an internal rotation parameter leads to a direct link between spin and statistics and to a physical rationale for the Pauli exclusion principle.

KEYWORDS

particle-field coupling, resonant response, quantum statistics, symmetry/antisymmetry, Pauli exclusion principle

1 Introduction

The statistics of identical particles is one of the most fundamental quantum features: all quantum particles are known to obey either Fermi–Dirac or Bose–Einstein statistics. It is also well known that the intrinsic angular momentum (spin) of a particle determines its statistics and *vice versa*, with integral-spin particles being bosons and half-integral-spin particles being fermions. The symmetrization postulate and the spin statistics theorem are central to a number of key quantum applications, including all of atomic, molecular, and nuclear physics and quantum statistical physics. Nevertheless, a century after their establishment (Pauli, 1925; Heisenberg, 1926; Dirac, 1926), they continue to be taken as mathematically-justified empirical facts. All known experimental data are consistent with Pauli's exclusion principle, and experiments continue to be carried out to find possible violations of it (Kaplan, 2020). Pauli himself, who gave the first formal proof of the spin-statistics theorem in 1925, expressed his dissatisfaction with this state of affairs two decades later (Pauli, 1946; Pauli, 1950), but explanations continue to rely mainly on formal arguments based on topological properties, group-theoretical considerations, and the like.

All this leads to the conclusion that the physical underpinning of quantum statistics remains to be elucidated. What makes the state vectors of identical multipartite systems either symmetric or antisymmetric? What is the mechanism that "binds" identical particles in such a way that they obey either Fermi or Bose statistics?

The aim of this paper is to provide an answer to these questions based on general principles and previous results from stochastic electrodynamics (SED). Recent work has shown that consideration of the interaction of particles with the electromagnetic radiation field is key to understanding their quantum behavior (de la Peña et al., 2015). The ground state of the radiation field—the zero point field (ZPF)—has been identified as the source of quantum fluctuations and a key factor in driving a bound system to a stationary state. In addition, the quantum operator formalism has been obtained as the algebra describing the response of the particle's dynamical variables to the background field modes responsible for the transitions between stationary states (Cetto and de la Peña, 2024). Furthermore, bipartite entanglement was derived as a consequence of the interaction of two identical particles with the same field modes (de la Peña et al., 2015). Against this background, the theory provides us with a physically grounded explanation of the origin of the symmetry properties of identical quantum particle systems and the resulting statistics.

The paper is structured as follows. Section 2 summarizes the SED Hamiltonian derivation of the quantum operator formalism, which gives sense to this formalism as an algebraic description of the linear (dipolar) resonant response of the particle to a well-defined set of modes of the background radiation field. In Section 3, the expression of the dynamical variables of the particle in terms of linear response coefficients is applied to the analysis of a system of two identical particles in a stationary state. Section 4 identifies two types of particles according to the relative phase of their coupling to a common field mode in the bipartite case, and the multipartite case is briefly discussed. Section 5 shows that the analysis of two-particle correlations leads to entangled symmetric or antisymmetric state vectors. In Section 6, the intrinsic rotation is introduced in order to establish the connection between the spin and the quantum statistics as reflected in the symmetry of the state vector, leading to the Pauli exclusion principle for particles with half-integer spin.

2 Quantum operators as linear response functions

As shown in SED (de la Peña et al., 2015), the dynamics of an otherwise classical charged particle immersed in the zero-point radiation field of energy $\hbar\omega/2$ per mode (ZPF) and subject to a binding force and its own radiation reaction evolves irreversibly into the quantum regime, characterized by the stationary states reached as a result of the average energy balance between radiation reaction and the action of the background field. Cetto and de la Peña (2024) showed by means of a Hamiltonian analysis of the particle–field system that the *nature* of the particle dynamical variables—the kinematics—changes in the transition to the quantum regime. In this regime, $x(t)$, $p(t)$ no longer refer to trajectories but to the linear, resonant *response* of the particle to the driving force of the background field, which effects the transitions between stationary states. The radiative transitions between two states (n,k) involve precisely those field modes to which the particle responds resonantly. Thus, from the initially infinite, continuous set of canonical field variables (q,p), only those $(\mathrm{q}_{nk},\mathrm{p}_{nk})$ so defined are relevant for the description in the quantum regime. Since the memory of the initial particle variables $x(0)$, $p(0)$ is lost and the dynamics are now controlled by the field, the Poisson bracket of the particle canonical variables, which initially is taken with respect to the complete set of (particle + field) variables, reduces to the Poisson bracket with respect to the (relevant) field variables. Therefore, for the particle in a stationary state n (note that Roman letters are used for the canonical field variables),

$$\{x_n(t),p_n(t)\}_{\mathrm{qp}}=1, \tag{1}$$

where

$$\{x_n(t),p_n(t)\}_{\mathrm{qp}}=\sum_{k\neq n}\left(\frac{\partial x_n}{\partial \mathrm{q}_{nk}}\frac{\partial p_n}{\partial \mathrm{p}_{nk}}-\frac{\partial p_n}{\partial \mathrm{q}_{nk}}\frac{\partial x_n}{\partial \mathrm{p}_{nk}}\right).$$

Instead of the canonical field variables (the quadratures) $(\mathrm{q}_{nk},\mathrm{p}_{nk})$, it is convenient to use the (dimensionless) normal variables $a_{nk}=\exp(i\phi_{nk})$, where ϕ_{nk} is a random phase, which are related to the former by

$$\mathrm{q}_{nk}=\sqrt{\frac{\hbar}{2|\omega_{kn}|}}\,(a_{nk}+a_{nk}^{\star}),\quad \mathrm{p}_{nk}=-i\sqrt{\frac{\hbar|\omega_{kn}|}{2}}\,(a_{nk}-a_{nk}^{\star}). \tag{2}$$

This transformation, which takes into account the energy of the field mode of frequency ω_{kn} being equal to $\hbar\omega_{kn}$, is the entry point of Planck's constant in the equations that follow.

With the transformation (2), the Poisson bracket with respect to the normal variables becomes

$$\begin{aligned}\{x(t),p(t)\}_{nn}&\equiv\sum_{k\neq n}\left(\frac{\partial x_n}{\partial a_{nk}}\frac{\partial p_n}{\partial a_{nk}^{\star}}-\frac{\partial p_n}{\partial a_{nk}}\frac{\partial x_n}{\partial a_{nk}^{\star}}\right)\\&=i\hbar\sum_{k\neq n}\left(\frac{\partial x_n}{\partial \mathrm{q}_{nk}}\frac{\partial p_n}{\partial \mathrm{p}_{nk}}-\frac{\partial p_n}{\partial \mathrm{q}_{nk}}\frac{\partial x_n}{\partial \mathrm{p}_{nk}}\right),\end{aligned} \tag{3}$$

and, therefore, according to Equation 1, the transformed Poisson bracket must satisfy

$$\{x(t),p(t)\}_{nn}=i\hbar. \tag{4}$$

From this and Equation 3, it is clear that $x_n(t)$, $p_n(t)$ must indeed be linear functions of the normal variables $\{a_{nk}\}$, $k\neq n$. Thus, $x_n(t)$ becomes expressed in the form (in one dimension, for simplicity)

$$x_n(t)=x_{nn}+\sum_{k\neq n}x_{nk}a_{nk}e^{-i\omega_{kn}t}+\text{c.c.}, \tag{5}$$

where the index k denotes any other state that can be reached by means of a transition from n (hence $k\neq n$), and ω_{kn} is the corresponding transition frequency. The coefficient x_{nk} is the response amplitude of the particle to the field mode of frequency ω_{kn}. More generally, since the field variables connecting different states n,n' are independent random variables, $(\partial a_{nk}/\partial a_{n'k})=\delta_{nn'}$ (for equal times, one may omit the time dependence in the expression) and

$$\{x,p\}_{nn'}=i\hbar\delta_{nn'}. \tag{6}$$

Using Equation 5 for $x_n(t)$ and

$$p_n(t)=m\dot{x}_n(t)=-im\sum_{k\neq n}\omega_{kn}x_{nk}a_{nk}e^{-i\omega_{kn}t}+\text{c.c.} \tag{7}$$

to calculate the derivatives involved in Equation 3, we obtain

$$\{x(t), p(t)\}_{nn} = 2im\sum_{k\neq n}\omega_{kn}|x_{nk}|^2 = i\hbar. \tag{8}$$

For x and p real, $x^*_{nk}(\omega_{nk}) = x_{kn}(\omega_{kn})$, $p^*_{nk}(\omega_{nk}) = p_{kn}(\omega_{kn})$, $a^*_{nk}(\omega_{nk}) = a_{kn}(\omega_{kn})$. This allows us to write Equation 6 in the explicit form

$$\sum_{k\neq n}(x_{nk}p_{kn'} - p_{n'k}x_{kn}) = i\hbar\delta_{nn'}, \tag{9}$$

and to identify the response coefficients x_{nk}, $p_{n'k}$ as the elements of matrices $\hat{x}$, $\hat{p}$ such that

$$[\hat{x}, \hat{p}] = i\hbar. \tag{10}$$

This central result of SED reveals the quantum commutator as *the matrix expression of the Poisson bracket* of the particle variables (x_n, p_n) in any state n with respect to the (relevant) normal field variables corresponding to the modes $\{nk\}$ to which the particle responds resonantly from that state. Furthermore, Equation 8 is identified with the Thomas–Reiche–Kuhn sum rule,

$$2im\sum_{k\neq n}\omega_{kn}|x_{nk}|^2 = i\hbar. \tag{11}$$

In summary, this is the physical essence of the quantum operators: they describe the linear, resonant response of the (bound) particle to a well-defined set of field modes. The response coefficients x_{nk} and the transition frequencies ω_{kn} contained in Equation 5 are characteristic of the mechanical system; the corresponding random normal variables a_{nk} in turn contain information about the (stationary, random) background field. By taking the derivatives of x_n and p_n given by Equations 5, 7 with respect to a_{nk}, a^*_{nk} to calculate the Poisson bracket, the latter are removed from the description; the problem seems to be reduced to be purely mechanical, although it is in essence electrodynamic. Once the operator formalism is adopted, the factor $\hbar$, coming from the transformation expressed in Equation 2, remains the only conspicuous imprint left by the field.

We further note that the structure of the commutator is a direct consequence of the symplectic structure of the problem; this is a feature of the Hamiltonian dynamics that remains intact in the evolution from the initial classical to the quantum regime. The correspondence between classical Poisson brackets and quantum commutators, insightfully established by Dirac on formal grounds, thus finds a physical explanation.

To connect with quantum formalism in the Heisenberg representation, we consider an appropriate Hilbert space on which the operators act. In the present case, the natural choice is the Hilbert space spanned by the set of orthonormal vectors $\{|n\rangle\}$ representing the stationary states with energy $\mathcal{E}_n$. With the components of $\hat{x}(t)$ given by $x_{nk}e^{-i\omega_{kn}t}$ (see Equation 5), we have

$$\hat{x}(t) = \sum_{n,k} x_{nk}e^{-i\omega_{kn}t}|n\rangle\langle k|. \tag{12}$$

The matrix elements of $\hat{x}(t)$ are

$$x_{nk}(t) = \langle n|\hat{x}(t)|k\rangle \tag{13}$$

in the Heisenberg picture, or

$$x_{nk}(t) = \langle n(t)|\hat{x}|k(t)\rangle \tag{14}$$

in the Schrödinger picture, where the time dependence has been transferred to the state vector,

$$|n(t)\rangle = e^{-i\mathcal{E}_nt/\hbar}|n\rangle. \tag{15}$$

Finally, with the evolution of x, p into operators, the initial Hamiltonian equations evolve in the quantum regime into the Heisenberg equations

$$\frac{1}{i\hbar}\left[\hat{x}, \hat{H}\right] = \dot{\hat{x}}, \quad \frac{1}{i\hbar}\left[\hat{p}, \hat{H}\right] = \dot{\hat{p}}, \tag{16}$$

with $\hat{H} = \frac{\hat{p}^2}{2m} + \hat{V}$, $\dot{\hat{x}} = \hat{p}/m$ and $\dot{\hat{p}} = -(\widehat{dV/dx})$. By taking the matrix element (nk) of the first of these equations, we confirm that $\omega_{kn} = (\mathcal{E}_n - \mathcal{E}_k)/\hbar$—that is, that the energy $\hbar\omega_{kn}$ transferred to (or from) the field to the particle in a transition is equal to the energy difference between the two stationary states.

3 Response of a bipartite system to the background field

Now consider a system consisting of two identical particles. When the particles are isolated from each other, they are subject to different realizations of the background field, in which case their behavior can be studied separately for each particle using the procedure above. However, if they are part of one and the same system, they are subject to the same realization of the field and, being identical, they respond to the same set of relevant field modes, whether or not they interact with each other. In the following, we assume that the particles do not interact directly with each other.

Our purpose is to describe the response of the composite system to the background field when in a stationary state characterized by the total energy $\mathcal{E}_{(nm)} = \mathcal{E}_n + \mathcal{E}_m$ with $\mathcal{E}_n \neq \mathcal{E}_m$, the subindices n and m referring to single-particle states. If particle 1 is in state n, it responds to the set of modes $\{nk\}$, and similarly particle 2 in state m responds to the set $\{ml\}$,

$$\begin{aligned} x_{1n}(t) &= \sum_k e^{i\theta^1_{nk}}x_{1nk}a_{nk}e^{-i\omega_{kn}t} + \text{c.c.}, \quad x_{2m}(t) \\ &= \sum_l e^{i\theta^2_{ml}}x_{2ml}a_{ml}e^{-i\omega_{lm}t} + \text{c.c.} \end{aligned} \tag{17}$$

where we have added the factor $\exp(i\theta)$ to each term to allow for the (random) phase of the response of the particle to the field modes.

When $n \neq m$, the sums in Equation 17 involve the different, mutually independent normal variables a_{nk} and a_{ml}, except when $k = m$ and $l = n$, since $a_{nm} = a^*_{mn}$. Therefore, the Poisson bracket of $x_1(t)$ and $x_2(t)$, calculated in the state of the composite system (nm), reduces to a single term:

$$[x_1, x_2]_{(nm)} = \left(\frac{\partial x_{1n}}{\partial a_{nm}}\frac{\partial x_{2m}}{\partial a^*_{nm}} - \frac{\partial x_{2m}}{\partial a_{nm}}\frac{\partial x_{1n}}{\partial a^*_{nm}}\right) = 2i|x_{nm}|^2\sin\theta^{12}_{nm}. \tag{18}$$

Since the particles are identical, the interchange of labels 1 and 2 should not alter the value of the Poisson bracket, and therefore this equation must be equal to 0. This sets an important restriction on the possible values of the phase difference. With

$$\left|\theta^1_{nm} - \theta^2_{nm}\right| = \left|\theta^{12}_{nm}\right| \equiv \pi\zeta^{12}_{nm}, \tag{19}$$

we see that ζ^{12}_{nm} must be an integer so that

$$[x_1, x_2]_{(nm)} = 0 \ \ (n \neq m). \tag{20}$$

Furthermore, with $p_2(t)$ obtained from the second Equation 17,

$$p_{2m}(t) = -im \sum_l e^{i\theta^2_{ml}} \omega_{lm} x_{2ml} a_{ml} e^{-i\omega_{lm}t} + \text{c.c.},$$

the Poisson bracket of $x_1(t)$ and $p_2(t)$ calculated for the same state (nm) gives

$$[x_1, p_2]_{(nm)} = \left(\frac{\partial x_{1n}}{\partial a_{nm}} \frac{\partial p_{2m}}{\partial a^\star_{nm}} - \frac{\partial p_{2m}}{\partial a_{nm}} \frac{\partial x_{1n}}{\partial a^\star_{nm}} \right) = 2im\omega_{mn} |x_{nm}|^2 \cos\theta^{12}_{nm}. \tag{21}$$

In terms of the parameter ζ^{12}_{nm} defined in Equation 19, we have

$$\cos\theta^{12}_{nm} = (-1)^{\zeta^{12}_{nm}}, \ \ \zeta^{12}_{nm} = 0, 1, 2, \ldots. \tag{22}$$

and therefore, from Equation 21,

$$[x_1, p_2]_{(nm)} = (-1)^{\zeta^{12}_{nm}} 2im\omega_{mn} |x_{nm}|^2. \tag{23}$$

This result shows that a correlation is established between the response variables of the two particles to the shared field mode (nm) for $n \neq m$; in other words, the field mode serves as a bridge between the particles and correlates their responses. It is important to note that Equation 23 involves only the field mode connecting the two states with $\mathcal{E}_n \neq \mathcal{E}_m$, and it is different from O only when these states are connected by a dipolar transition element, $x_{nm} \neq 0$.

We now consider two equal particles in the same energy state: $n = m$. In this case, the particles share all field modes, so that the Poisson brackets become, by virtue of Equation 22,

$$[x_1, x_2]_{(nn)} = \sum_k \left(\frac{\partial x_{1n}}{\partial a_{nk}} \frac{\partial x_{2n}}{\partial a^\star_{nk}} - \frac{\partial x_{2n}}{\partial a_{nk}} \frac{\partial x_{1n}}{\partial a^\star_{nk}} \right) = 2i \sum_k \sin\theta^{12}_{nk} |x_{nk}|^2 = 0, \tag{24}$$

$$[x_1, p_2]_{(nn)} = \sum_k \left(\frac{\partial x_{1n}}{\partial a_{nk}} \frac{\partial p_{2n}}{\partial a^\star_{nk}} - \frac{\partial p_{2n}}{\partial a_{nk}} \frac{\partial x_{1n}}{\partial a^\star_{nk}} \right)$$
$$= 2im \sum_k \omega_{kn} \cos\theta^{12}_{nk} |x_{nk}|^2 = 2im \sum_k (-1)^{\zeta^{12}_{nk}} \omega_{kn} |x_{nk}|^2. \tag{25}$$

4 Two families of particles

Equation 23 indicates that there are two distinct types of identical particles, depending on whether the phase parameter ζ^{12}_{nm} given by Equation 19 is an even or odd number. Since this condition applies to all modes that are shared by the two particles, we can write, using Equation 19:

$$\zeta^{12}_{nm} = \zeta^{12} = |\zeta^1 - \zeta^2|, \tag{26}$$

so that the two types of particles are characterized by

$$\text{Type B:} \ \ \zeta^{12}_B = 0, 2, 4, \ldots, \tag{27a}$$
$$\text{Type F:} \ \ \zeta^{12}_F = 1, 3, 5, \ldots. \tag{27b}$$

In Appendix A, it is shown that for all ζ^{12}_B to be even, the individual ζ^i_B must be integers, and that for all ζ^{12}_F to be odd, the individual ζ^i_F must be half-integers:

$$\text{Type B:} \ \ |\zeta^i_B| = 0, 1, 2, \ldots \Upsilon_B, \tag{28a}$$
$$\text{Type F:} \ \ |\zeta^i_F| = \frac{1}{2}, \frac{3}{2}, \frac{5}{2}, \ldots \Upsilon_F, \tag{28b}$$

where Υ_B and Υ_F are the maximum values of the individual ζ^i_B, ζ^i_F. This means that B and F actually stand for two distinct families of particles, the members of which are characterized by the respective value of Υ. Identical particles of family B can have any value of ζ^i_B integer such that $|\zeta^i_B| \leq \Upsilon_B$, but when combined they must satisfy Equation 27a; similarly, those of family F must satisfy Equation 27b. In other words, according to Equations 27a, b, only pairwise combinations of ζ^i_B that are even and only pairwise combinations of ζ^i_F that are odd are allowed. Since, in both cases, ζ^i can be positive or negative, this gives a total of $g = 2\Upsilon + 1$ possible different states of the bipartite system.

With these results, Equation 17 take the form (except for a remaining common phase factor $e^{i\theta}$ that can be neglected)

$$x_{1n}(t) = e^{i\pi\zeta^1} \sum_k x_{1nk} a_{nk} e^{-i\omega_{kn}t} + \text{c.c.},$$
$$x_{2m}(t) = e^{i\pi\zeta^2} \sum_l x_{2ml} a_{ml} e^{-i\omega_{lm}t} + \text{c.c.}, \tag{29}$$

and Equation 25 is reduced to

$$[x_1, p_2]_{(nn)} = (-1)^{\zeta^{12}} i\hbar. \tag{30}$$

Therefore, in comparison with the one-particle commutator $[x_1, p_1]_{(nn)} = i\hbar$, we note that in the B case—when Equation 27a holds—particle 2 responds in the same way as particle 1. Indeed, according to Equation 19, the response of the two particles to the shared field modes is *in phase*, and a correlation is established between the particles. By contrast, according to Equation 27b, ζ^{12}_F is an odd number; hence, the response of the two identical type F particles to the shared field modes is *in antiphase*.

4.1 Extension to three or more particles

In light of the above results, we now briefly analyze the possible correlations for a system composed of three or more identical particles.

In the first case of three type-B particles, when total energy $\mathcal{E}_{(nml)} = \mathcal{E}_n + \mathcal{E}_m + \mathcal{E}_l$ with $\mathcal{E}_n \neq \mathcal{E}_m \neq \mathcal{E}_l$, Equation 27a applies, and the three particles are pairwise correlated. According to Equation 30, correlation also exists when $\mathcal{E}_n \neq \mathcal{E}_m = \mathcal{E}_l$ or $\mathcal{E}_n = \mathcal{E}_m = \mathcal{E}_l$ because the responses of the three particles to common field modes are always in phase. Therefore, all three particles may in principle occupy the same state n and respond coherently. The argument can of course be extended to four or more particles; consequently, there may in principle be an arbitrary number N of type-B particles in the same state and responding coherently to the field modes, like a well-disciplined troop.

In the type-F case, we have already concluded that particles 1 and 2 respond in antiphase to a common mode, and the same applies of course to any pair of identical particles. When total energy $\mathcal{E}_{(nml)} = \mathcal{E}_n + \mathcal{E}_m + \mathcal{E}_l$ with $\mathcal{E}_n \neq \mathcal{E}_m \neq \mathcal{E}_l$, the three particles are pairwise correlated according to Equation 27b. However, when at least two energy levels coincide, two particles respond in antiphase

to the shared modes, thus preventing a third one from responding in antiphase to the same modes and therefore from being correlated to the other two. Therefore, contrary to the type-B case, there can be no coherent response of more than two type-F particles in this case.

5 Field-induced covariance and entanglement

To calculate the effect of the background field on the correlation of the responses, we consider two generic dynamical variables associated with particles 1 and 2. These can be the variables $x(t)$ and $p(t)$ considered so far, a linear combination of them, or any other variable of the form given by Equation 29, where n, m are, as before, two stationary states of the system, with energies $\mathcal{E}_n, \mathcal{E}_m$,

$$f_{1n}(t) = f_{1nn} + e^{i\pi\zeta^1} \sum_{k\neq n} f_{1nk} a_{nk} e^{-i\omega_{kn}t} + \text{c.c.}, \tag{31}$$

$$g_{2m}(t) = g_{2mm} + e^{i\pi\zeta^2} \sum_{l\neq m} g_{2ml} a_{ml} e^{-i\omega_{lm}t} + \text{c.c.}, \tag{32}$$

The time-independent terms in these equations represent in each case the average value of the function, taken over the distribution of the normal variables $a_{nk} = \exp(i\phi_{nk})$ where ϕ_{nk} is a random phase, as mentioned in Section 2,

$$\overline{f_{1n}(t)} = f_{1nn},\ \overline{g_{2m}(t)} = g_{2mm}. \tag{33}$$

To calculate the correlation, we take the average of the product of $f_1(t)$ and $g_2(t)$. When particles 1 and 2 do not form part of the same system, they respond to independent realizations of the field modes, and therefore the covariance is given by

$$\Gamma(f_{1n}g_{2m}) = \left(\overline{f_{1n}(t)} - f_{1nn}\right)\left(\overline{g_{2m}(t)} - g_{2mm}\right) = 0, \tag{34}$$

which simply confirms that the variables are not correlated.

However, when the particles form a bipartite system, they respond to the same realization of the field modes. To calculate the covariance in this case, we must take into account the double degeneracy of the combined state, $\mathcal{E} = \mathcal{E}_{1n} + \mathcal{E}_{2m} = \mathcal{E}_{1m} + \mathcal{E}_{2n}$. In order to distinguish between the two configurations, we define

$$\mathcal{E}_C = \mathcal{E}_{1n} + \mathcal{E}_{2m},\ \mathcal{E}_D = \mathcal{E}_{1m} + \mathcal{E}_{2n}. \tag{35}$$

Let us consider the first case, $\mathcal{E}_C = \mathcal{E}_{1n} + \mathcal{E}_{2m}$, and use Equations 31, 32 to calculate the average product of $f_1(t)$ and $g_2(t)$, which we call $\overline{fg}^C$ (the left factor always refers to particle 1 and the right to particle 2, so that we omit the indices 1 and 2 in the following). Taking into account that, for random independent normal variables, $\overline{a_{ij}a_{jk}} = \overline{a_{ij}a_{kj}^*} = \delta_{ik}$ and hence

$$\overline{a_{nk}a_{ml}} = \delta_{nk}\delta_{ml} + \delta_{nl}\delta_{km}, \tag{36}$$

we obtain

$$\overline{fg}^C = f_{nn}g_{mm} + (-1)^\zeta f_{nm}g_{mn}. \tag{37}$$

Similarly, for the D configuration, we obtain

$$\overline{fg}^D = f_{mm}g_{nn} + (-1)^\zeta f_{mn}g_{nm}. \tag{38}$$

Since the two configurations have the same weight, the averages of $f_1(t)$ and $g_2(t)$ are

$$\bar{f} = \frac{1}{2}(f_{nn} + f_{mm}),\ \bar{g} = \frac{1}{2}(g_{nn} + g_{mm}),$$

and the average of the product of $f_1(t)$ and $g_2(t)$ is given by

$$\begin{aligned}\overline{fg} &= \frac{1}{2}\left(\overline{fg}^C + \overline{fg}^D\right)\\ &= \frac{1}{2}\left[f_{nn}g_{mm} + (-1)^\zeta f_{nm}g_{mn} + f_{mm}g_{nn} + (-1)^\zeta f_{mn}g_{nm}\right].\end{aligned} \tag{39}$$

The covariance is therefore given by

$$\begin{aligned}\Gamma(fg) &= \overline{fg} - \bar{f}\bar{g}\\ &-\frac{1}{4}(f_{nn} - f_{mm})(g_{nn} - g_{mm}) + \frac{1}{2}(-1)^\zeta\left[f_{nm}g_{mn} + f_{mn}g_{nm}\right].\end{aligned} \tag{40}$$

In this equation, the two contributions to the covariance are of a very different nature: the first is a classical covariance of f_1 and g_2 due to the different average values of these functions in states n, m under the condition of degeneracy, $\mathcal{E}_{1n} + \mathcal{E}_{2m} = \mathcal{E}_{1m} + \mathcal{E}_{2n}$. The second term, though, has no classical counterpart: it is entirely due to the joint response of particles 1 and 2 to the shared mode (nm) and is therefore a signature of the matter–field interaction. Evidently, both particles must respond to the mode (nm) for this term not to be zero; if any of the two matrices $\hat{f}, \hat{g}$ is diagonal, there is no quantum contribution to $\Gamma(fg)$.

5.1 Emergence of entanglement

In quantum formalism, entanglement is reflected in the non-factorizability of the bipartite state vector. Therefore, in order to show the emergence of entanglement in the present context, we will translate Equation 40 into the language of the product Hilbert space $\mathrm{H}_1 \otimes \mathrm{H}_2$, where $\mathrm{H}_1, \mathrm{H}_2$ are respectively spanned by the sets of orthonormal state vectors $\{|n\rangle\}$ of particles 1 and 2 (see Section 2 for the one-particle case). In the shorthand notation introduced above, configurations C, D are represented by the product state vectors

$$|C\rangle = |n\rangle_1|m\rangle_2,\ |D\rangle = |m\rangle_1|n\rangle_2. \tag{41}$$

In this notation, Equation 40 reads

$$\begin{aligned}\Gamma(fg) = &-\frac{1}{4}(f_{nn} + f_{mm})(g_{nn} + g_{mm})\\ &+\frac{1}{2}\langle C + (-1)^\zeta D|\hat{f}\hat{g}|C + (-1)^\zeta D\rangle.\end{aligned} \tag{42}$$

In writing the second term, we have used the fact that $(-1)^\zeta = \pm 1$ according to Equations 27a and b. Note that the average of fg is now taken over the (normalized) state vector

$$|\Psi\rangle \equiv \frac{1}{\sqrt{2}}|C + (-1)^\zeta D\rangle, \tag{43}$$

or in terms of the individual state vectors,

$$|\Psi\rangle = \frac{1}{\sqrt{2}}\left[|n\rangle_1|m\rangle_2 + (-1)^\zeta|m\rangle_1|n\rangle_2\right]. \tag{44}$$

As a result, we obtain

$$\Gamma(fg) = \langle\Psi|\hat{f}\hat{g}|\Psi\rangle - \langle\Psi|\hat{f}|\Psi\rangle\langle\Psi|\hat{g}|\Psi\rangle, \tag{45}$$

which is exactly the quantum covariance of $\hat{f}\hat{g}$ calculated in the entangled state given by Equation 44. The covariance coincides with the correlation of f and g since the state vector $|\Psi\rangle$ is normalized to unity.

We stress that the above calculation is restricted to the case $n \neq m$; when $n = m$, there is no field mode correlating the responses of the two particles, so there is no entanglement. On the other hand, if there is degeneracy—that is, $\mathcal{E}_C = \mathcal{E}_D$—the two-particle system is necessarily in an entangled state if f_{nm}, g_{mn} are different from zero—that is, if the response variables f, g connect the single-particle states n, m. The origin of the entanglement is thus traced back to the action of the common relevant field mode (nm), and the responses of the two particles to this mode are maximally correlated (anticorrelated) according to Equation 40 with $(-1)^\zeta = +1$ (-1). More generally, entanglement occurs whenever there is degeneracy, be it in energy or any other variable that defines the state of the bipartite system, as discussed in the next section.

Equations 43–45 were previously obtained in the context of SED by a somewhat laborious procedure using the Hilbert-space formalism. In contrast to such an abstract procedure, the present derivation has the advantage of keeping track at every moment of the physical quantities involved: the field mode variables, the particles' response variables, and the phase difference of the responses.

It is clear from Equation 44 that the two families of identical particles identified in Section 4 are distinguished by their entangled state vectors. The symmetry or antisymmetry of the state vector is uniquely linked to the phase difference of the responses of the two particles to the shared field mode. When the coupling is in phase (type B particles), the state vector is symmetric with respect to the exchange of particles; when the relative coupling is out of phase (type F particles), the state vector is antisymmetric.

It should be stressed that no direct interaction between the components of the system is involved in the derivation leading to entangled states; entanglement arises as a result of their indirect interaction via the shared field modes and, therefore, does not entail a non-local action.

6 The Pauli exclusion principle

6.1 Introduction of spin

Among the various proposals that have been made to justify the spin-statistics theorem, some that are relevant to this work involve the inclusion of the internal (spin) coordinates among the parameters affected by the exchange operation (e.g. Hunter et al., 2005 and Jabs, 2010, and additional references cited the latter). In particular, in Jabs (2010), the spin–statistics connection is derived under the postulates that the original and the exchange wave functions are simply added and the azimuthal phase angle, which defines the orientation of the spin part of each single-particle spin component in the plane normal to the spin-quantization axis, is exchanged along with the other parameters.

In dipolar transitions, atomic electrons interact with field modes of circular polarization, as expressed in the selection rule $\triangle l = \pm 1$, and is increasingly exploited for practical applications in spin-resolved spectroscopy and magneto-optics (e.g. Okuda et al., 2011; De et al., 2021). Furthermore, the interaction of the particle with circular polarized modes of the ZPF, which are known to have an intrinsic angular momentum equal to $\hbar/2$ (Sobelman, 1979; Mandel and Wolf, 1995), was indeed shown in Cetto et al. (2014) to be responsible for the origin of the electron spin itself. It is reasonable to assume that a similar mechanism is responsible for the neutron spin, since the neutron has a magnetic moment that couples to the radiation field.

Therefore, following Jabs (2010) and Cetto and de la Peña (2015), in order to include the spin in the present analysis, we add an (internal) rotation angle ϕ to the expression for the dynamic variables. Strictly speaking, the problem becomes a three-dimensional one. However, for simplicity, we can still use our one-dimensional expressions for the dynamic variables if we decompose the radiation field into (statistically independent) modes of circular polarization. So instead of (31) and (32), we write

$$f_{1n}(t,\phi) = e^{i\pi\zeta^1} \sum_k f_{1nk} a_{nk} e^{i\gamma_{nk}\phi - i\omega_{kn}t} + \text{c.c.}, \tag{46}$$

$$g_{2m}(t) = e^{i\pi\zeta^2} \sum_l g_{2ml} a_{ml} e^{i\gamma_{ml}\phi - i\omega_{lm}t} + \text{c.c.}, \tag{47}$$

where $\gamma_{nk}\phi$ is the difference of two rotation angles,

$$\gamma_{nk}\phi = (\gamma_n - \gamma_k)\phi, \tag{48}$$

and γ_n, γ_k stand for counterclockwise (clockwise) rotation. If n, m are two stationary states of a system of identical particles, as before, we obtain for the partial covariances in configurations C and D (see Equations 37 and 38)

$$\overline{fg}^C = f_{nn} g_{mm} + (-1)^\zeta f_{nm} e^{i\gamma_{nm}\phi} g_{mn} e^{i\gamma_{mn}\phi}, \tag{49}$$

$$\overline{fg}^D = f_{mm} g_{nn} + (-1)^\zeta f_{mn} e^{i\gamma_{mn}\phi} g_{nm} e^{i\gamma_{nm}\phi}, \tag{50}$$

and, therefore,

$$\overline{fg} = \frac{1}{2}\left(\overline{fg}^C + \overline{fg}^D\right) = \frac{1}{2}\left[f_{nn} g_{mm} + f_{mm} g_{nn}\right] + \frac{1}{2}(-1)^\zeta \left[f_{nm} e^{i\gamma_{nm}\phi} g_{mn} e^{i\gamma_{mn}\phi} + f_{mn} e^{i\gamma_{mn}\phi} g_{nm} e^{i\gamma_{nm}\phi}\right]. \tag{51}$$

By translating this result into the language of the product Hilbert space and using Equation 48, we obtain after some algebra

$$\Gamma(fg) = \langle\Psi|\hat{f}\hat{g}|\Psi\rangle - \langle\Psi|\hat{f}|\Psi\rangle\langle\Psi|\hat{g}|\Psi\rangle, \tag{52}$$

where $|\Psi\rangle$ now stands for the complete bipartite state vector, including the internal rotation components,

$$|\Psi\rangle \equiv \frac{1}{\sqrt{2}}\left|e^{-i\gamma_n\phi} e^{-i\gamma_m\phi} C + (-1)^\zeta e^{-i\gamma_m\phi} e^{-i\gamma_n\phi} D\right\rangle = \frac{1}{\sqrt{2}}\left|e^{-i\gamma_n\phi}|n\rangle_1 e^{-i\gamma_m\phi}|m\rangle_2 + (-1)^\zeta e^{-i\gamma_m\phi}|m\rangle_1^{-i\gamma_n\phi}|n\rangle_2\right\rangle. \tag{53}$$

In Equation 53, the first angular factor is always associated with particle 1 and the second with particle 2. This suggests writing each individual state vector in the form $e^{-i\gamma\phi}|n\rangle$. In quantum language, this implies the introduction of two orthonormal vectors $|\gamma\rangle = |+\rangle, |-\rangle$ spanning the two-dimensional Hilbert space, $|n\rangle|\gamma\rangle \equiv |n\gamma\rangle$; Equation 53 thus takes the form

$$|\Psi\rangle = \frac{1}{\sqrt{2}}\left[|n\gamma_n\rangle_1 |m\gamma_m\rangle_2 + (-1)^\zeta |m\gamma_m\rangle_1 |n\gamma_n\rangle_2\right]. \tag{54}$$

Since the parameter γ is associated with the internal rotation, we identify it with the spin of the electron, which means that

$$\gamma_{n,m} = \pm\frac{1}{2}. \tag{55}$$

6.2 The connection between spin and symmetry

We now examine the symmetry properties of the complete entangled state function (53) under particle exchange. When particles 1 and 2 are exchanged, in addition to switching their positions in three-dimensional space, their internal angles change: particle 1 rotates to the azimuthal position of particle 2 and *vice versa*, with both rotations occurring in the same direction (clockwise or counterclockwise). Consider a clockwise rotation. As shown in Jabs (2010) and Cetto and de la Peña (2015), when $\phi_2 > \phi_1$ ϕ_1 transforms into ϕ_2 and ϕ_2 transforms into $\phi_1 + 2\pi$,

$$\phi_2 - \phi_1 \rightarrow \phi_1 - \phi_2 + 2\pi, \tag{56}$$

and $|\Psi\rangle$ given by Equation 53 transform into

$$|\Psi\rangle_{1\longleftrightarrow 2} = \frac{1}{\sqrt{2}}\left|e^{-i\gamma_m(\phi+2\pi)}|m\rangle_1 e^{-i\gamma_n\phi}|n\rangle_2 + (-1)^{\zeta}e^{-i\gamma_n(\phi+2\pi)}|n\rangle_1 e^{-i\gamma_m\phi}|m\rangle_2\right\rangle.$$

Since γ_n, γ_m are half-integers, the overall effect of the particle exchange is to multiply the original state vector by a factor of

$$|\Psi\rangle_{1\longleftrightarrow 2} = (-1)^{\zeta}(-1)^{2\gamma_n}|\Psi\rangle. \tag{57}$$

If instead $\phi_2 < \phi_1$, ϕ_2 transforms into ϕ_1 and ϕ_1 transforms into $\phi_2 + 2\pi$, so that

$$\phi_2 - \phi_1 \rightarrow \phi_1 - \phi_2 - 2\pi, \tag{58}$$

and the transformation of the state vector is again given by Equation 57. Of course, the same result is obtained if the rotation is anticlockwise. Since particles 1 and 2 are identical, their exchange should have no effect on the state vector, which implies that

$$(-1)^{\zeta}(-1)^{2\gamma_n} = 1. \tag{59}$$

Therefore, taking into account Equation 55, we conclude that $(-1)^{\zeta} = -1$. Thus, symmetry of the total state vector under particle exchange, obtained from Equation 54 with $(-1)^{\zeta} = -1$,

$$|\Psi\rangle = \frac{1}{\sqrt{2}}\left[|n\gamma_n\rangle_1|m\gamma_m\rangle_2 - |m\gamma_m\rangle_1|n\gamma_n\rangle_2\right]. \tag{60}$$

implies antisymmetry of the (energy) state vector (44),

$$|\Psi\rangle = \frac{1}{\sqrt{2}}\left[|n\rangle_1|m\rangle_2 - |m\rangle_1|n\rangle_2\right]. \tag{61}$$

6.3 The Pauli principle

The above procedure is of course applicable to particles with higher spin; thus, for any half-integer value of γ, $(-1)^{2\gamma} = -1$ and according to Equation 59, the bipartite (energy) state vector will be antisymmetric with respect to particle exchange, as in Equation 61.

We recall that Equation 61 is valid for $|n\rangle \neq |m\rangle$. If $|n\rangle = |m\rangle$ and the spin is not taken into account, the state vector is simply the product of the individual energy eigenvectors, $|\Psi\rangle = |n\rangle_1|n\rangle_2$; according to Equation 40 the particle variables are not correlated and the bipartite system is obviously not entangled. However, with the introduction of spin, the complete state function is different from zero for $|n\rangle = |m\rangle$, under the condition that $|\gamma_n\rangle \neq |\gamma_m\rangle$. If this is the case, Equation 60 is reduced to

$$|\Psi\rangle = \frac{|n\rangle_1|n\rangle_2}{\sqrt{2}}\left[\left|\gamma_1\right\rangle\left|\gamma_2\right\rangle - \left|\gamma_2\right\rangle\left|\gamma_1\right\rangle\right]. \tag{62}$$

In other words, entanglement can arise from energy degeneracy, if $\mathcal{E} = \mathcal{E}_n + \mathcal{E}_m$ with $\mathcal{E}_n \neq \mathcal{E}_m$, or from spin degeneracy, if $\gamma = \gamma_1 + \gamma_2$ with $\gamma_1 \neq \gamma_2$. Since for the electron (and other spin-1/2 particles) $\gamma_i = \pm\frac{1}{2}$, Equation 62 takes the form (except for an irrelevant overall sign)

$$|\Psi\rangle = \frac{|n\rangle_1|n\rangle_2}{\sqrt{2}}\left[\left|\frac{1}{2}\right\rangle\left|-\frac{1}{2}\right\rangle - \left|-\frac{1}{2}\right\rangle\left|\frac{1}{2}\right\rangle\right]. \tag{63}$$

In Section 5, it was shown that the correlation between particle variables results from the antiphase response to the single common field mode of frequency ω_{mn} with $\mathcal{E}_n \neq \mathcal{E}_m$. On the other hand, when $|n\rangle = |m\rangle$, we note from Equation 25 that the two particles respond in antiphase to all (common) field modes; in this case, correlation is established as a result of the response of both particles to a common field mode of circular polarization. In other words, the entanglement results not from the response to a single mode connecting two states separated by their energies, $\triangle\mathcal{E}_{nm} = |\mathcal{E}_n - \mathcal{E}_m|$ but from a mode connecting two states separated by their spins, $\triangle\gamma_{12} = |\gamma_1 - \gamma_2|$. Just as in the first case $\triangle\mathcal{E} = \hbar\omega_{mn}$ is the energy exchanged with the field in a transition, in the second case $\hbar\triangle\gamma_{12} = \hbar$ is the angular momentum exchanged with the field in a transition.

Equation 63 leaves no room for a third electron in the same energy state $|n\rangle$ because its spin parameter would be either equal to γ_1 or γ_2. The conclusion holds for any pair of identical half-integer spins because the condition $\triangle\gamma_{ij} = |\gamma_i - \gamma_j| = 1$ cannot be satisfied simultaneously for $i.j = 1, 2, 3$: if two half-integer values of γ satisfy $\triangle\gamma_{ij} = 1$, the third value of γ differs from the first two by an even number. To illustrate, consider $\Gamma_F = \frac{3}{2}$. Possible pairs (γ_1, γ_2) are $(\frac{3}{2}, \frac{1}{2})$, $(\frac{3}{2}, \frac{-3}{2})$, and $(-\frac{3}{2}, -\frac{1}{2})$; there is no γ_3 that simultaneously satisfies $\triangle\gamma_{31} = |\gamma_3 - \gamma_1| = 1$ and $\triangle\gamma_{32} = |\gamma_3 - \gamma_2| = 1$.

This is a clear example of Pauli's exclusion principle. The present discussion reveals the physical basis of the phenomenon: two particles in the same energy state respond in antiphase to a single (circularly polarized) mode of the field and a third particle cannot respond in antiphase to the first two.

7 Discussion

In this work, the symmetrization postulate and the spin-statistics theorem were shown to follow from the in-phase or antiphase response of identical particles to specific modes of the common background radiation field. The inclusion of spin in the

analysis allowed the identification of the type B and F families introduced in Section 4 as bosons and fermions and led to the Pauli exclusion principle in the case of fermions.

Key quantum phenomena that were introduced as postulates in the foundational phase of quantum mechanics and that have been repeatedly confirmed both formally and experimentally thus find a physical justification. The picture provided by the present approach is very suggestive. In particular, it shows that the collective behavior of identical particles, which leads to the respective quantum statistics, is a consequence of the mediation of specific field modes that "connect" the particles and correlate their dynamics, producing entanglement. A mysterious, apparently non-local connection between particles, as described by quantum formalism, is thus shown to be an entirely causal and local effect of the bridging role of the common background field. Given the increasing attention paid to entanglement phenomena and their applications, particularly in the fields of quantum information, computing, and communication, the insight gained from this perspective should prove highly fruitful. In particular, since entanglement and other quantum phenomena discussed here are shown to depend critically on the correlations established between identical particles by their coherent binding to certain common field modes, the cancellation or significant modification of these modes by Casimir cavity techniques (e.g. Kleppner, 1986; Walther et al., 2006) could be an interesting way to analyze the effect on such correlations.

The results reported here suggest further investigation. In particular, extending the one-dimensional analysis carried out here to three dimensions would allow an adequate treatment of more general problems involving additional dynamical variables, including orbital angular momentum.

Data availability statement

The original contributions presented in the study are included in the article; further inquiries can be directed to the corresponding author.

Author contributions

AC: conceptualization, investigation, writing – original draft, and writing – review and editing. LP: writing – original draft, writing – review and editing, conceptualization, and investigation.

Funding

The author(s) declare that no financial support was received for the research and/or publication of this article.

Acknowledgments

We would like to thank the reviewers for their constructive comments, which helped improve the clarity of the exposition.

Conflict of interest

The authors declare that the research was conducted in the absence of any commercial or financial relationships that could be construed as a potential conflict of interest.

Generative AI statement

The author(s) declare that no Generative AI was used in the creation of this manuscript.

Publisher's note

References

Cetto, A. M., and de la Peña, L. (2015). Electron system correlated by the zero-point field: physical explanation for the spin-statistics connection. *J. Phys. Conf. Ser.* 701, 012008. doi:10.1088/1742-6596/701/1/012008

Cetto, A. M., and de la Peña, L. (2024). The radiation field, at the origin of the quantum canonical operators. *Found. Phys.* 54, 51. doi:10.1007/s10701-024-00775-5

Cetto, A. M., de la Peña, L., and Valdés-Hernández, A. (2014). Emergence of quantization: the spin of the electron. *J. Phys. Conf. Ser.* 504, 012007.

De, A., Bhowmick, T. K., and Lake, R. K. (2021). Anomalous magneto-optical effects in an antiferromagnet–topological-insulator heterostructure. *Phys. Rev. Appl.* 16, 014043. doi:10.1103/physrevapplied.16.014043

de la Peña, L., Cetto, A. M., and Valdés-Hernández, A. (2015). "The emerging quantum," in *The physics behind quantum mechanics.* Springer. doi:10.1007/978-3-319-07893-9

Dirac, P. A. M. (1926). On the theory of quantum mechanics. *Proc. R. Soc. Lond. A* 112, 661–677.

Heisenberg, W. (1926). Mehrkörperproblem und Resonanz in der Quantenmechanik. *Zeitschr. F. Phys.* 38, 411–426.

Hunter, G., and Schlifer, I. (2005). Explicit spin coordinates. arXiv:quant-ph/0507008v1 1 Ju8l 2008.

Jabs, A. (2010). Connecting spin and statistics in quantum mechanics. *Found. Phys.* 40, 776–792. doi:10.1007/s10701-009-9351-4

Kaplan, I. G. (2020). The Pauli exclusion principle and the problems of its experimental verification. *Symmetry* 12, 320. doi:10.3390/sym12020320

Kleppner, D. (1986). "Cavity quantum electrodynamics," in *International Quantum Electronics Conference. OSA Technical Digest.* Editors M. Richardson, C. Tang, D. Grischkowsky, and T. Hansch Available online at: https://opg.optica.org/abstract.cfm?URI=IQEC-1986-WFF1.

Mandel, L., and Wolf, E. (1995). *Optical coherence and quantum optics*. Cambridge University Press. Chapter 10.

Okuda, T., Miyamaoto, K., Miyahara, H., Kuroda, K., Kimura, A., Namatame, H., et al. (2011). Efficient spin resolved spectroscopy observation machine at Hiroshima Synchrotron Radiation Center. *Rev. Sci. Instrum.* 82, 103302. doi:10.1063/1.3648102

Pauli, W. (1925). Über den Zusammenhang des Abschlusses der Elektronengruppen im Atom mit der Komplexstruktur der Spektren. *Zeitschr. F. Phys.* 31 (1), 765–783. doi:10.1007/bf02980631

Pauli, W. (1946). *Exclusion Principle and Quantum Mechanics*. Nobel lecture. Available online at: https://www.nobelprize.org/uploads/2018/06/pauli-lecture.pdf.

Pauli, W. (1950). On the connection between spin and statistics. *Prog. Theor. Phys.* 5, 526–543. doi:10.1143/ptp.5.526

Sobelman, I. I. (1979). *Atomic Spectra and Radiative Transitions*. Springer.

Walther, H., Varcoe, B., Englert, B. G., and Becker, T. H. (2006). Cavity quantum electrodynamics. *Rep. Prog. Phys.* 69 (5), 1325–1382. doi:10.1088/0034-4885/69/5/R02

Appendix A

Equations 24, 25 must be satisfied for any pair of identical particles—that is, ζ^{ij} is either even or odd for identical particles $i, \quad j = 1, 2, \ldots$. This means that ζ^{12} expresses a distinctive property of the particles themselves, which manifests when the particles form part of the same system and couple either in phase or antiphase to the shared modes. This property is identified in Equation 26 and the following with the parameters $\zeta^i_B, \quad \zeta^i_F$, $i = 1, 2$, which must satisfy either Equation 27a or 27b, respectively.

If we take the smallest possible value of ζ^1 in the F case, which is $|\zeta^1_m| = 1/2$, any integer value of another type-F particle would violate both Equations 27a, b; hence, type-F particles can only have half-integer values of the parameter ζ^i. Similarly, taking the smallest possible value of ζ^1 in the B case, which is $|\zeta^1_m| = 0$, any half-integer value for another type-B particle would violate both Equations 27a, b, so type-B particles can only have integer values of the parameter ζ^i.

This confirms the correctness of Equations 28a, b.

frontiers | Frontiers in Quantum Science and Technology

TYPE Original Research
PUBLISHED 21 July 2025
DOI 10.3389/frqst.2025.1603372

OPEN ACCESS

EDITED BY
Karl Hess,
University of Illinois at Urbana-Champaign,
United States

REVIEWED BY
Marcin Wieśniak,
University of Gdansk, Poland
Bryan Sanctuary,
McGill University, Canada

*CORRESPONDENCE
Theodorus Maria Nieuwenhuizen,
t.m.nieuwenhuizen@uva.nl

RECEIVED 31 March 2025
ACCEPTED 16 May 2025
PUBLISHED 21 July 2025

CITATION
Nieuwenhuizen TM (2025) Dynamics of the ideal quantum measurement of a spin-1 with a Curie–Weiss magnet.
Front. Quantum Sci. Technol. 4:1603372.
doi: 10.3389/frqst.2025.1603372

Dynamics of the ideal quantum measurement of a spin-1 with a Curie–Weiss magnet

Theodorus Maria Nieuwenhuizen*

Institute for Theoretical Physics, University of Amsterdam, Amsterdam, Netherlands

Quantum measurement is a dynamical process involving an apparatus coupled to a test system. The ideal measurement of the z-component of a spin-$\frac{1}{2}$ ($s_z = \pm\frac{1}{2}$) has been modeled by the Curie–Weiss model for quantum measurement. Recently, the model was generalized to higher spins, and its thermodynamics were solved. Here, the dynamics are considered. To this end, the dynamics for the spin-$\frac{1}{2}$ case are cast in general notation. The dynamics of the measurement of the z-component of a spin-1 ($s_z = 0, \pm 1$) are solved in detail and evaluated numerically. The energy costs of the measurement, which are macroscopic, are evaluated. The generalization to higher spin is straightforward.

KEYWORDS

ideal quantum measurement, dynamics, Curie–Weiss model, higher spin, exact solution

1 Introduction

This year, we celebrate the centennial of the formulation of quantum theory; see Capellmann (2017) for the prehistory. After the "Zur Quantummechanik" by Born and Jordan (1925), the Dreimänner Arbeit by Born et al. (1926) on the matrix mechanics was soon followed by Schrödinger's (1926) formulation of wave mechanics, inspired by the insights of De Broglie (1924). The predictive power of the theory was expressed by Born's (1926) rule. For a compilation of historical contributions, see Wheeler and Zurek (2014).

The interpretation of quantum mechanics has been discussed throughout the century since then. The Copenhagen interpretation— with the Born rule and the collapse postulate—emerged as the most reasonable. Many attempts to deepen understanding begin with these postulates. However, they are merely shortcuts for what happens in a laboratory. With our collaborators Armen Allahverdyan and Roger Balian, we have taken the viewpoint of starting from the uninterpreted quantum formalism and applied it to the dynamics of an idealized measurement. The elements of this approach that have already been solved do not need to be interpreted; interpretation is needed to put the results in a proper, global context. As discussed below, this effort has led to a specified version of the statistical interpretation of quantum mechanics, popularized by Ballentine (1970).

The present study deals with the dynamics of an ideal quantum measurement. It is based on the Curie–Weiss model for measuring the z-component of a spin $\frac{1}{2}$, introduced by Allahverdyan et al. (2003a). After reviewing various models for quantum measurement, it was considered in great detail by Allahverdyan et al. (2013). The apparatus consists of a mean-field type magnet having $N \gg 1$ spins $\frac{1}{2}$ coupled to a harmonic oscillator bath. The magnet starts in a metastable, long-lived, paramagnetic state, which is separated by free energy barriers from the stable states with upward or downward magnetization. It is in a "ready" state for use in a measurement.

When employed as an apparatus, the magnetization acts as a pointer for the outcome. The coupling to the tested spin causes a quick transition to one of the stable states, thereby registering the measurement. For this to succeed, the coupling must be large enough to overcome the free energy barrier. While the final state of the magnet is described by thermodynamics, much detail is contained in the dynamical evolution toward this state.

In an ideal measurement, the Born rule appears due to the non-disturbance of the measured operator. It provides probabilities for the pointer, that is, for the final magnetization to be upward or downward. The state of the microscopic spin is correlated with it and inferred from the pointer indication.

Understanding the dynamics also provides a natural route toward the interpretation of quantum mechanics. Indeed, when assuming the quantum formalism, the task is to work out its predictions, and only then to interpret the results. This leads to viewing the wave function, or, more generally, the density matrix, as a state of best knowledge and the "collapse of the wave function" or "disappearance of cat states" as an update of knowledge after the selection of the runs with identical outcomes, compatible with the quantum formalism. Notably, quantum theory is not a theory of Nature based on an ontology; rather, it is an abstract construct to explain its probabilistic features.

The "measurement problem," that is, describing the individual experiments that occur in a laboratory, is, in our view, still the most outstanding challenge of modern science. Many attempts have been made to solve it by making adaptations or small alterations to quantum mechanics or by interpreting it differently. We hold the opinion that this entire enterprise is in vain; one should start completely from scratch to "derive quantum mechanics," that is to say, establish the origin of quantum behavior in Nature[1].

Various formalisms of quantum mechanics were reviewed by David (2015). The insight that quantum mechanics is only meaningful in a laboratory context, stressed in particular by Bohr, is central to the approaches of Auffeves and Grangier (2016) and Auffeves and Grangier (2020), it leads to new insights regarding the Heisenberg cut between quantum and classical (Van Den Bossche and Grangier, 2023). One century of interpretation of the Born rule, including the modern one, was overviewed by Neumaier (2025).

1.1 The Curie–Weiss model for quantum measurement

A macroscopic material consists of atoms, which are quantum particles. The starting point for their dynamics lies in quantum statistical mechanics. For a measurement, the apparatus must be macroscopic and have a macroscopic pointer so that the outcome of the measurement can be read off or processed automatically. Hereto, an operator formalism is required, with dynamics set by the Liouville–von Neumann equation, the generalization of the Schrödinger equation to mixed states.

Progress on solvable models for quantum measurement has been made in recent decades when we, together with A. Allahverdyan and R. Balian introduced and solved the so-called Curie–Weiss model for quantum measurement (Allahverdyan A. E. et al., 2003) in our "ABN" collaboration. Here, the classical Curie–Weiss model of a magnet is taken in its quantum version and applied to the measurement of a quantum spin $\frac{1}{2}$. Various further aspects were presented in Allahverdyan A. E. et al. (2003), Allahverdyan et al. (2005a), Allahverdyan et al. (2005b), Allahverdyan et al. (2007), and Allahverdyan et al. (2006). They were reviewed and greatly expanded in Allahverdyan et al. (2013). Lecture notes were presented by Nieuwenhuizen et al. (2014). A straightforward interpretation for a class of these measurement models was provided by Allahverdyan et al. (2017); it is a specified version of the statistical interpretation made popular by Ballentine (1970).

Simultaneous measurement of two noncommuting quantum variables was worked out (Perarnau-Llobet and Nieuwenhuizen, 2017a), as well as an application to Einstein-Podolsky-Rosen type of measurements (Perarnau-Llobet and Nieuwenhuizen, 2017b). A numerical test on a simplified version of the Curie–Weiss model reproduced nearly all of its properties (Donker et al., 2018).

Our ensuing insights, which are suitable for teachers of quantum theory (at the high school, bachelor's, or master's levels), are presented in Allahverdyan et al. (2024) and summarized in a feature article (Allahverdyan et al., 2025).

1.2 Higher-spin Curie–Weiss models

The mentioned Curie–Weiss model was recently generalized by us to measure a spin $l > \frac{1}{2}$ (Nieuwenhuizen, 2022). This study will be termed "Models" henceforth. For spin l, the state of the magnet is described by $2l$ order parameters. To assure an unbiased measurement, the Hamiltonian of the apparatus and the interaction Hamiltonian with the tested system have Z_{2l+1} symmetry. The statics were solved for spin-1, $\frac{3}{2}$, 2, and $\frac{5}{2}$.

Here, the dynamics are worked out for spin-1, laying the groundwork for higher-spin dynamics. In the spin $\frac{1}{2}$ Curie–Weiss model, it was found that Schrödinger cat terms disappear through two mechanisms: dephasing of the magnet, possibly followed by decoherence due to the thermal bath. Similar behavior is now investigated for spin-1.

The setup of the article is as follows. In Section 2, we recall the formulation of the Curie–Weiss model for general spin-l and discuss aspects of its physical implementation for spin $\frac{1}{2}$ and spin-1. In

1 An analogy is offered by the dark matter problem in cosmology. Abandoning particle dark matter, we view dark "matter" as a form of energy and assume new properties of vacuum energy. This provides a description of black holes with a core rather than a singularity (Nieuwenhuizen, 2023), aspects of dark matter throughout the history and future of the Universe (Nieuwenhuizen, 2024a), and the giant dark matter clouds around isolated galaxies (Nieuwenhuizen, 2024b), explaining the "indefinite flattening" of their rotation curves (Mistele et al., 2024). Remarkably, this approach is a generalization of the classical Lorentz–Poincaré electron—a charged, non-spinning spherical shell filled with vacuum energy (Nieuwenhuizen, 2025).

Section 3, we revisit the spin-$\frac{1}{2}$ case and cast its dynamics in a general form. In Section 4, we analyze the dynamics of the spin-1 situation. We close with a summary in Section 5.

2 Higher-spin Curie–Weiss Hamiltonian models

We start by recalling some properties of higher-spin models that we introduced in "Models" (Nieuwenhuizen, 2022). The statics were considered there; here, we define and study the dynamics, recalling parts of the spin $\frac{1}{2}$ case. We often refer to the review by Allahverdyan et al. (2013) to be termed "Opus."

In the following, we denote quantum operators by a hat, specifically $\hat{\mathbf{s}}$ and $\hat{s}_z$ for the measured spin and $\hat{\sigma}^{(i)}$ and $\hat{\sigma}_z^{(i)}$ for the spins of the apparatus. For simplicity of notation, we follow Models and denote the eigenvalues without a hat, notably those of $\hat{s}_z$ by s and the ones of $\hat{\sigma}_z^{(i)}$ by σ_i. Sums over i lead to the operators $\hat{m}_k$ and their scalar values m_k for $k = 1, 2, \ldots, 2l$. Switching between these operators and their eigenvalues is straightforward.

The strategy is to measure the z-component of a quantum spin-l with $(l = \frac{1}{2}, 1, \frac{3}{2}, \cdots)$. The eigenvalues s of the operator $\hat{s}_z$ lie in the spectrum[2]

$$s \in \mathrm{spec}_l = \{-l, -l+1, \ldots, l-1, l\}. \tag{2.1}$$

The measurement will be performed by employing an apparatus with $N \gg 1$ vector spins-l having operators $\hat{\sigma}^{(i)}$, $i = 1, \ldots, N$. They have components $\hat{\sigma}_a^{(i)}$ $(a = x, y, z)$, with eigenvalues $\sigma_a^{(i)} \in \mathrm{spec}_l$. These operators are mutually coupled in the Hamiltonian of M. For each $i = 1, \cdots N$, and for each $\hat{\sigma}_a^{(i)}$, $a = x, y, z$, they are also coupled to a thermal harmonic oscillator bath; for the case $l = \frac{1}{2}$, this was worked out by Allahverdyan et al. (2003a), Allahverdyan et al. (2003b), and Allahverdyan et al. (2013). The generalization of such a bath for arbitrary spin-l is straightforward and will be applied to the spin-1 model.

2.1 Spin–spin Hamiltonian of the magnet

A quantum measurement is often assumed to be "instantaneous." In our idealized modeling, it will take a finite time, but the tested spin will not evolve in the meantime. In other words, the spin itself is "sitting still" and waiting to be measured. Neither should it evolve during the "fast" measurement. This is realized when its Hamiltonian $\hat{H}_S$ commutes with $\hat{s}_z$; we consider the simplest case: $\hat{H}_S = 0$.

In order to have an unbiased apparatus, the Hamiltonian of the magnet should have degenerate minima and maximal symmetry. To construct such a functional, we consider, in the eigenvalue presentation, the form

$$C_2 = \nu^2 \sum_{i,j=1}^{N} \cos \frac{2\pi(\sigma_i - \sigma_j)}{2l+1}, \quad \nu \equiv \frac{1}{N}, \tag{2.2}$$

which is maximal in ferromagnetic states $\sigma_i = \sigma_1$ $(i = 2, \ldots, N)$. In general, these interactions do not seem realistic, but here, the cosine rule allows expressing this as spin–spin interactions,

$$C_2 = \mathrm{co}_l^2 + \mathrm{si}_l^2, \tag{2.3}$$

which is bilinear in the single-spin sums

$$\mathrm{co}_l = \frac{1}{N}\sum_{i=1}^{N} \cos \frac{2\pi\sigma_i}{2l+1}, \quad \mathrm{si}_l = \frac{1}{N}\sum_{i=1}^{N} \sin \frac{2\pi\sigma_i}{2l+1}. \tag{2.4}$$

The discrete values of the spin projections allow expressing these terms in the $2l$ spin moments,

$$m_k = \frac{1}{N}\sum_{i=1}^{N} \sigma_i^k, \qquad (k = 1, \ldots, 2l), \tag{2.5}$$

while $m_0 \equiv 1$. For $l = \frac{1}{2}$, the values $s = \pm\frac{1}{2}$ imply

$$\cos \pi s = 0, \quad \sin \pi s = 2s. \tag{2.6}$$

Applying this for $s \to \sigma_i$ and summing over i yields

$$\mathrm{co}_{\frac{1}{2}} = 0, \quad \mathrm{si}_{\frac{1}{2}} = 2m_1, \quad m_1 = \frac{1}{N}\sum_{i=1}^{N} \sigma_i. \tag{2.7}$$

In the case $l = 1$, one has $s = 0, \pm 1$. The rule

$$\cos \frac{2\pi s}{3} = 1 - \frac{3}{2}s^2, \quad \sin \frac{2\pi s}{3} = \frac{\sqrt{3}}{2}s, \tag{2.8}$$

leads to $s \to \sigma_i$ and summing over i leads to

$$\mathrm{co}_1 = 1 - \frac{3}{2}m_2, \quad \mathrm{si}_1 = \frac{\sqrt{3}}{2}m_1, \tag{2.9}$$

Here, m_2 ranges from 0 to 1 with steps of $\nu \equiv 1/N$, while m_1 ranges from $-m_2$ to m_2 with steps of 2ν. At finite N, one can label the discrete $m_{1,2}$ as

$$\begin{aligned} &m_1 = (2n_1 - n_2)\nu, \quad m_2 = n_2\nu, \\ &(0 \le n_2 \le N, \quad 0 \le n_1 \le n_2). \end{aligned} \tag{2.10}$$

The results for $s = \frac{3}{2}$, 2, and $\frac{5}{2}$ are given in Models.

Let out of the N spins σ_i, a number $N_\sigma = \sum_i \delta_{\sigma_i,\sigma}$ take the value $\sigma \in \mathrm{spec}_l$ and let $x_\sigma = N_\sigma/N$ be their fraction. The sum rule $\sum_\sigma N_\sigma = N$ implies $m_0 \equiv \sum_\sigma x_\sigma = 1$. The moments read

$$m_k = \sum_{\sigma=-l}^{l} x_\sigma \sigma^k, \quad k = 1, \ldots, 2l, \tag{2.11}$$

Inversion of these relations determines the x_σ as linear combinations of the m_k. For $l = \frac{1}{2}$, one has

$$m_1 = \frac{1}{2}x_{\frac{1}{2}} - \frac{1}{2}x_{-\frac{1}{2}}, \quad x_{\pm\frac{1}{2}} = \frac{1}{2} \pm m_1. \tag{2.12}$$

For spin-1 $(l = 1)$, one has

$$m_1 = -x_{-1} + x_1, \qquad m_2 = x_{-1} + x_1. \tag{2.13}$$

2 To simplify the notation, we replace the standard notation for spins with $s \to l$ and $s_z \to s$. For an angular momentum $L^2 = l(l+1)$, the model also applies to the measurement of $\hat{L}_z$ with eigenvalues $m \to s$. We employ units $\hbar = k = 1$.

With $x_{-1} + x_0 + x_1 = 1$, their inversion reads

$$x_0 = 1 - m_2, \qquad x_{\pm 1} = \frac{m_2 \pm m_1}{2}. \tag{2.14}$$

In a quantum approach, one goes to operators and sets $s \to \hat{s}_z$, $\sigma_i \to \hat{\sigma}_z^{(i)}$, and $m_k \to \hat{m}_k$. For the Hamiltonian $\hat{H}_{\rm M} = N\hat{H}$, we follow Allahverdyan et al. (2003a) and Allahverdyan et al. (2003b) and adopt the spin–spin and four–spin interactions:

$$\hat{H}_{\rm M} = N\hat{H}, \quad \hat{H} = -\frac{1}{2}J_2\hat{C}_2 - \frac{1}{4}J_4\hat{C}_2^2. \tag{2.15}$$

Multispin interaction terms like $-\frac{1}{6}J_6\hat{C}_2^3 - \frac{1}{8}J_8\hat{C}_2^4$ can be added without changing the overall picture.

2.2 The interaction Hamiltonian

The coupling between the tested spin S and the magnet M is chosen similar to Equation 2.2,

$$\hat{H}_{\rm SA} = N\hat{I}, \ \hat{I} = \frac{g}{N}\sum_{i=1}^{N}\cos\frac{2\pi\left(\hat{s}_z\hat{\sigma}_z^{(i)}\right)}{2l+1}, \tag{2.16}$$

where g is the coupling constant. It takes the values

$$I_s(\{\sigma_i\}) = -\frac{g}{N}\sum_{i=1}^{N}\Big(\cos\frac{2\pi s}{2l+1}\cos\frac{2\pi\sigma_i}{2l+1} + \sin\frac{2\pi s}{2l+1}\sin\frac{2\pi\sigma_i}{2l+1}\Big), \tag{2.17}$$

This can be expressed as a linear combination of the moments $m_1, \cdots, m_{2l}$. For $l = \frac{1}{2}$, one has

$$I_s(m_1) = -4gsm_1, \tag{2.18}$$

and for $l = 1$, denoting $\mathbf{m} = (m_1, m_2)$,

$$I_s(\mathbf{m}) = -g\Big[\Big(1 - \frac{3}{2}s^2\Big)\Big(1 - \frac{3}{2}m_2\Big) + \frac{3}{4}sm_1\Big]. \tag{2.19}$$

The total spin Hamiltonian,

$$\hat{H} = \hat{H}_{\rm M} + \hat{H}_{\rm SA} = \hat{H}_{\rm M} - N\hat{I}, \tag{2.20}$$

has Z_{2l+1} symmetry: on the diagonal basis, a shift $s \to s + \bar{s}$ with $\bar{s} = 1, 2, \ldots, 2l+1$ can be accompanied by a shift $\sigma_i \to \sigma_i + \bar{s}$ for all i. This is evident in the cosine expressions and implies a somewhat hidden invariance in the formulation in terms of the moments m_k, as discussed in Models.

2.3 Coupling to a harmonic oscillator bath

For a general spin l, the magnet–bath coupling is taken as the spin–boson coupling of Opus Equation 3.10,

$$\hat{H}_{\rm MB} \equiv \sqrt{\gamma}\sum_{i=1}^{N}\sum\nolimits_{a=x,y,z}\hat{\sigma}_a^{(i)}\hat{B}_a^{(i)}, \tag{2.21}$$

with $\gamma \ll 1$, where the bath operators read

$$\hat{B}_a^{(i)} = \sum\nolimits_k \sqrt{c_k}\Big(\hat{b}_{k,a}^{(i)} + \hat{b}_{k,a}^{\dagger(n)}\Big), \tag{2.22}$$

for each i, a, there is a large set of oscillators labeled by k, having a common coupling parameter c_k. These bosons have the Hamiltonian

$$\hat{H}_{\rm B} = \sum_{i=1}^{N}\sum_{a=x,y,z}\sum_k \hbar\omega_k\hat{b}_{k,a}^{\dagger(i)}\hat{b}_{k,a}^{(i)}, \tag{2.23}$$

with the ω_k also identical for all n, a. The autocorrelation function of B defines a bath kernel K, which is identical for all i, a,

$$\begin{aligned}\mathrm{tr}_{\rm B}\Big[\hat{R}_{\rm B}(0)\hat{B}_a^{(i)}(t)\hat{B}_b^{(j)}(t')\Big] &= \delta_{i,j}\delta_{a,b} \quad K(t-t'),\\ \hat{B}_a^{(i)}(t) &\equiv e^{i\hat{H}_{\rm B}t}\hat{B}_a^{(i)}e^{-i\hat{H}_{\rm B}t}.\end{aligned} \tag{2.24}$$

Writing $c_k = c(\omega_k)$, this leads to

$$\begin{aligned}K(t) &= \sum\nolimits_k c(\omega_k)\Big(\frac{e^{i\omega_k t}}{e^{\beta\omega_k}-1} + \frac{e^{-i\omega_k t}}{1-e^{-\beta\omega_k}}\Big)\\ &\equiv \frac{1}{2\pi}\int_{-\infty}^{+\infty}\mathrm{d}\omega \quad e^{i\omega t}\tilde{K}(\omega).\end{aligned} \tag{2.25}$$

The kernel $\tilde{K}(\omega)$ can be read off and expressed in the spectral density $\rho_c(\omega) = \sum_k c(\omega_k) \quad \delta(\omega - \omega_k)$,

$$\tilde{K}(\omega) = \frac{2\pi}{|\omega|}\rho_c(|\omega|)\frac{\omega}{e^{\beta\omega}-1}. \tag{2.26}$$

We adopt an Ohmic spectrum with a Debye cutoff,

$$\tilde{K}(\omega) = \frac{e^{-|\omega|/\Gamma}}{4}\frac{\omega}{e^{\omega/T}-1}, \tag{2.27}$$

where $T = 1/\beta$ is the temperature of the phonon bath, and Γ the typical cutoff frequency. In Opus, we also consider a Lorentzian (power law) cutoff, for which the statics allows analytic results.

With the couplings in Equations 2.21, 2.22, and 2.23 independent of a, $\hat{H}_{\rm MB}$ is statistically invariant under Z_{2l+1}. Combined with the invariance of $\hat{H}_{\rm M}$ and $\hat{H}_{\rm SA}$, this ensures an unbiased measurement.

2.4 Evolution of the density matrix

The evolution of the density matrix of the total system is given by the Liouville–von Neumann equation. On the eigenbasis of $\hat{s}_z$, its elements $\hat{R}_{s\bar{s}}$ evolve independently as given in Equation 4.8 of Opus; this involves the apparatus spins and the bath. The procedure of Opus for spin $l = \frac{1}{2}$ appears to hold for general spin-l operators.

Let us consider the time evolution of $\hat{R}_{s\bar{s}}$ as given in Equation 4.8 of Opus (we now denote $i \to s$, $j \to \bar{s}$), where the action of the harmonic oscillator bath has been expressed in the bath kernel $K(t)$ and which involves commutators of $\hat{R}_{s\bar{s}}$ with the spin operators $\hat{\sigma}_a^{(i)}$, $a = x, y, z$; $i = 1, \ldots, N$.

Formally, the initial state (Equation 5.4) is a constant function of the $\hat{\sigma}_z^{(i)}$. In addition, $\dot{\hat{R}}_{s\bar{s}}(t_{\rm i})$ is a function of them, so it is consistent to assume that, at all t, $\hat{R}_{s\bar{s}}$ only depends on the $\hat{\sigma}_z^{(i)}$. As a result, the $a = z$ terms of Equation 4.8 in Opus have vanishing commutators for any spin l. Left with the x, y commutators, we define (using the index n rather than i to label the $\hat{\sigma}_{x,y}$)

$$\hat{\sigma}_{\pm}^{(n)} = \hat{\sigma}_x^{(n)} \pm i\hat{\sigma}_y^{(n)}. \tag{2.28}$$

Because $\sum_{ax,y}\hat{\sigma}_a^{(n)}\hat{O}\hat{\sigma}_a^{(n)} = \frac{1}{2}\sum_{\alpha=\pm1}\hat{\sigma}_\alpha^{(n)}\hat{O}\hat{\sigma}_{-\alpha}^{(n)}$ for any operator $\hat{O}$, Equation 4.8 in Opus takes the form

$$\frac{\mathrm{d}\hat{R}_{s\bar{s}}(t)}{\mathrm{d}t} = -i\hat{H}_s\hat{R}_{s\bar{s}}(t) + i\hat{R}_{s\bar{s}}(t)\hat{H}_{\bar{s}} + \frac{\gamma}{2}\sum_{\alpha,\beta=\pm1}\sum_{n=1}^{N}\int_0^t \mathrm{d}u \quad K(\beta u)\hat{C}_{s\bar{s},\beta}^{(\alpha,n)}(u), \tag{2.29}$$

where

$$\hat{C}_{s\bar{s},+}^{(\alpha,n)}(u) = \left[e^{-iu\hat{H}_s}\hat{\sigma}_{-\alpha}^{(n)}e^{iu\hat{H}_{\bar{s}}}\hat{R}_{s\bar{s}}(t), \quad \hat{\sigma}_\alpha^{(n)}\right],$$
$$\hat{C}_{s\bar{s},-}^{(\alpha,n)}(u) = \left[\hat{\sigma}_{-\alpha}^{(n)}, \quad \hat{R}_{s\bar{s}}(t)e^{-iu\hat{H}_{\bar{s}}}\hat{\sigma}_\alpha^{(n)}e^{iu\hat{H}_{\bar{s}}}\right], \tag{2.30}$$

are commutators involving the Hamiltonian of M coupled to S in state s, without the bath, viz.

$$\hat{H}_s = \hat{H}_{\mathrm{M}} + \hat{H}_{\mathrm{SA}}^s = NH(\hat{m}_1) + NI_s(\hat{m}_1). \tag{2.31}$$

The action of the bath is expressed in the kernel $K(\pm u)$, with the smallness of γ allowing truncation at its first order. Equations 2.29, 2.30 are valid for general spin $l = \frac{1}{2}, 1, \frac{3}{2}, \cdots$.

Most importantly, the $\hat{R}_{s\bar{s}}$ are decoupled in the separate $s, \bar{s}$ sectors, a property of ideal measurement but absent in general. Examples of these non-idealities are a spin S having nontrivial dynamics during the measurement and a biased measurement, in which the Hamiltonian of the magnet and/or the bath depends on the state of S.

2.5 Physical implementation of the model

The spin-$\frac{1}{2}$ Curie–Weiss model for quantum measurement (Allahverdyan A. et al., 2003) was initially conceived as a tool to understand the dominant physical aspects of idealized quantum measurements. It has served this purpose well. Let us look here at possible realizations of the model.

Curie–Weiss models are mean-field types of spin models. Their distance-independent couplings apply to a small magnetic grain. The grain need not be very large. From studies of spin glasses and cluster glasses, it is known that "fat spins," clusters of hundreds or thousands of coherent spins, are easily detectable (Mydosh, 1993).

The Ising nature of the couplings refers to fairly anisotropic spin–spin interactions. For spin $\frac{1}{2}$, Equation 2.15 expresses the pair and quartet couplings between the z-components of the spins. Multispin interactions are a natural result of the overlap of electronic orbits; here, they are approximated as not decaying with the distance between the spins in the grain. How reasonable this approximation is must be considered in each separate application. The main feature of our modeling, a first-order phase transition in the magnet, suggests that it represents a large class of short-range systems. This is underlined by the model's support of the Copenhagen postulates of collapse and Born probabilities.

These features also hold for the spin-1 Curie–Weiss model. However, on top of this, Equation 2.8 produces the combination $\hat{\Sigma}_i \equiv \hat{\sigma}_z^{(i)2} - 2/3$, which takes the values 1/3 for the "out-of-plane" cases $\sigma_i = \pm 1$ and −2/3 for the "in-plane" case $\sigma_i = 0$. Separate-spin terms of the form $\sum_i D\hat{\sigma}_z^{(i)2}$ are well known, stemming from crystal fields. For the apparatus, the co_1^2 term of Equation 2.3 relates to the interaction $\sum_{ij}\hat{\Sigma}_i\hat{\Sigma}_j$ between the $\hat{\Sigma}_i$, so it involves both the aforementioned D-term and also the terms $\hat{\sigma}_z^{(i)2}\hat{\sigma}_z^{(j)2}$. How to implement these crystal-field-type spin–spin interactions in practice is an open question.

Concerning numerical implementations, Donker et al. (2018)'s approximation of the Curie–Weiss model can be generalized to higher spin.

3 The spin $\frac{1}{2}$ case revisited

3.1 Elements of the statics

We set the stage by considering the spin-$\frac{1}{2}$ situation, the original Curie–Weiss model for quantum measurement in slightly adapted notation[3]. The spin operators are $\hat{\sigma}_{x,y,z}$, with $\hat{\sigma}_z = \mathrm{diag}(\frac{1}{2}, -\frac{1}{2})$. It holds that $[\hat{\sigma}_a, \hat{\sigma}_b] = i\varepsilon_{abc}\hat{\sigma}_c$ and $\hat{\sigma}_x^2 + \hat{\sigma}_y^2 + \hat{\sigma}_z^2 = \frac{3}{4}\hat{\sigma}_0$ with $\hat{\sigma}_0 = \mathrm{diag}(1, 1)$.

The magnet has N these spins $\hat{\sigma}_{x,y,z}^{(i)}$, $i = 1, 2, \ldots, N$. They have magnetization operator

$$\hat{M}_1 = N\hat{m}_1, \quad \hat{m}_1 = \frac{1}{N}\sum_{i=1}^{N}\hat{\sigma}_z^{(i)}, \tag{3.1}$$

taking eigenvalues $-\frac{1}{2} \le m_1 \le \frac{1}{2}$. In the paramagnetic state, $m_1 = 0$. The Hamiltonian is taken as pair and quartet interactions,

$$\hat{H}_{\mathrm{M}} = N\hat{H}, \qquad \hat{H} = -2J_2\hat{m}_1^2 - 4J_4\hat{m}_1^4. \tag{3.2}$$

With $\hat{x}_\sigma = \hat{N}_\sigma/N$, it holds that

$$\hat{m}_1 = \frac{1}{2}\hat{x}_{1/2} - \frac{1}{2}\hat{x}_{-1/2}, \quad \hat{x}_{\pm1/2} = \frac{1}{2}\hat{I} \pm \hat{m}_1. \tag{3.3}$$

The spins have eigenvalues $\sigma_i = \pm\frac{1}{2}$, so that $\hat{m}_1$ has eigenvalues $m_1 = \nu\sum_i\sigma_1$ ranging from $-\frac{1}{2}$ to $\frac{1}{2}$ with steps of ν.

3.2 The interaction Hamiltonian

To use the magnet coupled to its bath as an apparatus for a quantum measurement, a system–apparatus (SA) coupling is needed. According to Equation 2.18, it is chosen as a spin–spin coupling,

$$\hat{H}_{\mathrm{SA}} = -4g\sum_{i=1}^{N}\hat{s}\hat{\sigma}_z^{(i)} = -4gN\hat{s}\hat{m}_1, \tag{3.4}$$

and takes the values $H_{\mathrm{SA}}^s(m_1) = -4gsNm_1$. The full Hamiltonian of S + A in the sector s thus reads

$$\hat{H}_s = -2J_2N\hat{m}_1^2 - 4J_4N\hat{m}_1^4 - 4gsN\hat{m}_1. \tag{3.5}$$

The eigenvalues of $\hat{s}_z$ are $s = \pm\frac{1}{2}$ and those of $\hat{\sigma}_z^{(i)}$ are $\sigma_i = \pm\frac{1}{2}$, so that $\hat{m}_1$ has the eigenvalues $\nu\sum_{i=1}^{N}\sigma_i$. The degeneracy of a state with magnetization m_1 is

3 For the connection with the parameters in Opus, see ref 1.

$$G_N = \frac{N!}{N_{-\frac{1}{2}}!\ \ N_{\frac{1}{2}}!} = \frac{N!}{\left(Nx_{-\frac{1}{2}}\right)!\left(Nx_{\frac{1}{2}}\right)!}, \tag{3.6}$$

and entropy $S_N = \log G_N$. At large N, we get the standard result for the entropy $S_N = NS$ with

$$S = \frac{1-2m_1}{2}\log\frac{1-2m_1}{2} - \frac{1+2m_1}{2}\log\frac{1+2m_1}{2}. \tag{3.7}$$

Combining Equation 3.5 and Equation 3.6, the free energy in the s-sector reads

$$F_s(m_1) = -2J_2Nm_1^2 - 4J_4Nm_1^4 \ - 4gsNm_1 - T\log G_N(m_1), \tag{3.8}$$

which yields, for large N,

$$\frac{F_s}{N} = -2J_2m_1^2 - 4J_4m_1^4 - 4gsm_1 - TS(m_1). \tag{3.9}$$

3.3 Dynamics of the spin $\frac{1}{2}$ model

At the initial time t_i of the measurement, the state of the tested system, S, here $\hat{\mathbf{s}}$, a spin-$\frac{1}{2}$ operator, is described by its 2×2 density matrix $\hat{r}(t_\mathrm{i})$ with elements $r_{s\bar{s}}(t_\mathrm{i})$ for $s, \bar{s} = \pm\frac{1}{2}$. The magnet M has $N \gg 1$ quantum spins-$\frac{1}{2}$ $\hat{\sigma}^{(i)}$ $(i = 1, \ldots, N)$. In each $s, \bar{s}$ sector, S + M lie in the state $\hat{R}_{s\bar{s}}(t) = \hat{R}^\dagger_{\bar{s}s}(t)$, which is an operator that can be represented by a $2^N \times 2^N$ matrix. At t_i, M is assumed to lie in the paramagnetic state wherein the spins are fully disordered and uncorrelated. Multiplying by the respective element of $\hat{r}(t_\mathrm{i})$ leads to the elements of the initial density matrix of S + M

$$\hat{R}_{s\bar{s}}(t_\mathrm{i}) = r_{s\bar{s}}(t_\mathrm{i})\frac{\hat{\sigma}_0^{(1)}}{2}\otimes\frac{\hat{\sigma}_0^{(2)}}{2}\otimes\cdots\otimes\frac{\hat{\sigma}_0^{(N)}}{2}. \tag{4.1}$$

3.4 Truncation for spin $\frac{1}{2}$

The dynamics of the off-diagonal elements (cat terms) were worked out in Opus. In the relevant short-time domain, the spin–spin couplings are ineffective; therefore, it suffices to study independent spins coupled by the interaction Hamiltonian and the bath. These elements vanish dynamically, truncating the density matrix $\hat{R}$ to a form diagonal on the eigenbasis of $\hat{s}_z$. There is no reason to repeat that here; for spin-1, this will be worked out in Section 4.1.

3.5 Registration for spin $\frac{1}{2}$

Registration of the measurement is described by the evolution of the diagonal elements of the density matrix of the full system. For the situation of higher spin, it is instructive to reconsider and slightly reformulate the spin $\frac{1}{2}$ situation.

For $\bar{s} = s$, the Hamiltonian terms drop out of Equation 2.29; hence, the dynamics are a relaxation set by

$$\frac{\mathrm{d}\hat{R}_{ss}(t)}{\mathrm{d}t} = \frac{\gamma}{2}\sum_{\alpha,\beta=\pm1}\sum_{n=1}^{N}\int_0^t \mathrm{d}u \quad K(\beta u)\hat{C}^{(\alpha,n)}_{ss,\beta}(u). \tag{4.2}$$

For $l = \frac{1}{2}$, the spin operators $\hat{\sigma}_{x,y,z}$ anticommute; hence, for any function f of the $\hat{\sigma}_z^{(i)}$, it holds that

$$\begin{aligned}\hat{\sigma}_\alpha^{(n)} f\left(\left\{\hat{\sigma}_z^{(i)}\right\}\right) &= \hat{f}\left(\left\{(-1)^{\delta_{i,n}}\hat{\sigma}_z^{(i)}\right\}\right)\hat{\sigma}_\alpha^{(n)} \\ &\equiv f^{(n)}\left(\left\{\hat{\sigma}_z^{(i)}\right\}\right)\hat{\sigma}_\alpha^{(n)}.\end{aligned} \tag{4.3}$$

This brings the $\hat{\sigma}_\alpha^{(n)}$ and $\hat{\sigma}_{-\alpha}^{(n)}$ next to each other, which allows to eliminate them using the sum $\sum_{\alpha=\pm1}\hat{\sigma}_\alpha^{(n)}\hat{\sigma}_{-\alpha}^{(n)} = \hat{\sigma}_0^{(n)}$. With only functions of the $\hat{\sigma}_z^{(i)}$ $(i = 1, \ldots, N)$ remaining, we can go to their diagonal bases to work with scalar functions of their eigenvalues $\sigma_i = \pm\frac{1}{2}$ (see also Opus, Section 4.4). This expresses Equation 2.30 as

$$\begin{aligned}C^{(n)}_{s\bar{s},+}(u) &\equiv \sum_{\alpha=\pm1} C^{\alpha\ \ n}_{s\bar{s},+}(u) = e^{-iuH_s}e^{iuH_s^{(n)}}R^{(n)}_{s\bar{s}}(t) - e^{-iuH_s^{(n)}}e^{iuH_s}R_{s\bar{s}}(t), \\ C^{(n)}_{s\bar{s},-}(u) &\equiv \sum_{\alpha=\pm1} C^{\alpha\ \ n}_{s\bar{s},-}(u) = R^{(n)}_{s\bar{s}}(t)e^{-iuH_{\bar{s}}^{(n)}}e^{iuH_{\bar{s}}} - R_{s\bar{s}}(t)e^{-iuH_{\bar{s}}}e^{iuH_{\bar{s}}^{(n)}},\end{aligned} \tag{4.4}$$

where for any function $f(\{\sigma_i\})$, $f^{(n)}$ has the sign of σ_n reversed,

$$f^{(n)}(\{\sigma_i\}) = f\left(\left\{(-1)^{\delta_{i,n}}\sigma_i\right\}\right). \tag{4.5}$$

We employed the obvious rules $(fg)^{(n)} = f^{(n)}g^{(n)}$ and $[f(g)]^{(n)} = f(g^{(n)})$. The terms in Equation 4.4, being scalars, yield the relation $C^{(n)}_{s\bar{s},-}(u) = C^{(n)}_{s\bar{s},+}(-u)$, which allows combining the integrals of Equations 2.29 and 2.30 as a single one from $u = -t$ to t. Because $\gamma \ll 1$, the typical scale of t, the registration time $1/\gamma T$ is much larger than the bath equilibration time $1/T$. Hence, we may now take the integral over the entire real axis to arrive at the Fourier-transformed kernel $\bar{K}(\omega)$ at specific frequencies.

The next step is to reduce the $2^N \times 2^N$ matrix problem to a problem of $N+1$ variables by considering $R_{ss}(\{\sigma_i\}) = R_{ss}(m_1)$ to be functions of the order parameter $m_1 = \nu\sum\sigma_i$. This is formally true at t_i and valid for $\dot{R}_{s\bar{s}}(t_\mathrm{i})$; hence, it remains valid over time. Denoting $P_s(m_1)$ as the probability that $R_{ss}(\{\sigma_i\})/r_{ss}(t_\mathrm{i})$ involves $m_1 = \nu\sum_i\sigma_i$, it picks up the degeneracy number G_N in Equation 3.6 of realizations $\{\sigma_i\}$ with the same m_1,

$$P_s(m_1) = G_N(m_1)\frac{R_{ss}(m_1)}{r_{ss}(t_\mathrm{i})}. \tag{4.6}$$

To obtain the evolution of $\dot{P}_s$, we multiply Equation 4.2 by $G_N(m_1)/r_{ss}(t_\mathrm{i})$. At given m_1, one has $m_1^{(n)} = m_1 - 2\nu\sigma_n$, so we can split the terms with $\sigma_n = \frac{1}{2}$ (and $-\frac{1}{2}$) and perform the sum over n. The fraction of terms that flips an up spin $\sigma_n = \frac{1}{2}$ is $x_{\frac{1}{2}}(m_1)$, which multiplies $P(m_1 - \nu)$; flipping a down spin $\sigma_n = -\frac{1}{2}$ happens with probability $x_{-\frac{1}{2}}(m_1)$, which multiplies $P(m_1 + \nu)$. Due to Equation 4.6, these Ps involve the ratios

$$\begin{aligned}\frac{G_N(m_1)}{G_N(m_1-\nu)} &= \frac{x_{-\frac{1}{2}}(m_1-\nu)}{x_{\frac{1}{2}}(m_1)}, \\ \frac{G_N(m_1)}{G_N(m_1+\nu)} &= \frac{x_{\frac{1}{2}}(m_1+\nu)}{x_{-\frac{1}{2}}(m_1)},\end{aligned} \tag{4.7}$$

which has the effect of eliminating the $x_{\pm\frac{1}{2}}(m_1)$. Introducing the operators $E_\pm$ and $\Delta_\pm = E_\pm - 1$ by

$$\begin{aligned}E_\pm f(m_1) &= f(m_1 \pm \nu), \\ \Delta_\pm f(m_1) &= f(m_1 \pm \nu) - f(m_1),\end{aligned} \tag{4.8}$$

the evolution of P_s gets condensed as

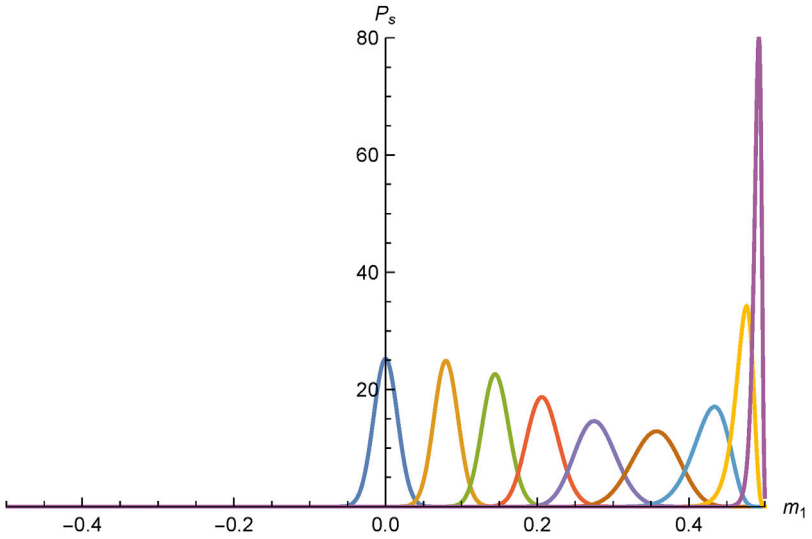

FIGURE 1
Evolution of the magnetization distribution $P_s(m_1;t)$ for $s = +\frac{1}{2}$ at times $0, 1, \ldots, 8$ in units of $1/\gamma T$. The paramagnetic state at $t = 0$ is peaked around $m_1 = 0$; the coupling between S and A moves the peak toward $m_1 = +\frac{1}{2}$. In doing so, it first broadens and later narrows significantly.

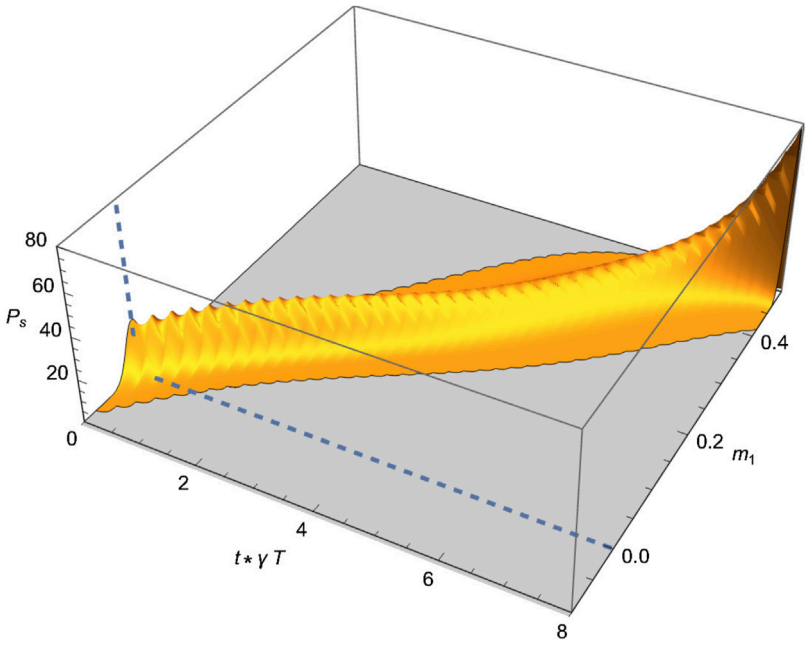

FIGURE 2
The case of Figure 1 plotted in 3*d* at intervals $\Delta t = 0.2/\gamma T$.

$$\dot{P}_s(m_1) = \frac{\gamma N}{2} \sum_{\alpha=\pm 1} \Delta_\alpha \left\{ x_{\frac{1}{2}\alpha}(m_1) \tilde{K}[\Omega_{s\alpha}(m_1)] P_s(m_1) \right\}. \tag{4.9}$$

where

$$\Omega_{s\pm}(m_1) = \Delta_\mp H_s = H_s(m_1 \mp \nu) - H_s(m_1). \tag{4.10}$$

This is now a problem for $N + 1$ functions $P(m_1;t)$ subject to the normalization $\sum_{m_1} P(m_1;t) = 1$.

In Figure 1, the distribution of the magnetization m_1 is depicted at various times. In Figure 2, this evolution is represented in a 3*d* plot.

3.6 *H*-theorem and relaxation to equilibrium

The dynamical entropy of the distribution $P_s(m_1;t) = G_N(m_1) R_{ss}(\{\sigma_i\};t)/r_{ss}(t_i)$ is defined as

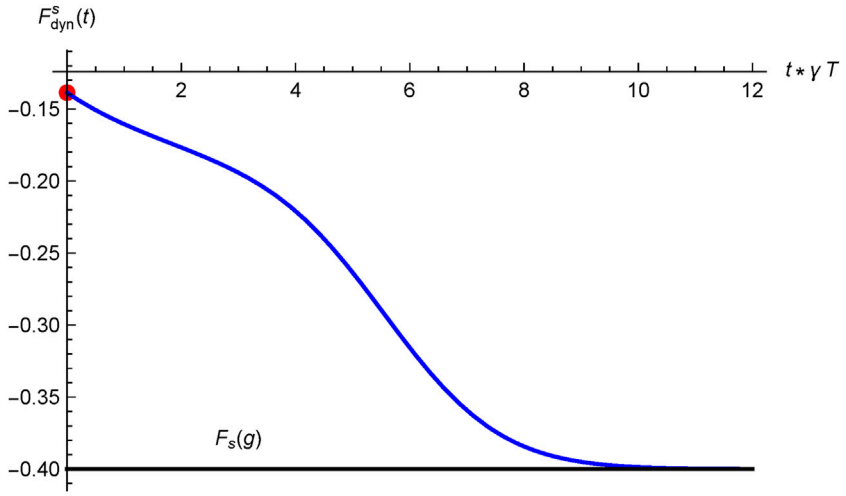

FIGURE 3
Evolution of the dynamical free energy $F^s_{\rm dyn}(t)$, identical in both sectors $s = \pm\frac{1}{2}$, after coupling the apparatus to a spin-$\frac{1}{2}$ at time $t = 0$. Its approach to the Gibbs state with $F_s(g)$ (bottom line), exponential in t, expresses the registration of the measurement.

$$S_s(t) = -\mathrm{Tr}\frac{\hat R_{ss}(t)}{r_{ss}(t_i)}\log\frac{\hat R_{ss}(t)}{r_{ss}(t_i)} = -\sum_{m_1} P_s(m_1;t)\log\frac{P_s(m_1;t)}{G_N(m_1)}. \tag{4.11}$$

As in Opus, we introduce a dynamical free energy:

$$F^s_{\rm dyn}(t) = U_s(t) - TS_s(t) = \sum_{m_1} P_s(m_1;t)\left[H_s(m_1) + T\log\frac{P_s(m_1;t)}{G_N(m_1)}\right], \tag{4.12}$$

which adds the $P_s \log P_s$ term to the average of the free energy functional $F_N(m_1) = H_s(m_1) - TS_N(m_1)$. With $\beta = 1/T$, Equation 5.36 yields.

$$\dot F^s_{\rm dyn} = T\sum_{m_1}\dot P_s(m_1)\log\frac{P_s(m_1)e^{\beta H_s(m_1)}}{G_N(m_1)} = \frac{\gamma NT}{2}\sum_{\alpha=\pm1}\sum_{m_1}\Delta_\alpha\left[x_{\frac12\alpha}\tilde K(\Omega_{s\,\alpha})P_s\right]\log\frac{P_s e^{\beta H_s}}{G_N}.$$

For general functions $f_{1,2}(m_1)$ and $\alpha = \pm 1$, partial summation yields

$$\sum_{m_1}(\Delta_\alpha f_1)f_2 = \sum_{m_1} f_1(\Delta_{-\alpha}f_2) = \sum_{m_1} E_\alpha[f_1(\Delta_{-\alpha}f_2)] = -\sum_{m_1}(E_\alpha f_1)(\Delta_\alpha f_2). \tag{4.13}$$

provided that the boundary terms $f_{1,2}(m^\nu_\pm)$ at $m^\nu_\pm = \pm(1+\nu)$ vanish. As discussed, this holds for P_s but also for the logarithm in Equation 4.13 because we may insert a factor $(1 - \delta_{m_1,m^\nu} - \delta_{m_1,-m^\nu})$ that makes this explicit. For $\alpha = +1$, we now use the last expression, and for $\alpha = -1$, we use the second one, which yields, also using Equation 4.10 and the property $\tilde K(-\omega) = \tilde K(\omega)e^{\beta\omega}$ satisfied in (Equations 2.26, 2.27), the result

$$\dot F^s_{\rm dyn} = -\gamma NT\sum_{m_1}\tilde K(\Delta_+H_s)\times\left\{e^{\Delta_+\beta H_s}\left(E_+x_{\frac12}\right)(E_+P_s)x_{-\frac12}P_s\right\}\Delta_+\log\frac{P_s e^{\beta H_s}}{G_N}. \tag{4.14}$$

The various x–factors are such that a term $G_N(m_1)x_{-\frac12}$ can be factored out to yield

$$\dot F^s_{\rm dyn} = -\gamma NT\sum_{m_1}\sum_{\beta=\pm1}G_N x_{-\frac12}\tilde K(\Delta_+H_s)\times\left\{e^{\Delta_+\beta H_s}\left(E_+\frac{P_s}{G_N}\right)\frac{P_s}{G_N}\right\}\Delta_+\log\frac{P_s e^{\beta H_s}}{G_N}. \tag{4.15}$$

With $\Delta_+H_s = E_+H_s - H_s$, $G_N = \exp(S_N)$ and $F_s(m_1) = H_s(m_1) - TS_N(m_1)$, this can finally be expressed as

$$\dot F^s_{\rm dyn}(t) = -\gamma NT\sum_{m_1}x_{-\frac12}\tilde K(\Delta_+H_s)e^{-\beta F_s}\times\left(\Delta_+\frac{P_s}{e^{-\beta F_s}}\right)\left(\Delta_+\log\frac{P_s}{e^{-\beta F_s}}\right). \tag{4.16}$$

The last factors have the form $(x'-x)\log(x'/x)$, which is nonnegative, so that $F^s_{\rm dyn}$ is a decreasing function of time. Dynamic equilibrium occurs when these factors vanish, which happens when the magnet has reached the thermodynamic equilibrium set by the Gibbs state $P_s = e^{-\beta F_s}/Z_s$ and $\hat R_{ss} = e^{-\beta\hat H_s}/Z_s$, with $Z_s = \sum_{m_1}\exp(-\beta F_s) = \sum_{m_1}G_N(m_1)$ $\exp(-\beta H_s) = \mathrm{Tr}\exp(-\beta\hat H_s)$, as usual. The dynamical free energy (Equation 4.12) indeed ends up at the thermodynamic one,

$$F^s_{\rm dyn}(\infty) = -T\log Z_s = F_s(g). \tag{4.17}$$

This constitutes an example of the apparatus going dynamically to its lowest thermodynamic state and the pointer state indicating the measurement outcome $s = \pm\frac12$. The temporal evolution from $F_{dyn}(0)$ to $F_s(g)$ is depicted in Figure 3.

3.7 Decoupling the apparatus

Near the end of the measurement, at a suitable time $t_{\rm dc}$, the apparatus is decoupled from the system, by setting $g = 0$; in doing so, an energy $U_{\rm dc} = -\sum_{m_1}P_s(m_1;t_{\rm dc})H_{\rm SA}(m_1)$ must be supplied to the magnet, which will then relax further its nearby minimum of the $g = 0$ situation, to provide a stable

pointer indication with a macroscopic order parameter $M_1 = Nm_1$ that can be read off.

4 Dynamics of the spin-1 model

We now focus on the spin-1 case, in which the tested system, S, is $\hat{\mathbf{s}}$, a spin-1 operator with $\hat{s}_z$ having eigenvalues $s_z = -1, 0, 1$. Our magnet M has $N \gg 1$ quantum spins-1 $\hat{\sigma}^{(i)}$ $(i = 1, \ldots, N)$. According to Equation 2.5, one now deals with two order parameters,

$$\hat{m}_1 = \frac{1}{N}\sum_{i=1}^{N}\hat{\sigma}_i, \qquad \hat{m}_2 = \frac{1}{N}\sum_{i=1}^{N}\hat{\sigma}_i^2. \tag{5.1}$$

While $\hat{m}_1$ is the usual magnetization in the z-direction, $\hat{m}_2$ is a spin-anisotropy order parameter that discriminates the sectors with eigenvalues $\sigma_i = \pm 1$ from the sector with eigenvalues $\sigma_i = 0$.

The quantity $\hat{C}_2$, the operator-form of Equation 2.2, is our starting point for a permutation-invariant Hamiltonian that ensures unbiased measurement. Expanding the cosine, employing Equation 2.8 for each spin $\hat{\sigma}_i$, and summing over i yields a polynomial in the moments $\hat{m}_{1,2}$,

$$\hat{C}_2 = \left(1 - \frac{3}{2}\hat{m}_2\right)^2 + \frac{3}{4}\hat{m}_1^2. \tag{5.2}$$

For the Hamiltonian, we take as in Equation 3.2

$$\hat{H}_N = N\hat{H}, \qquad \hat{H} = -\frac{1}{2}J_2\hat{C}_2 - \frac{1}{4}J_4\hat{C}_2^2. \tag{5.3}$$

It can be understood as containing the single-spin term $\hat{m}_2$, the pair couplings $\hat{m}_1^2 = 1/N^2\sum_{ij}\hat{\sigma}_i\hat{\sigma}_j$ and $\hat{m}_2^2 = 1/N^2\sum_{ij}\hat{\sigma}_i^2\hat{\sigma}_j^2$, the triplet couplings $\hat{m}_1^2\hat{m}_2$ and the quartet couplings $\hat{m}_1^4$, $\hat{m}_1^2\hat{m}_2^2$, and $\hat{m}_2^4$. However, note its different conception in Section 2.5.

At the initial time t_i of the measurement, its state is described by its 3×3 density matrix $\hat{r}(t_\mathrm{i})$ with elements $r_{s\bar{s}}(t_\mathrm{i})$ for $s, \bar{s} = -1, 0, 1$.

In each $s, \bar{s}$ sector, M lies in its state $\hat{R}_{s\bar{s}}(t) = \hat{R}_{\bar{s}s}^\dagger(t)$, which is an operator that can be represented by a $3^N \times 3^N$ matrix. This exponential problem gets transformed into a polynomial one, a step that is exact for the considered mean-field-type Hamiltonian.

At t_i, M is assumed to lie in a paramagnetic state, wherein the spins are fully disordered and uncorrelated. For each spin, its state is thus $\hat{\sigma}_0^{(i)}/3$ where $\hat{\sigma}_0^{(i)} = \mathrm{diag}(1, 1, 1)$. Multiplying by the respective element of $\hat{r}(t_\mathrm{i})$ leads to the elements of the initial density matrix of S + M in the $s, \bar{s} = 0, \pm 1$ sector,

$$\hat{R}_{s\bar{s}}(t_\mathrm{i}) = r_{s\bar{s}}(t_\mathrm{i})\frac{\hat{\sigma}_0^{(1)}}{3}\otimes\frac{\hat{\sigma}_0^{(2)}}{3}\cdots\otimes\frac{\hat{\sigma}_0^{(N)}}{3}. \tag{5.4}$$

For general angular momentum, the commutation relations $[\hat{L}_a, \hat{L}_b] = i\varepsilon_{abc}\hat{L}_c$ and $\hat{L}_x^2 + \hat{L}_y^2 + \hat{L}_z^2 = l(l+1)\hat{I}$ carry over to general spin

$$[\hat{\sigma}_a, \hat{\sigma}_b] = i\varepsilon_{abc}\hat{\sigma}_c, \quad \hat{\sigma}_x^2 + \hat{\sigma}_y^2 + \hat{\sigma}_z^2 = l(l+1)\hat{\sigma}_0, \tag{5.5}$$

While we considered $l = \frac{1}{2}$ in Section 3, we now focus on $l = 1$.

We proceed as for spin $\frac{1}{2}$. The $a = z$ commutator in Equation 2.29 does again not contribute. We introduce $\hat{\sigma}_\alpha = \hat{\sigma}_x + i\alpha\hat{\sigma}_y$ for $\alpha = \pm 1$. From Equation 5.5, it follows for general l that

$$\begin{aligned}\hat{\sigma}_\alpha\hat{\sigma}_{-\alpha} &= l(l+1)\hat{\sigma}_0 + \alpha\hat{\sigma}_z - \hat{\sigma}_z^2\\ (\hat{\sigma}_\alpha\hat{\sigma}_{-\alpha})_{\sigma\sigma'} &= (l + 1 - \alpha\sigma)(l + \alpha\sigma)\delta_{\sigma\sigma'}.\end{aligned} \tag{5.6}$$

In the present case $l = 1$, this has nontrivial values

$$(\hat{\sigma}_\alpha\hat{\sigma}_{-\alpha})_{\sigma\sigma} = 2\delta_{\sigma,\alpha} + 2\delta_{\sigma,0}, \quad (\sigma = 0, \pm 1), \tag{5.7}$$

with Equation 5.6 implying that the $\sigma = -\alpha$ term indeed drops out. The SO(3) generators

$$\begin{aligned}\hat{\sigma}_x &= \frac{1}{\sqrt{2}}\begin{pmatrix}0&1&0\\1&0&1\\0&1&0\end{pmatrix}, \quad \hat{\sigma}_y = \frac{1}{\sqrt{2}}\begin{pmatrix}0&-i&0\\i&0&-i\\0&i&0\end{pmatrix},\\ \hat{\sigma}_z &= \begin{pmatrix}1&0&0\\0&0&0\\0&0&-1\end{pmatrix},\end{aligned} \tag{5.8}$$

allow verifying these relations. Each of the $\hat{\sigma}^{(i)}$ $(i = 1, \ldots, N)$ has such a presentation. In Equation 2.30, the interchange of the $\hat{\sigma}_\alpha^{(i)}$ with the $\hat{\sigma}_z^{(n)}$ will be needed. For $i \neq n$, they commute, while for $i = n$,

$$\begin{aligned}\hat{\sigma}_\alpha^{(n)}\hat{\sigma}_z^{(n)\ k} &= \left(\hat{\sigma}_z^{(n)} - \alpha\hat{\sigma}_0^{(n)}\right)^k\hat{\sigma}_\alpha^{(n)},\\ \hat{\sigma}_z^{(n)\ k}\hat{\sigma}_\alpha^{(n)} &= \hat{\sigma}_\alpha^{(n)}\left(\hat{\sigma}_z^{(n)} + \alpha\hat{\sigma}_0^{(n)}\right)^k.\end{aligned} \tag{5.9}$$

Valid for $k = 1$, induction yields this for higher k. For functions of the $\{\hat{\sigma}_z^{(i)}\}$, $(i = 1, \ldots, N)$, that can be expanded in a power series, it follows that

$$\begin{aligned}\hat{\sigma}_\alpha^{(n)} f\left(\left\{\hat{\sigma}_z^{(i)}\right\}\right) &\equiv f^{(n,\alpha)}\left(\left\{\hat{\sigma}_z^{(i)}\right\}\right)\hat{\sigma}_\alpha^{(n)},\\ f^{(n,\alpha)}\left(\left\{\hat{\sigma}_z^{(i)}\right\}\right) &= f\left(\left\{\hat{\sigma}_z^{(i)} - \delta_{i,n}\alpha\hat{\sigma}_0^{(n)}\right\}\right).\end{aligned} \tag{5.10}$$

Now the $\hat{\sigma}_\pm$ can be eliminated using Equation 5.6, which leaves functions of only the $\hat{\sigma}_z^{(i)}$, with the shifts in their arguments arising as the cost for this. As before, we can assume that $\hat{R}_{s\bar{s}}(t) = R_{s\bar{s}}(\{\hat{\sigma}_z^{(i)}\}, t)$, where $R_{s\bar{s}}(\{\sigma_i\}, t)$ is a *scalar* function of the eigenvalues $\sigma_i = 0, \pm 1$ of the $\hat{\sigma}_z^{(i)}$. Valid at t_i, this holds for $(\mathrm{d}\hat{R}_{s\bar{s}}/\mathrm{d}t)(t_\mathrm{i})$, so it remains valid in time. Hence, it is possible to go from the matrix equations to scalar equations. With the equality in Equation 5.6 applied for spin n, we end up with the scalar expressions

$$\begin{aligned}C_{s\bar{s},+}^{(n,\alpha)}(u) &= (\delta_{\sigma_n,-\alpha} + \delta_{\sigma_n,0})e^{-iuH_s}e^{iuH_s^{(n,\alpha)}}R_{s\bar{s}}^{(n,\alpha)}(t)\\ &\quad -(\delta_{\sigma_n,\alpha} + \delta_{\sigma_n,0})e^{-iuH_s^{(n,-\alpha)}}e^{iuH_s}R_{s\bar{s}}(t),\\ C_{s\bar{s},-}^{(n,\alpha)}(u) &= C_{s\bar{s},+}^{(n,\alpha)}(-u),\end{aligned} \tag{5.11}$$

where for any function $R_{s\bar{s}}$ expandable in powers of the $\sigma_i = 0, \pm 1$ $(i = 1, \ldots, N)$, it holds that

$$R_{s\bar{s}}^{(n,\alpha)} = R_{s\bar{s}}(\{\sigma_i \to \sigma_i + \alpha\delta_{i,n}\}), \tag{5.12}$$

Now that all terms are scalar functions of the $\hat{\sigma}_z^{(i)}$, it is seen that $C_{s\bar{s},-}^{(n,\alpha)}(u) = C_{s\bar{s},+}^{(n,\alpha)}(-u; H_s \to H_{\bar{s}})$. We no longer need to track the operator structure and can work with scalar functions of the eigenvalues.

4.1 Off-diagonal sector: truncation of Schrödinger cat terms

In the spin $\frac{1}{2}$ Curie–Weiss model, it was found that the Schrödinger cat terms disappear by two mechanisms: dephasing of the magnet, possibly followed by decoherence due to the thermal bath. Similar behavior is now investigated for spin-1.

4.1.1 Initial regime: dephasing

Truncation of the density matrix (disappearance of the cat states) is a collective effect that takes place within an initial time window, in which the magnet stays in the paramagnetic phase, so that the mutual spin couplings $J_{2,4}$ and the coupling to the bath can be neglected. The spins of M act individually by their coupling to the tested spin S and do not get correlated yet. In the sector where the eigenvalue of the operator $\hat{s}_z$ is s, the Hamiltonian of the magnet is

$$\begin{aligned}\hat{H}_{\rm SA} &= \sum_n \hat{H}^{sn}_{\rm SA},\\ \hat{H}^{sn}_{\rm SA} &= -g\Big[\Big(1-\frac{3}{2}s^2\Big)\Big(\hat{\sigma}^{(n)}_0 - \frac{3}{2}\hat{\sigma}^{(n)\,2}_z\Big) + \frac{3}{4}s\hat{\sigma}^{(n)}_z\Big].\end{aligned} \tag{5.13}$$

At a given s, this is a trace-free diagonal matrix with elements $\frac{1}{2}g$ (twice) and $-g$,

$$\begin{aligned}\big(H^{sn}_{\rm SA}\big)_{\sigma\tilde{\sigma}} &= \frac{g}{2}\delta_{\sigma,\tilde{\sigma}}(1-3\delta_{\sigma,s}),\\ \delta_{\sigma,s} &= \frac{1}{3} + \Big(\frac{2}{3}-s^2\Big)\Big(1-\frac{3}{2}\sigma^2\Big) + \frac{1}{2}s\sigma,\end{aligned} \tag{5.14}$$

for $(s,\sigma,\tilde{\sigma} = 0,\pm 1)$. In this approximation, the $3^N \times 3^N$ density matrix of the magnet in each sector $s\bar{s}$ maintains the product structure (Equation 5.4) of uncorrelated spins at $t = t_{\rm i}$,

$$\hat{R}_{s\bar{s}}(t) = r_{s\bar{s}}(t_{\rm i})\hat{\rho}^{(1)}_{s\bar{s}}(t)\cdots\otimes\hat{\rho}^{(2)}_{s\bar{s}}(t)\cdots\otimes\hat{\rho}^{(N)}_{s\bar{s}}(t), \tag{5.15}$$

where, setting $t_{\rm i} = 0$, for each n,

$$\begin{aligned}\hat{\rho}^{(n)}_{s\bar{s}}(t) &= e^{-it\hat{H}^{s,n}_{\rm SA}}\frac{\hat{\sigma}^{(n)}_0}{3}e^{it\hat{H}^{\bar{s}n}_{\rm SA}} = \big(\hat{\rho}^{(n)}_{\bar{s}s}(t)\big)^\dagger,\\ \big(\rho^{(n)}_{s\bar{s}}(t)\big)_{\sigma\tilde{\sigma}} &= \frac{1}{3}\delta_{\sigma,\tilde{\sigma}}\exp\Big[\frac{3}{2}igt\,(\delta_{\sigma,s}-\delta_{\sigma,\bar{s}})\Big].\end{aligned} \tag{5.16}$$

Diagonal elements $s = \bar{s}$ thus essentially do not evolve in this short-time window. The off-diagonal ones imply for $s \neq \bar{s}$

$$r_{s\bar{s}}(t) = {\rm Tr}_{\rm M}\hat{R}_{s\bar{s}}(t) = r_{s\bar{s}}(0)\Big(\frac{1}{3}+\frac{2}{3}\cos\frac{3}{2}gt\Big)^N. \tag{5.17}$$

For small t, this decays as $r_{s\bar{s}}(0)\exp(-t^2/\tau^2_{\rm dph})$ with the dephasing time $\tau_{\rm dph} = 2/g\sqrt{3N}$, very short for large N. The undesired recurrences at $t_n = 4\pi n/3g$, where the cosine equals 1 again, can be suppressed by assuming that the $g \to g_n = \bar{g} + \delta g_n$ values in Equation 5.16 have a small spread δg_n (see Opus, Section 6.1.1). If the thermal oscillator bath has proper parameters, it will cause decoherence, as seen next.

4.1.2 Second step: decoherence

To include the bath in Equation 5.16, we now make the generalized Ansatz:

$$\big(\hat{\rho}^{(n)}_{s\bar{s}}(t)\big)_{\sigma\tilde{\sigma}} = \delta_{\sigma,\tilde{\sigma}}\frac{1}{3}\exp[-B_\sigma(t)]\times\ \exp\Big[-itH^{(s,n)}_{\rm SA}(\sigma) + itH^{(\bar{s},n)}_{\rm SA}(\sigma)\Big]. \tag{5.18}$$

In the commutators (Equation 5.11), H_s now reduces to the $H^{s,n}_{\rm SA}$ of Equation 5.14, and the terms are identical for all n. We can neglect $B \sim \gamma$ in the exponents of Equation 2.29 and find, putting $-\alpha \to \alpha$ in the minus terms,

$$\begin{aligned}\dot{B}_\sigma = \frac{\gamma}{2}\sum_\alpha\{&[K_{t>}(\Delta^\sigma_\alpha H_s) + K_{t<}(\Delta^\sigma_\alpha H_{\bar{s}})]\\ &-[K_{t>}(-\Delta^\sigma_\alpha H_s) + K_{t<}(-\Delta^\sigma_\alpha H_{\bar{s}})]e^{\alpha\sigma}_{s\bar{s}}(t)\},\end{aligned} \tag{5.19}$$

with

$$\begin{aligned}K_{t>}(\omega) &= \int_0^t {\rm d}u\quad K(u)e^{-i\omega u},\\ K_{t<}(\omega) &= \int_{-t}^0 {\rm d}u\quad K(u)e^{-i\omega u}.\end{aligned} \tag{5.20}$$

Here, $K_{t>}(\omega) = K^*_{t>}(\omega)$ because the kernel $\tilde{K}(\omega)$ is real valued; see the example in Equation 2.27, and

$$\begin{aligned}\Delta^\sigma_\alpha H_s &= H_s(\sigma+\alpha) - H_s(\sigma)\\ &= \frac{3g}{2}\Big[\Big(1-\frac{3}{2}s^2\Big)(1+2\alpha\sigma) - \frac{1}{2}s\alpha\Big],\end{aligned} \tag{5.21}$$

with a similar expression for $\Delta^\sigma_\alpha H_{\bar{s}}$, and finally

$$e^{\alpha\sigma}_{s\bar{s}}(t) = \exp[-it\quad(\Delta^\sigma_\alpha H_s - \Delta^\sigma_\alpha H_{\bar{s}})]. \tag{5.22}$$

For $\bar{s} = s$, one has $e^{\alpha\sigma}_{s\bar{s}}(t) = 1$. For $t \gg 1/2\pi T$, one gets, using $\tilde{K}(-\omega) = e^{\beta\omega}\tilde{K}(\omega)$,

$$\begin{aligned}\dot{B}_\sigma &= \frac{\gamma}{2}\sum_\alpha \tilde{K}(\Delta^\sigma_\alpha H_s) - \tilde{K}(-\Delta^\sigma_\alpha H_s)\\ &= \frac{\gamma}{2}\sum_\alpha(\Delta^\sigma_\alpha H_s)e^{-|\Delta^\sigma_\alpha H_s|/T} \sim \frac{\gamma}{N},\end{aligned} \tag{5.23}$$

because $H_s \sim N$, $\Delta^\sigma_\alpha H_s \sim N^0$, and $\sum_\alpha \Delta^\sigma_\alpha H_s \sim 1/N$. Therefore, for $s = \bar{s}$, this confirms that hardly any dynamics take place in this time window. In the next subsection, we show that they occur on a longer time scale $\tau_{\rm reg} = 1/\gamma T$.

For off-diagonal elements $\bar{s} \neq s$, it is seen that $e^{\alpha\sigma}_{s\bar{s}}(t)$ has terms $e^{\pm 3igt/2}$ and $e^{\pm 3igt}$, so that

$$\begin{aligned}e^{\alpha\sigma}_{s\bar{s}}(t) &= \sum_{j=-2,-1,1,2} c_j e^{3ijgt/2},\\ \int_0^t {\rm d}u\quad e^{\alpha}_{s\bar{s}}(\sigma;u) &= \sum_{j=-2,-1,1,2} c_j\frac{e^{3ijgt/2}-1}{3ijg/2}.\end{aligned} \tag{5.24}$$

The exponentials are equal to unity, making $E^\alpha_{s\bar{s}} = 1$, at the times $t_n = 4\pi n/3g$, $n = 1,2,\cdots$, encountered below Equation 5.17, when appearing in the dephasing process, and thus also as times where $\dot{B}_\sigma(t) = 0$. To suppress recurrences like in the dephasing, we again set in each n-term $g \to g_n = \bar{g} + \delta g_n$ with small Gaussian distributed δg_n. For times well exceeding the coherence time $1/2\pi T$ of the bath, the $K_{t>}$ and $K_{t<}$ reach their finite limits, so that we have

$$\begin{aligned}\int_0^t {\rm d}t'\quad K_{t'>}(\omega)E^\alpha_{s\bar{s}}(\sigma;t') &= \int_0^t {\rm d}t'\quad [K_{t'>}(\omega) - K_{\infty>}(\omega)]E^\alpha_{s\bar{s}}(\sigma;t')\\ &+ K_{\infty>}(\omega)\int_0^t {\rm d}u\quad E^{\alpha\sigma}_{s\bar{s}}(u),\end{aligned} \tag{5.25}$$

The first part is small, and the second is given in Equation 5.24. After canceling out its exponents by the δg_n, an imaginary part remains. Hence, for $t \gg 1/2\pi T$, the $E^{\alpha\sigma}_{s\bar{s}}$ terms can be neglected in $\Re B$. We keep

$$\begin{aligned}\Re B_\sigma(t) &\approx \Re\dot{B}_\sigma \times t,\\ \Re\dot{B}_\sigma &\approx \frac{\gamma}{2}\sum_\alpha\big[\tilde{K}(\Delta^\sigma_\alpha H_s) + \tilde{K}(\Delta^\sigma_\alpha H_{\bar{s}})\big],\end{aligned} \tag{5.26}$$

which is positive, so that $|\exp(-NB_\sigma)| = \exp(-N\Re B_\sigma)$ with $N\Re B_\sigma \sim \gamma N g t$ leads for large enough values of N to a decoherence of the off-diagonal elements $r_{s\bar{s}}(t)$ of the density matrix at the characteristic decoherence time $t_{dec} = 1/\gamma gN$ and $\gamma N g\tau_{\rm reg} \sim Ng/T$.

Decoherence is a combined effect of the N apparatus spins; despite it, the individual elements of $\hat{R}_{s\bar{s}}$ hardly decay in this time window, behaving as $\exp(-\gamma g t) = \exp(-t/N\ t_{dec}) \approx 1$.

4.2 Registration dynamics for spin-1

In Section 3, a difference equation was derived for the distribution of the magnetization of the magnet for any number N of spins-$\frac{1}{2}$. Our aim here is to derive an analogous equation for the spin-1 case.

In the paramagnet, one has the form $R_{ss}(\{\sigma_i\}) = r_{ss}(t_i)/3^N$. Let $P_s(\mathbf{m})$ with $\mathbf{m} = (m_1, m_2)$ be the probability for a state of the magnet M characterized by the moments $m_{1,2}$. It gathers the value $R_{ss}(\mathbf{m})/r_{ss}(t_i)$ for all sequences $\{\sigma_i\}$ compatible with $m_{1,2}$, the number of which is the degeneracy factor $G_N = \exp S_N$,

$$\begin{aligned} P_s(\mathbf{m};t) &= G_N(\mathbf{m})\frac{R_{ss}(\mathbf{m};t)}{r_{ss}(t_i)},\\ G_N(\mathbf{m}) &= \frac{N!}{(N_{-1})!\quad (N_0)!\quad (N_1)!},\qquad N_\sigma = x_\sigma N, \end{aligned} \tag{5.27}$$

with the $x_{\pm1} = \frac{1}{2}(m_2 \pm m_1)$ and $x_0 = 1 - m_2$ from Equation 2.14. The normalizations are

$$\begin{aligned} \sum_{\sigma^{(1)}=-1}^{1}\cdots\sum_{\sigma^{(N)}=-1}^{1} R_{ss}\big(\{\sigma^{(i)}\};t\big) &= r_{ss}(t_i),\\ \sum_{m_2=0}^{1}\sum_{m_1=-m_2}^{m_2} P_s(m_1,m_2;t) &= 1. \end{aligned} \tag{5.28}$$

Due to the relations described by Equations 2.13 and 2.14 between the spin moments $m_{0,\pm1}$ and the spin fractions $x_{0,\pm1}$, the shifts in $m_{1,2}$ induce the shifts $N'_\sigma = N_\sigma + \delta N_\sigma$ and $x'_\sigma = x_\sigma + \nu\delta N_\sigma$, with

$$\delta N_{\pm1} = \frac{1\pm\alpha}{2} + \alpha\sigma_n,\ \ \delta N_0 = -1 - 2\alpha\sigma_n, \tag{5.29}$$

which are integers, as they should be. The degeneracies for $\sigma_n = -\alpha, 0, \alpha$ lead to the respective factors

$$\begin{aligned} \frac{G_N}{(G_N)'} = \frac{N'_{-1}!N'_0!N'_1!}{N_{-1}!N_0!N_1!} &= \frac{x_0+\nu}{x_{-\alpha}}\delta_{\sigma_n,-\alpha}\\ +\frac{x_\alpha+\nu}{x_0}\delta_{\sigma_n,0} &+ \frac{(x_{-1}+\nu)(x_1+\nu)+(x_\alpha+2\nu)}{x_0(x_0-\nu)(x_0-2\nu)}\delta_{\sigma_n,\alpha}, \end{aligned} \tag{5.30}$$

where $N_\sigma = Nx_\sigma$ is used. The complicated last term is fortunately not needed, while the denominators of the first two will factor out.

Going to the functions P_s of the moments $m_{1,2}$, we proceed as for the spin $\frac{1}{2}$ situation. The $C_\pm$ terms of Equation 5.11 can again be combined and performing the u-integrals in Equation 4.2 leads for $t \gg 1/T$ to the kernel $\tilde{K}(\omega)$ at the frequencies

$$\Omega^\beta_\alpha(\mathbf{m}) = H_s(m_1\alpha - \nu, m_2 - \beta\nu) - H_s(\mathbf{m}), \tag{5.31}$$

for $\alpha, \beta = \pm1$. Multiplying Equation 4.2 by G_N and summing over α, there results an evolution equation for the distribution P_s at each discrete value of $m_{1,2}$,

$$\begin{aligned} \dot{P}_s(m_1,m_2;t) = \gamma N\sum_{\alpha=\pm1}\Big\{&(x_0+\nu)\tilde{K}\big(-\Omega^+_{s,-\alpha}\big)P^-_{s\alpha}(m_1,m_2;t)\\ &+(x_\alpha+\nu)\tilde{K}\big(-\Omega_{s,-\alpha}{}^{-}\big)P^+_{s\alpha}(m_1,m_2;t)\\ &-\big[x_\alpha\tilde{K}(\Omega^+_{s\alpha}) + x_0\tilde{K}(\Omega^-_{s\alpha})\big]P_s(m_1,m_2;t)\Big\}. \end{aligned} \tag{5.32}$$

Let us condense notation and introduce the shift operators E^β_α and $\Delta^\beta_\alpha = E^\beta_\alpha - 1$ by their action

$$\begin{aligned} E^\beta_\alpha f(\mathbf{m}) &= f(m_1+\alpha\nu, m_2+\beta\nu),\\ \Delta^\beta_\alpha f(\mathbf{m}) &= f(m_1+\alpha\nu, m_2+\beta\nu) - f(\mathbf{m}). \end{aligned} \tag{5.33}$$

on any $f(\mathbf{m})$. They have the properties

$$\begin{aligned} &E^\beta_\alpha\Delta^{-\beta}_{-\alpha} = -\Delta^\beta_\alpha, \qquad \Omega^\beta_{s\alpha} = \Delta^{-\beta}_{-\alpha}H_s,\\ &E^\beta_\alpha\Omega^\beta_{s\alpha} = -\Delta^\beta_\alpha H_s = -\Omega^{-\beta}_{s,-\alpha}.\\ &E^\beta_\alpha x_\alpha = x_\alpha + \frac{1+\beta}{2}\nu, \quad E^\beta_\alpha x_0 = x_0 - \beta\nu. \end{aligned} \tag{5.34}$$

Hence, Equation 5.32 can be expressed as

$$\dot{P}_s(m_1,m_2;t) = \gamma N\sum_{\alpha=\pm1}\Big(\Delta^+_\alpha\big[x_\alpha\tilde{K}(\Omega^+_{s\alpha})P_s\big] + \Delta^-_\alpha\big[x_0\tilde{K}(\Omega^-_{s\alpha})P_s\big]\Big), \tag{5.35}$$

which has a remarkable analogy to Equation 4.9 and Equation 4.16 of Opus for the spin-$\frac{1}{2}$ case. By denoting $x^+_\alpha = x_\alpha$ above and $x^-_\alpha = x_0$, this is condensed further,

$$\dot{P}_s(m_1,m_2;t) = \gamma N\sum_{\alpha,\beta=\pm1}\Delta^\beta_\alpha\big[x^\beta_\alpha\tilde{K}\big(\Omega^\beta_{s\alpha}\big)P_s\big]. \tag{5.36}$$

4.3 H-theorem and relaxation to equilibrium

We now exhibit a H theorem that assures the relaxation of the magnet towards its Gibbs equilibrium state and, thus, a successful measurement. The dynamical entropy of the distribution $P_s(\mathbf{m};t) = G_N(\mathbf{m})R_{ss}(\{\sigma_i\})/r_{ss}(t_i)$ is defined as

$$\begin{aligned} S_s(t) &= -\mathrm{Tr}\frac{\hat{R}_{ss}(t)}{r_{ss}(t_i)}\log\frac{\hat{R}_{ss}(t)}{r_{ss}(t_i)}\\ &= -\sum_{\mathbf{m}}P_s(\mathbf{m};t)\log\frac{P_s(\mathbf{m};t)}{G_N(\mathbf{m})}. \end{aligned} \tag{5.37}$$

Following Opus and Equation 4.12 above, we consider the dynamical free energy

$$F^s_{\mathrm{dyn}}(t) = U_s(t) - TS_s(t) = \sum_{\mathbf{m}}P_s(\mathbf{m};t)\left[H_s(\mathbf{m}) + T\log\frac{P_s(\mathbf{m};t)}{G_N(\mathbf{m})}\right]. \tag{5.38}$$

It appears to depend on s. The simultaneous change $s \to -s$, $m_1 \to -m_1$ implies that $F^1_{\mathrm{dyn}}(t) = F^{-1}_{\mathrm{dyn}}(t)$ at all t, as happened for $s = \pm\frac{1}{2}$ in the spin $\frac{1}{2}$ case, but the $F^{\pm1}_{\mathrm{dyn}}(t)$ differ from $F^0_{\mathrm{dyn}}(t)$, except in the thermal situations at $t = 0$ and $t \to \infty$.

With $\beta = 1/T$, not to be confused with the index $\beta = \pm1$, Equation 5.36 yields

$$\begin{aligned} \dot{F}^s_{\mathrm{dyn}} &= T\sum_{\mathbf{m}}\dot{P}_s(\mathbf{m})\log\frac{P_s(\mathbf{m})e^{\beta H_s(\mathbf{m})}}{G_N(\mathbf{m})}\\ &= \gamma NT\textstyle\sum_{\alpha,\beta=\pm1}\sum_{\mathbf{m}}\Delta^\beta_\alpha\big[x^\beta_\alpha\tilde{K}(\Omega^\beta_{s\alpha})P_s\big]\log\frac{P_se^{\beta H_s}}{G_N}. \end{aligned} \tag{5.39}$$

For general functions $f_{1,2}(\mathbf{m})$ with vanishing boundary terms, partial summation yields

$$\begin{aligned} \sum_{\mathbf{m}}\big(\Delta^\beta_\alpha f_1\big)f_2 &= \sum_{\mathbf{m}}f_1\big(\Delta^{-\beta}_{-\alpha}f_2\big) = \sum_{\mathbf{m}}E^\beta_\alpha\big[f_1\big(\Delta^{-\beta}_{-\alpha}f_2\big)\big]\\ &= -\sum_{\mathbf{m}}\big(E^\beta_\alpha f_1\big)\big(\Delta^\beta_\alpha f_2\big). \end{aligned} \tag{5.40}$$

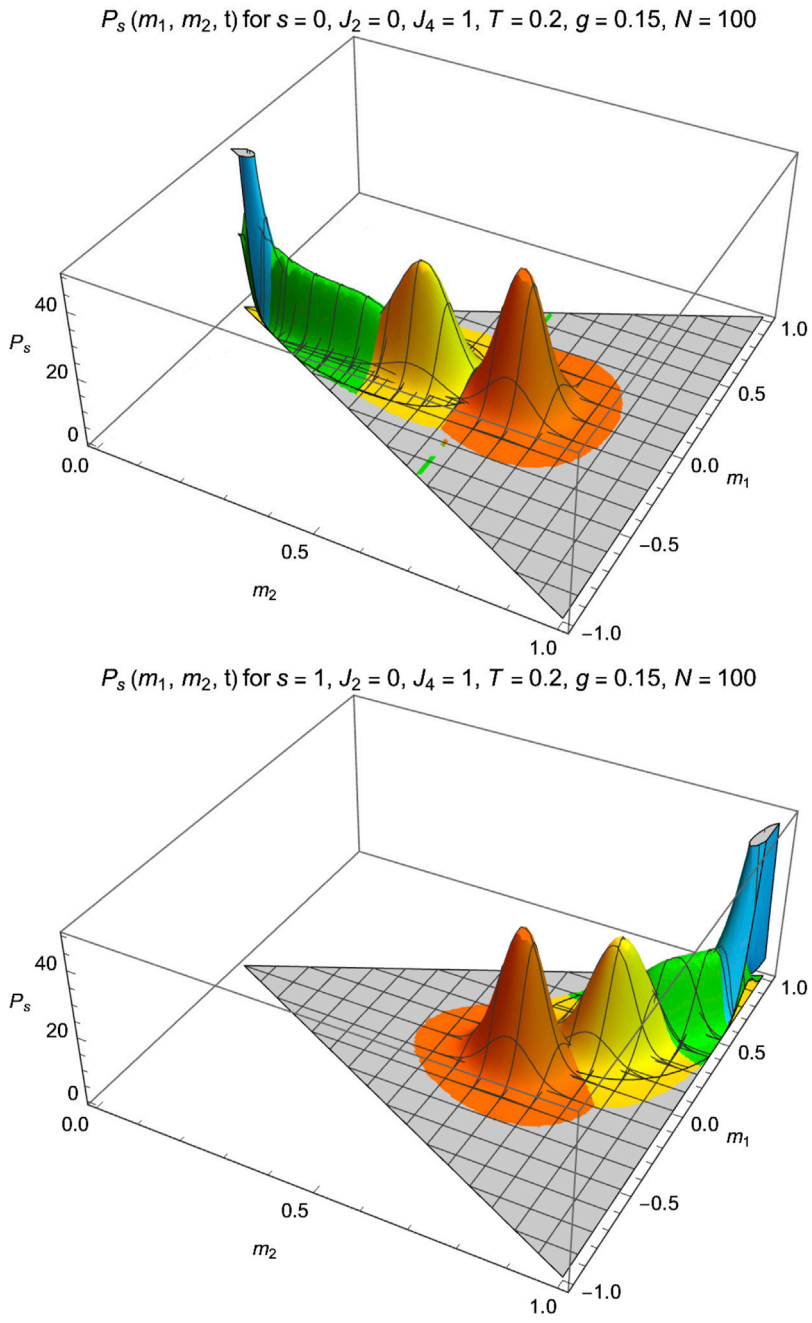

FIGURE 4
Snapshots of the distribution P_s of the magnetization moments $m_{1,2}$ for registration of the spin-1 measurement. Upper: $P_s \geq 10^{-3}$ data in the $s = 0$ sector at times $t = (0, 1, 2, 3) \times 2/\gamma T$ from right to left. Lower: the $s = 1$ sector at $t = (0, 1, 2, 3) \times 5/\gamma T$ from left to right; it evolves more slowly. The parameters are listed in Equation 5.46.

For $\alpha = +1$, we use the last expression, and for $\alpha = -1$, we use the second one, while taking $\beta \to -\beta$, and also using Equation 5.34 and the property $\tilde{K}(-\omega) = \tilde{K}(\omega)e^{\beta\omega}$ satisfied generally in Equation 2.26, which yields the result

$$\dot{F}^s_{\rm dyn} = -\gamma NT \sum_{\mathbf{m}} \sum_{\beta=\pm 1} \tilde{K}\left(\Delta^\beta_+ H_s\right) \times \left\{ e^{\Delta^\beta_+ \beta H_s} \left(E^\beta_+ x^\beta_+\right)\left(E^\beta_+ P_s\right) - x^{-\beta}_{-1} P_s \right\} \Delta^\beta_+ \log \frac{P_s e^{\beta H_s}}{G_N}. \quad (5.41)$$

The various parts are such that a term $G_N(\mathbf{m})x^{-\beta}_{-1}$ can be factored out, to express this as

$$\dot{F}^s_{\rm dyn} = \gamma NT \sum_{\mathbf{m}} \sum_{\beta=\pm 1} G_N x^{-\beta}_{-1} \tilde{K}\left(\Delta^\beta_+ H_s\right) \times \left\{ e^{\Delta^\beta_+ \beta H_s} \left[E^\beta_+ \left(\frac{P_s}{G_N} \right) \right] - \frac{P_s}{G_N} \right\} \Delta^\beta_+ \log \frac{P_s e^{\beta H_s}}{G_N}. \quad (5.42)$$

With $\Delta^\beta_+ H_s = E^\beta_+ H_s - H_s$, $G_N = \exp(S_N)$, and $F_s(\mathbf{m}) = H_s(\mathbf{m}) - TS_N(\mathbf{m})$, this is equal to

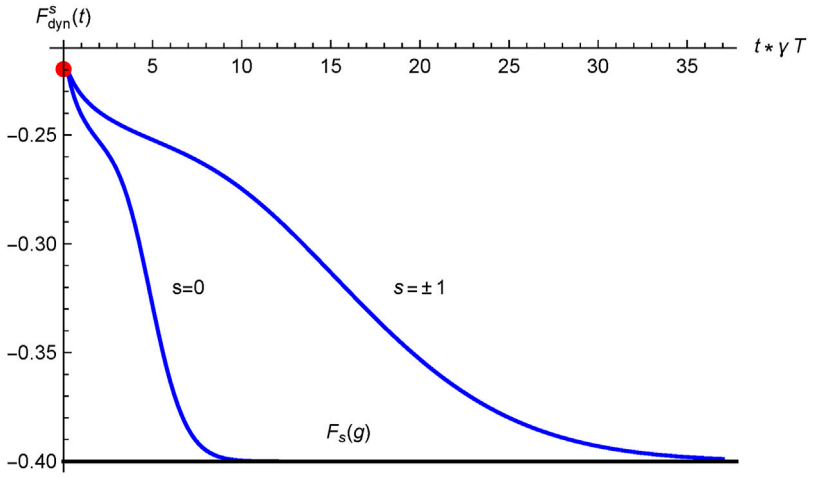

FIGURE 5
The spin-1 dynamical free energy $F^s_{\rm dyn}$ of Equation 5.38 relaxes from its $t = 0$ value to its thermodynamic value. $F_s(g)$ of Equation 5.44, thereby registering the measurement. Parameters are as in Figures 4A,B, and time is expressed in units of $1/\gamma T$. The relaxation for $s = \pm 1$ is slower than for $s = 0$ due to the occurrence of zero frequencies. The initial "shoulders" describe the initial broadenings in Figures 4A,B.

$$\dot{F}^s_{\rm dyn}(t) = -\gamma NT \sum_{\mathbf{m}} \sum_{\beta=\pm1} x_{-1}^{-\beta} \tilde{K}(\Delta_+^\beta H_s) e^{-\beta F_s} \times \left(\Delta_+^\beta \frac{P_s}{e^{-\beta F_s}}\right)\left(\Delta_+^\beta \log \frac{P_s}{e^{-\beta F_s}}\right). \tag{5.43}$$

The last factors have the form $(x' - x)\log(x'/x)$, which is nonnegative, implying that $F^s_{\rm dyn}$ is a decreasing function of time. Dynamic equilibrium occurs when these factors vanish, which happens when the magnet has reached thermodynamic equilibrium, that is, the Gibbs state $P_s = e^{-\beta F_s}/Z_s$ and $\hat{R}_{ss} = e^{-\beta \hat{H}_s}/Z_s$, with $Z_s = \sum_{\mathbf{m}} \exp(-\beta F_s) = \sum_{\mathbf{m}} G_N(\mathbf{m}) \exp(-\beta H_s) = \mathrm{Tr} \exp(-\beta \hat{H}_s)$, as usual. The dynamical free energy (Equation 5.38) then ends up at the thermodynamic free energy,

$$F^s_{\rm dyn}(\infty) = -T \log Z_s, \tag{5.44}$$

which actually does not depend on s due to the invariance map of the static state, reflecting that the measurement is unbiased. This constitutes an explicit example of the apparatus going dynamically to its lowest thermodynamic state, the pointer state registering the measurement outcome.

Although the statics are identical for $s = 0, \pm 1$, this does not hold for the dynamics. While it is similar for $s = \pm 1$ (to change the sign of $s = \pm 1$, also change the sign of m_1), this deviates from the $s = 0$ dynamics. For $s = 0$, all $\Omega^\beta_\alpha(\mathbf{m})$ are finite, but for $s = \pm 1$, there are cases where $\Omega^\beta_\alpha(\mathbf{m})$ vanishes, which leads to a slower dynamics; see Figure 5.

4.4 Numerical analysis

The initial spin-1 Hamiltonian leads to a $3^N \times 3^N$ matrix problem, which is numerically hard. For the considered mean-field-type model, the formulation in terms of the order parameters $m_{1,2}$ is exact; it lowers the dimensionality considerably. The variable $m_2 = (1/N)\sum_{i=1}^N \sigma_i^2$ can take $N + 1$ values between 0 and 1. The value of $M_2 = Nm_2$ indicates that $N - M_2$ of the σ_i take the value 0, while the other M_2 of the σ_i are ± 1. Given this number, $m_1 = (1/N)\sum_{i=1}^N \sigma_i$ can take $M_2 + 1$ values between $-m_2$ and m_2. Accounting for conservation of total probability, this leads to $N(N + 3)/2$ dynamical variables, a polynomial problem.

(Concerning higher spin: For spin $\frac{3}{2}$, one separates terms with $s_i = \pm\frac{3}{2}$ from those with $s_i = \pm\frac{1}{2}$; for spin-2, one selects terms with $s_i = 0, \pm 1$, or ± 2, etc.)

Equation 5.32 can be solved numerically as a set of linear differential equations. Programming it is straightforward; the vanishing of boundary terms and conservation of the total probability must be verified as a check on the code.

The magnet starts in the paramagnetic initial state

$$P_s(\mathbf{m}; 0) = \frac{1}{3^N} G_N(\mathbf{m}) \approx \frac{3^{3/2}}{2\pi N} \exp\left\{-N\left[\frac{3}{4}m_1^2 + \left(\frac{3}{2}m_2 - 1\right)^2\right]\right\}. \tag{5.45}$$

The sum of P_s over $m_{1,2}$ equals unity and, with the mesh $\Delta m_1 \Delta m_2 = 2\nu^2$, so does its integral.

The dynamics (Equation 5.32) can be solved numerically, and the results are presented in upcoming figures. We consider the parameters, with g large enough,

$$N = 100, \quad J_2 = 0, \quad J_4 = 1, \quad g = 0.15, \quad T = 0.2, \quad \Gamma = 10. \tag{5.46}$$

We plot in Figures 4A,B snapshots of $P_s/(2\nu^2)$ at four times, for $s = 0$ and $s = 1$. The case $s = -1$ follows from the case $s = 1$ by setting $m_1 \to -m_1$.

Figure 5 shows the evolution of the dynamical free energy $F^s_{\rm dyn}(t)$.

4.5 Decoupling of the apparatus

Near the end of the measurement, the interaction between the system and the apparatus is cut off by setting $g = 0$; in doing so, at

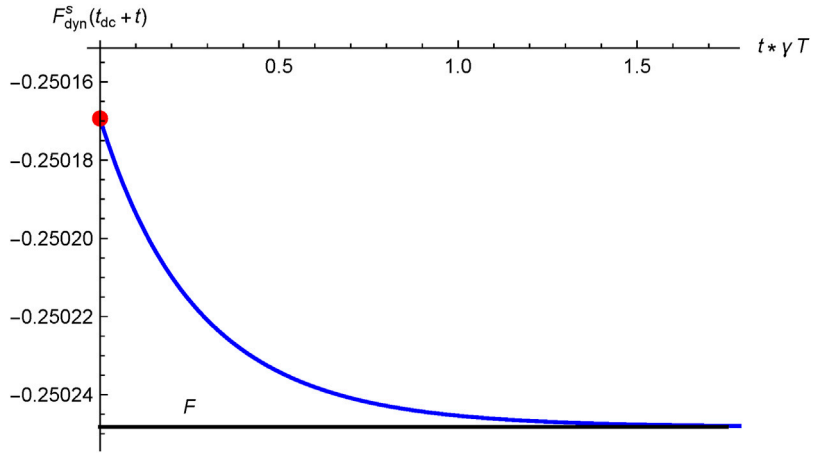

FIGURE 6
After decoupling the apparatus from the system, the magnet relaxes to its nearby $g = 0$ equilibrium. If this happens at a time t_{dc} where finite-g equilibrium has been reached, this goes identical in the sectors $s = 0, \pm 1$. The dynamical free energy is plotted with parameters as in Figures 4, 5, relaxing from its decoupled value (indicated by the dot) to its $g = 0$ thermodynamic limit F (lower line). Compared to Figure 5, this macroscopic energy cost is a permille effect.

decoupling time t_{dc}, Equation 5.13 expresses that an amount of energy

$$U_{dc} = -\sum_{\mathbf{m}} P_s(\mathbf{m}; t_{dc}) H_{SA}(\mathbf{m})$$
$$= +gN \times \sum_{\mathbf{m}} P_s(\mathbf{m}; t_{dc}) \left[\left(1 - \frac{3}{2}s^2\right)\left(1 - \frac{3}{2}m_2\right) + \frac{3}{4}s\,m_1\right], \quad (5.47)$$

must be supplied to the magnet, leaving it with the post-decoupling free energy

$$F_{dc} = \sum_{\mathbf{m}} P_s(\mathbf{m}; t_{dc}) \left(H_M - T \log G_N\right). \quad (5.48)$$

This post-decoupling state is not an equilibrium state; the magnet will now relax to the nearby minimum of the $g = 0$ case. There follows a relaxation driven by bath, with the magnet evolving under the $g = 0$ Hamiltonian $H_M(\mathbf{m})$ to its Gibbs state $P_G(\mathbf{m}) = G_N \exp[-H_M(\mathbf{m})/T]/Z_G$, with free energy $F_G = \sum_{\mathbf{m}} P_G(\mathbf{m})[H_M(\mathbf{m}) - TS_N(\mathbf{m})]$.

When the decoupling time t_{dc} is large enough, the magnet M lies in its Gibbs state at coupling g, $P_s(t_{dc}) \sim \exp[-\beta H_s(\mathbf{m})]$. Due to the invariance of the $g = 0$ situation, the approach to it is identical for starting in any of the sectors $s = 0, \pm 1$.

To compare with the dynamics that end up in one of the minima, one must restrict the Gibbs state, which has three degenerate minima, to the nearby minimum. This is achieved numerically even at moderate N by discarding $\exp(-\beta H_s)$ well away from the peak of $P_s(t_{dc})$, also in Z_G. For $s = 0$, it suffices to keep $\exp(-\beta H_s)$ for $m_2 < \frac{1}{3}$; for $s = \pm 1$ by doing that for $m_1 s > \frac{1}{3}$.

The change of the state is also seen in $\langle m_2 \rangle(t) = \sum_{\mathbf{m}} m_2 P_s(\mathbf{m}; t)$. Let us consider the sector $s = 0$, where $\langle m_1 \rangle = 0$ at all t. Here, the coupling $H_{SA} = gN(\frac{3}{2}m_2 - 1)$ has the tendency to suppress m_2, so after decoupling, m_2 will relax to a larger value. For $N \to \infty$, we get from the Gibbs states at g and at $g = 0$, respectively,

$$\langle m_2(0) \rangle = 3.63\,10^{-4}, \langle m_2(\infty) \rangle = 11.5\,10^{-4}. \quad (5.49)$$

The full-time behavior for $N = 100$ and couplings as in Equation 5.46 is presented in Figure 6, with the finite-N values increasing from $\langle m_2(0) \rangle = 9.975\,10^{-4}$ to $\langle m_2(\infty) \rangle = 12.69\,10^{-4}$.

The relaxation in the sectors $s = \pm 1$ follows immediately from this. The map (Equation 5.50) yields. The maps (4.11) and (4.13) of Models lead to

$$\langle m_1 \rangle_{s=\pm 1} = \pm\left(1 - \frac{3}{2}\langle m_2 \rangle_{s=0}\right),$$
$$\langle m_2 \rangle_{s=\pm 1} = 1 - \frac{1}{2}\langle m_2 \rangle_{s=0}. \quad (5.50)$$

4.6 Energy cost of quantum measurement

The Copenhagen postulates obscure one of the facts of life in a laboratory: a firm cost for the energy needed to keep the setup running. In this work, we consider two intrinsic costs. In the previous subsection, we established the cost of decoupling the apparatus from the system. Here, we consider resetting the magnet for another run. It must be set from its stable state back to its metastable state. Being related to the magnet, both costs are macroscopic.

Our initial state, the paramagnet (pm), has zero magnetic energy and maximal entropy

$$F_{pm} = -NT \log 3, \quad (5.51)$$

The energy needed to reset the Gibbs state of the magnet to the paramagnetic one is

$$U_{reset} = F_{pm} - F_G = -\sum_{\mathbf{m}} P_G(\mathbf{m}) \left[H_M - T \log\left(G_N/3^N\right)\right]. \quad (5.52)$$

It is evidently macroscopic. The condition that U_{reset} is positive was identified in Opus and in Models as the condition that the initial paramagnetic state is metastable but not stable.

5 Conclusion

This article dealt with the dynamics of an ideal quantum measurement of the z-component of a spin-1. The statics for this task were worked out recently in our "Models" article (Nieuwenhuizen, 2022); it generalized to any spin $l > \frac{1}{2}$ the Curie–Weiss model to measure a spin $\frac{1}{2}$; the latter was considered in great detail in "Opus" (Allahverdyan et al., 2013). Here, we first reformulated the dynamics of the known case for spin $\frac{1}{2}$ and worked out some further properties. The resulting formalism is suitable as a basis for models to measure any higher spin.

The dynamics of measurement in the spin-1 case were analyzed in detail. Off-diagonal elements of the density matrix ("cat states") were shown to decay very fast ("truncation of the density matrix") due to dephasing, possibly followed by decoherence.

The evolution of the diagonal elements of the density matrix was expressed as coupled first-order differential equations for the distribution of two magnetization-type-order parameters, $m_{1,2}$. The approach to a Gibbs equilibrium was certified by demonstrating a H-theorem. The resulting scheme was found to be numerically a polynomial problem. These are easily solved with the present power of laptops for an apparatus consisting of a few hundred spins. The evolution of the probability density was evaluated, and the H-theorem was verified. The macroscopic energy costs for decoupling the apparatus from the spin and for resetting it from its stable state to its metastable state for use in the next run of the measurement were quantified.

For general spin l, this method simplified the numerically hard problem of dimension $(2l+1)^{2N} - 1$ by a polynomial problem of order N^{2l} for its $2l$-order parameters. For more complicated models of the apparatus, it will likewise pay off to focus on the order parameter of the dynamical phase transition of the pointer that achieves the registration of the measurement. The fact that the phase transition in the magnet is of first order underlines that our mean-field-type models, although of mathematical convenience, are not essential for the fundamental description of quantum measurements.

Data availability statement

The original contributions presented in the study are included in the article/supplementary material; further inquiries can be directed to the corresponding author.

Author contributions

TN: writing – original draft and writing – review and editing.

Funding

The author(s) declare that no financial support was received for the research and/or publication of this article.

Conflict of interest

The author declares that the research was conducted in the absence of any commercial or financial relationships that could be construed as a potential conflict of interest.

Generative AI statement

The author(s) declare that no Generative AI was used in the creation of this manuscript.

Publisher's note

References

Allahverdyan, A., Balian, R., and Nieuwenhuizen, T. M. (2003a). The quantum measurement process: an exactly solvable model. *Atti della Fondazione Giorgio Ronchi*, 719. Available online at: https://arxiv.org/abs/cond-mat/0309188.

Allahverdyan, A. E., Balian, R., and Nieuwenhuizen, T. M. (2003b). Curie-Weiss model of the quantum measurement process. *EPL Europhys. Lett.* 61, 452–458. doi:10.1209/epl/i2003-00150-y

Allahverdyan, A. E., Balian, R., and Nieuwenhuizen, T. M. (2005a). The quantum measurement process in an exactly solvable model. *AIP Conf. Proc.* 750, 26–34. doi:10.1063/1.1874554

Allahverdyan, A. E., Balian, R., and Nieuwenhuizen, T. M. (2005b). Dynamics of a quantum measurement. *Phys. E Low-dimensional Syst. Nanostructures* 29, 261–271. doi:10.1016/j.physe.2005.05.023

Allahverdyan, A. E., Balian, R., and Nieuwenhuizen, T. M. (2006). Phase transitions and quantum measurements. *AIP Conf. Proc.* 810, 47–58. doi:10.1063/1.2158710

Allahverdyan, A. E., Balian, R., and Nieuwenhuizen, T. M. (2007). "The quantum measurement process: lessons from an exactly solvable model," in *Beyond the quantum* (World Scientific), 53–65.

Allahverdyan, A. E., Balian, R., and Nieuwenhuizen, T. M. (2013). Understanding quantum measurement from the solution of dynamical models. *Phys. Rep.* 525, 1–166. doi:10.1016/j.physrep.2012.11.001

Allahverdyan, A. E., Balian, R., and Nieuwenhuizen, T. M. (2017). A sub-ensemble theory of ideal quantum measurement processes. *Ann. Phys.* 376, 324–352. doi:10.1016/j.aop.2016.11.001

Allahverdyan, A. E., Balian, R., and Nieuwenhuizen, T. M. (2024). Teaching ideal quantum measurement, from dynamics to interpretation. *Comptes Rendus. Phys.* 25, 251–287. doi:10.5802/crphys.180

Allahverdyan, A. E., Balian, R., and Nieuwenhuizen, T. M. (2025). Interpretation of quantum mechanics from the dynamics of ideal measurement. *Europhys. News, appear* 56, 23–25. doi:10.1051/epn/2025210

Auffèves, A., and Grangier, P. (2016). Contexts, systems and modalities: a new ontology for quantum mechanics. *Found. Phys.* 46, 121–137. doi:10.1007/s10701-015-9952-z

Auffèves, A., and Grangier, P. (2020). Deriving born's rule from an inference to the best explanation. *Found. Phys.* 50, 1781–1793. doi:10.1007/s10701-020-00326-8

Ballentine, L. E. (1970). The statistical interpretation of quantum mechanics. *Rev. Mod. Phys.* 42, 358–381. doi:10.1103/revmodphys.42.358

Born, M. (1926). Zur Quantenmechanik der Stoßvorgänge. *Z. für Phys.* 38, 803–827. doi:10.1007/bf01397184

Born, M., Heisenberg, W., and Jordan, P. (1926). Zur quantenmechanik. II. *Z. für Phys.* 35, 557–615. doi:10.1007/bf01379806

Born, M., and Jordan, P. (1925). Zur quantenmechanik. *Z. für Phys.* 34, 858–888. doi:10.1007/bf01328531

Capellmann, H. (2017). "The quantum theory of Born, Heisenberg, and Jordan," in *The development of elementary quantum theory* (Cham: Springer International Publishing), 23–39. Available online at: https://link.springer.com/content/pdf/10.1007/978-3-319-10539-0.pdf.

David, F. (2015). The formalisms of quantum mechanics. *Lect. notes Phys.* 893, 42–43. doi:10.1007/978-3-319-10539-0

De Broglie, L. (1924). *Recherches sur la théorie des quanta*. Paris: Migration-université en cours d'affectation. PhD thesis.

Donker, H., De Raedt, H., and Katsnelson, M. (2018). Quantum dynamics of a small symmetry breaking measurement device. *Ann. Phys.* 396, 137–146. doi:10.1016/j.aop.2018.07.010

Mistele, T., McGaugh, S., Lelli, F., Schombert, J., and Li, P. (2024). Indefinitely flat circular velocities and the baryonic tully–Fisher relation from weak lensing. *Astrophysical J. Lett.* 969, L3. doi:10.3847/2041-8213/ad54b0

Mydosh, J. A. (1993). *Spin glasses: an experimental introduction*. London: CRC Press. doi:10.1201/9781482295191

Neumaier, A. (2025). The Born rule–100 years ago and today. *arXiv Prepr. arXiv:2502.08545* 27, 415. doi:10.3390/e27040415

Nieuwenhuizen, T. (2022). Models for quantum measurement of particles with higher spin. *Entropy Basel, Switz.* 24, 1746. doi:10.3390/e24121746

Nieuwenhuizen, T. M. (2023). Exact solutions for black holes with a smooth quantum core. *arXiv Prepr. arXiv:2302.14653*.

Nieuwenhuizen, T. M. (2024a). Solution of the dark matter riddle within standard model physics: from black holes, galaxies and clusters to cosmology. *Front. Astronomy Space Sci.* 11, 1413816. doi:10.3389/fspas.2024.1413816

Nieuwenhuizen, T. M. (2024b). Indefinitely flat rotation curves from Mpc sized charged cocoons. *Europhys. Lett.* 148, 49002. doi:10.1209/0295-5075/ad895f

Nieuwenhuizen, T. M. (2025). How the vacuum rescues the Lorentz electron and imposes its Newton and geodesic motion, and the equivalence principle, *to appear Eur. J. Phys.*

Nieuwenhuizen, T. M., Perarnau-Llobet, M., and Balian, R. (2014). Lectures on dynamical models for quantum measurements. *Int. J. Mod. Phys. B* 28, 1430014. doi:10.1142/s021797921430014x

Perarnau-Llobet, M., and Nieuwenhuizen, T. M. (2017a). Simultaneous measurement of two noncommuting quantum variables: solution of a dynamical model, *Physical Review A* 95 (5), 052129.

Perarnau-Llobet, M., and Nieuwenhuizen, T. M. (2017b). Dynamics of quantum measurements employing two Curie–Weiss apparatuses, Philosophical Transactions of the Royal Society A: Mathematical, Physical and Engineering Sciences, 375 (2106), 20160386.

Schrödinger, E. (1926). An undulatory theory of the mechanics of atoms and molecules. *Phys. Rev.* 28, 1049–1070. doi:10.1103/physrev.28.1049

Van Den Bossche, M., and Grangier, P. (2023). Contextual unification of classical and quantum physics. *Found. Phys.* 53, 45. doi:10.1007/s10701-023-00678-x

Wheeler, J. A., and Zurek, W. H. (2014). *Quantum theory and measurement*, 15. Princeton University Press.

Frontiers in
Quantum Science and Technology

Explores innovation and tools enabled by quantum properties of nature

An exciting journal in a rapidly growing field researching how quantum properties of nature, such as entanglement and coherence, can provide modern society with new tools.

Discover the latest Research Topics

See more →

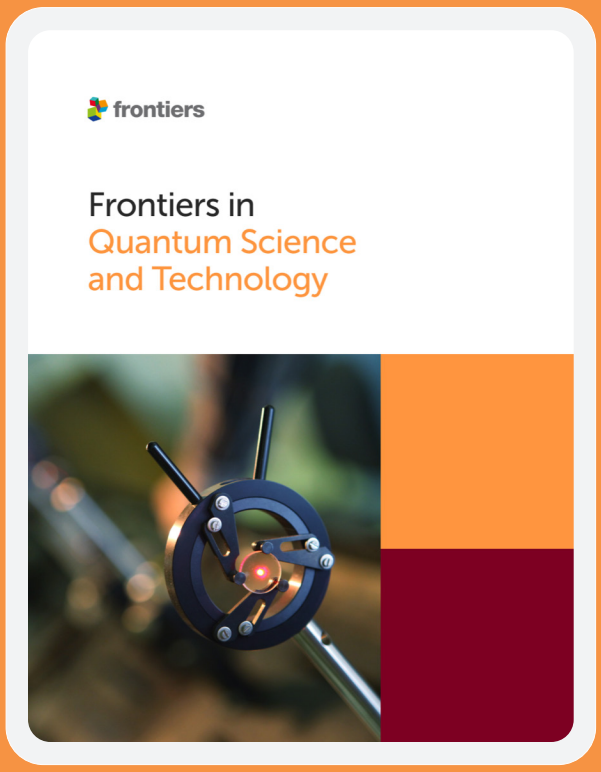

Frontiers

Avenue du Tribunal-Fédéral 34
1005 Lausanne, Switzerland
frontiersin.org

Contact us

+41 (0)21 510 17 00
frontiersin.org/about/contact